GEOLOGICAL, GEOCHEMICAL, AND GEOPHYSICAL SURVEYS OF THE GEOTHERMAL RESOURCES AT HOT SPRINGS BAY VALLEY, AKUTAN ISLAND, ALASKA

By

R.J. Motyka,[1] E.M. Wescott,[2] D.L. Turner,[2] S.E. Swanson,[2]
J.D. Romick,[1*] M.A. Moorman,[1] R.J. Poreda,[3] W. Witte,[2]
B.Petzinger,[2] R.D. Allely,[1] and M. Larsen[1]

General Editors: R.J. Motyka[1] and C.J. Nye[1]

Special Acknowledgments: J.W. Reeder,[1] S.A. Liss,[1] and G. LaRoche[1]

Alaska Division of
Geological and Geophysical Surveys

October 1985

794 University Avenue, Basement
Fairbanks, Alaska 99701

[1]Alaska Division of Geological and Geophysical Surveys*, 794 University Avenue, Basement, Fairbanks, Alaska 99701

[2]Geophysical Institute, University of Alaska, Fairbanks, Alaska 99701

[3]Scripps Institute of Oceanography, University of California

*Current Address: Department of Geological Sciences, Cornell University, Ithaca, N.Y. 14853

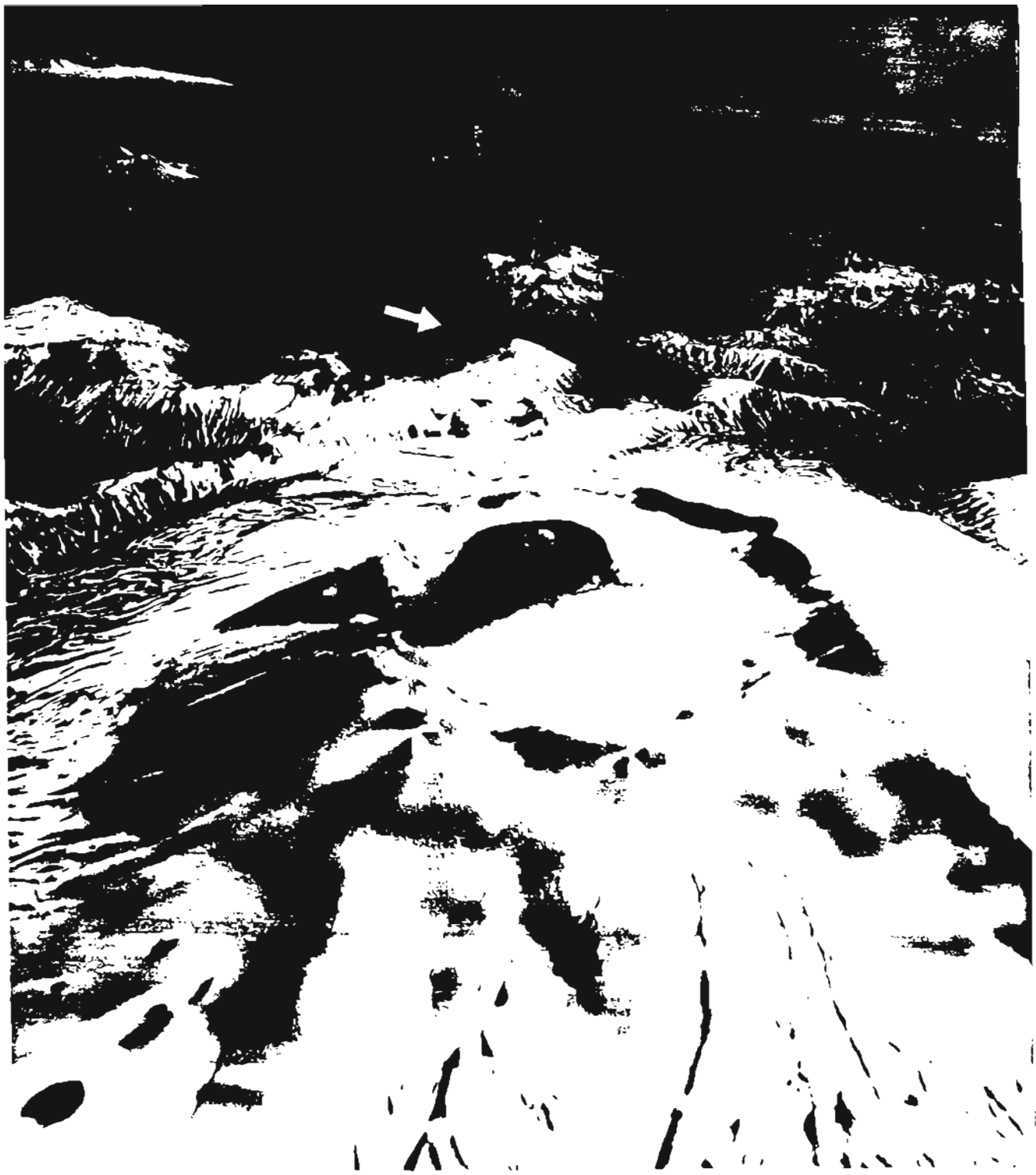

CONTENTS

Chapter 7. Appraisal of geothermal potential.

CHAPTER 1

GEOTHERMAL INVESTIGATIONS IN HOT SPRINGS BAY VALLEY, AKUTAN ISLAND, ALASKA, IN 1981

by

Roman J. Motyka,[1] Eugene M. Wescott,[2] Donald L. Turner,[2] Samuel E. Swanson,[2] Richard D. Allely,[1] and Mark Larsen[1]

[1]Alaska Division of Geological and Geophysical Surveys, 794 University Avenue, Fairbanks, Alaska 99701
[2]Geophysical Institute, University of Alaska, Fairbanks, Alaska 99701

INTRODUCTION

Regional and site-specific exploration and assessment of geothermal resources in the State of Alaska was initiated in 1979 by the Alaska Division of Geological and Geophysical Surveys (ADGGS) and the Geophysical Institute, University of Alaska, under a program jointly sponsored and funded by the U.S. Department of Energy and the State of Alaska, Department of Natural Resources. Impetus for the program was derived in part from federal policy of finding ways of decreasing national dependency on fossil-fuel energy sources and a state policy of fostering energy and economic independence in rural areas of Alaska. Early in the study it was recognized that the best potential for finding high-temperature geothermal resources, i.e. those capable of generating electrical power, lies in the Aleutian arc of active volcanism. State and local governments, Aleutian native corporations, and industries all expressed strong interest in the development of such resources as a means of providing stable and economical electrical power to support the state's growing fishing industry. The Bering Sea fishery is acknowledged to be one of the richest in the world. In addition, oil and gas exploration in the Bering Sea region has intensified in recent years putting a heavy strain on land-based support facilities.

An extensive geothermal reconnaissance of the Aleutian arc was made in 1980 by ADGGS. Using chemical and isotopic geothermometry and the existence of persistent solfatara fields as indicators, at least 13 sites were identified as potentially housing high-temperature hydrothermal systems (T>150°) (Motyka and others, 1981; Motyka, 1982). One of the most attractive of these sites in terms of potential future development is Hot Springs Bay Valley on

Akutan Island. Preliminary geothermometry applied to waters obtained from Akutan hot springs indicated reservoir temperatures of 180-190 C°, sufficient for electrical power generation. The resource is close to potential users, Akutan Village is 6 km away, and to Akutan Harbor, one of the few sheltered, deep-water harbors in the Aleutians. Several fish-processing plants operate in the area and a state-supported bottom-fish processing plant has recently been constructed near Akutan Village. For these reasons Hot Springs Bay Valley was chosen for more detailed geothermal exploration. The bulk of the field surveys were accomplished during July, 1981. This report describes these surveys and the results of the investigations.

REGIONAL SETTING

Akutan Island is located in the eastern Aleutian Islands between Unimak and Unalaska Islands (figs. 1-1 and 1-2). The Aleutian chain is composed predominately of volcanic rocks and most of the major islands, including Akutan, have active volcanoes. The volcanic arc lies immediately north of the Aleutian Trench, a convergent boundary between the North American and the Pacific lithospheric plates. This convergence produces a seismically active belt with much of the seismicity originating from the Benioff zone, the subcrustal region where the Pacific plate is being actively subducted under the North American plate. The eruption of Aleutian magmas, including Akutan, appears to be intimately related to this subduction process.

Akutan Island is mountainous and rugged with shorelines dominated by steep cliffs and rocky headlands. Akutan volcano (1,300 m), a composite shield volcano has erupted numerous times in recorded history and remains

active, with several eruptions occurring during the past decade. Portions of the island not covered by recent volcanic flows show signs of intense glaciation: serrated ridges, cirques, hanging valleys, and broad U-shaped valleys. The east end of the island is split by Akutan Harbor, a deep 8-km-long fiord. The lower elevations of the island are covered by a thin mantle of soil and recent volcanic ash, commonly blanketed by lush and verdant tundra vegetation.

The Akutan hot springs are located in Hot Springs Bay Valley, about 4 km northwest of Akutan Harbor and 10 km northeast of the active Akutan volcano (fig. 1-2, pl. 1). In addition to the hot springs, a solfatara field occurs several kilometers up-valley from the springs and is located at about 350 m elevation on the flank of Akutan Volcano. The glacial valley containing the hot springs has been carved from a sequence of interbedded volcanic breccias, debris flows, and lava flows that in places exceeds 700 m in thickness. Although the valley is relatively close to the volcano, an intervening valley and ridge help form barriers to lava flows or debris flows from the active vent.

Akutan Village, the only habitation on the island, is located on the east coast of the island at the base of a steep ridge that borders the north shore of Akutan Harbor (fig. 1-2, pl. 1). The village was established in 1879 as a fur storage and trading post; in 1912 a whale-processing station was built across the bay from Akutan and operated until 1939 (Morgan, 1980). The present population of about 120 inhabitants depends on subsistence, commercial fishing, and fish processing for their economy. Several floating fish processors now operate in the protected waters of Akutan Harbor, which bring in a seasonal influx of 200 - 700 nonresident workers. Boats and

amphibious aircraft are the only means of transportation into Akutan, which has no airstrip.

TOPOGRAPHIC BASE MAP

Until recently vertical aerial photography has been lacking for most of Akutan Island and, except for the coastline and areas immediately adjacent to it, topographic coverage on U.S. Geological Survey and U.S. Coast and Geodetic Survey maps is nonexistent or unreliable.* To facilitate geological mapping of Hot Springs Bay Valley and establish accurate locations of the various geophysical and geochemical surveys it was necessary to construct a topographic map of the valley. This was accomplished in the following manner:

1. A base network was established on the valley floor and a theodolite-distance range survey was made of selected points in and around the valley.

2. Surveyed positions were plotted on a base map and contours between points were sketched in the field.

3. Oblique aerial photos were taken of the valley and were subsequently used to define valley drainages and to modify contours sketched in the field.

*North Pacific Aerial Surveys (NPAS) of Anchorage acquired photogrammetric quality vertical aerial photos of Akutan Island on June 7, 1983. A proposal has been submitted to the U.S. Geological Survey by NPAS to produce topographic maps of the island.

4. The coastline used on the map was adopted from available U.S. Coast Guard nautical charts.

The geodetic survey was accomplished by R.D. Allely and M. Larsen of ADGGS. Contouring and drainage locations were interpreted by R.D. Allely. The final version of the topographic map was drafted by G. LaRoche, also of ADGGS (pl. 1). Contours appearing on the map are probably within ±6 m (20 ft) for steeper sections and ±1.5 m (5 ft) or better for the valley floor.

The geophysical grid used in this study was surveyed by theodolite and distance-ranger. This grid and lower valley topography are plotted on plate 2.

SUMMARY OF STUDIES

The primary goals of our studies were:

1. The construction of the topographic base map described above.

2. Reconnaissance geologic mapping of northern Akutan Island.

3. Detailed geologic mapping of Hot Springs Bay Valley.

4. Detailed geophysical surveys of lower Hot Springs Bay Valley.

5. Geochemical soil surveys.

6. Sampling, analysis, and geochemical interpretation of hot springs water and fumarolic gases.

Northern Akutan Island and Hot Springs Bay Valley were mapped with the aid of helicopter and of a zodiac raft and, wherever and whenever possible, by shoreline, valley and ridge traverses.

Funding and logistics limitations restricted detailed geophysical and geochemical-soil surveys to lower Hot Spring Bay Valley. Geophysical surveys included shallow-ground conductivity measurements, using a Geonics EM-31 meter; Schlumberger vertical electrical soundings; co-linear dipole-dipole sections; and seismic refraction profiles. Gravity profiling and VLF measurements were carried out but did not produce usable results. Distance between electrodes and the seismic shot spacing limited the depth of investigation to about 150 m.

Helium and mercury soil surveys were conducted in the vicinity of the lower valley hot springs.

Waters from the lower valley thermal springs were sampled in 1980 and 1981. Fumarolic gases and waters at the head of the valley were sampled in 1981 and again in 1983. Water samples were analyzed for major and minor element species and for stable isotope composition; the gases were analyzed for major, minor and trace constituents, and for carbon 13/carbon 12 and helium 3/helium 4 ratios.

SUMMARY OF RESULTS

Our geologic reconnaissance mapping found northern Akutan Island to be composed of three distinct volcanic units. The oldest, informally termed the

Hot Springs Bay volcanics in this report, is a Tertiary-aged sequence of mostly volcanic debris flows and volcanic breccias with minor intercalated lava flows that has been intruded by dikes, sills, and small stocks. This unit is overlain by the informally named Akutan volcanics which consist of Pleistocene-aged lava flows with minor dikes and sills. Holocene and historic lava flows from Akutan Volcano and Lava Point cinder cone overlie both the preceding units, and Recent volcanic debris flows and pyroclastic deposits fill several Pleistocene valleys. The volcanic rocks at Akutan are primarily tholeiitic basalts and andesites with major element chemistry consistent with simple low-pressure crystal fractionation of a single magmatic system.

The Hot Springs Bay Valley walls consist mostly of thick, poorly bedded debris flows with the high parts of ridges capped by basalt and andesite flows of the Akutan volcanics. The valley is floored by a Holocene volcanic debris flow which appears to be acting as an impermeable cap over the subsurface hydrothermal system. The outline of low resistivity from EM-31 surveys and helium and mercury soil surveys suggest that thermal waters ascend along buried stream channels which cut through the less permeable volcanic debris flows and allow the waters to emerge at the surface as springs along the present stream banks.

The electrical resistivity and seismic refraction surveys were able to distinguish three subsurface units: 1) an uppermost low velocity-high resistivity layer about 30 - 40 m in thickness believed to be composed of Holocene volcanic debris flows and valley alluvium; 2) a porous, medium velocity, low resistivity middle layer, 30 - 100 m thick that could be either

hydrothermally cemented glacial till and glacial-fluvial deposits or an ash flow tuff; and 3) a high-velocity bedrock layer thought to be similar to the Hot Spring Bay Valley volcanics exposed in the adjacent walls. The zone of low resistivity in the middle layer appears to be restricted to the northwest corner of the lower valley and extends under the region of hot spring activity.

Geochemical and isotopic investigations of thermal fluids provide substantial evidence that deeper thermal waters are mixing with cold meteoric waters before ascending to the surface. Isotopic and chemical geothermometry indicate parent thermal water temperatures are 170-190°C. The zone of mixing is inferred to be the seismically recognizable, low-resistivity layer at a depth of 30 to 100 m. Cold meteoric waters apparently infiltrate along valley walls and migrate laterally under the impermeable surface layers through the porous middle layer and then mix with the ascending thermal water to form a shallow reservoir of 120 to 135°C waters. Waters in this reservoir are under artesian pressure; they cool conductivity upon ascent and emerge as hot springs along the west side of the valley. Chloride concentrations of the mixed water are 400 ppm; the deeper parent thermal waters are estimated to have chloride concentrations of 600 ppm.

Heat discharged by spring flow from springs A through D is estimated at 4.4 to 7.4 MW. Substantial amounts of thermal waters probably also discharge directly into the sea beyond the confining surface volcanic debris flow layer as evidenced by sand temperatures and hot water outflow at the shoreline. The volume of the shallow reservoir as estimated from geophysical surveys and the size of the low resistivity layer is $\sim 9.4 \times 10^6$ m^3. For an assumed mean reservoir temperature of 127°C this is equivalent to $\sim 3 \times 10^{15}$ J of stored

heat energy. The heat discharge by natural flow-through, however, is on the order of 5 to 10 MW. The thermal waters under artesian pressure in the shallow reservoir could be tapped through relatively shallow drilling (50 - 150 m) and would be more than adequate for district heating and industrial processes at Akutan Village.

Geothermometry indicates that the parent thermal waters are derived from deeper reservoirs at 170 - 190°C, temperatures sufficient for generation of electrical power. If the reservoirs supplying fluids to the fumaroles and hot springs are interconnected, the deeper subsurface reservoir system may cover a distance of over 4 km and would represent a substantial geothermal energy resource.

ACKNOWLEDGMENTS

Funding for the Akutan geothermal investigations came from the U.S. Department of Energy, grant #DE-FC07-79ET27105 and from the State of Alaska, Department of Natural Resources Geothermal Program.

The authors wish to extend special acknowledgment to J. Reeder of the Alaska Division of Geological and Geophysical Surveys (ADGGS) for his help in coordinating logistics and field operations and to S.A. Liss and G. LaRoche, also of ADGGS, for their cartographic contributions to this report.

One of us (R. Motyka) wishes to acknowledge the help of W. Evans and C. Janik, U.S. Geological Survey, Menlo Park, California, and D. Sheppard, Department of Sciences and Industrial Research, New Zealand, in performing gas analyses.

Thanks is also extended to the helicopter pilot, Bruce Ricke, and to the camp manager, Scott Allen.

REFERENCES CITED

Morgan, L., (ed.), 1980, The Aleutians: Alaska Geographic, v. 7, no. 3, 224 p.

Motyka, R.J., 1982, High temperature hydrothermal resources in the Aleutian arc: Alaska Geological Society Symposium on Western Alaska Geology and Resource Potential, Anchorage, Proceedings, p. 87-99.

Motyka, R.J., Moorman, M.A., and Liss, S.A., 1981, Assessment of thermal spring sites, Aleutian arc, Atka Island to Becharof Lake - preliminary results and evaluation: Alaska Division of Geological and Geophysical Surveys Alaska Open-file Report 144, 173 p.

FIGURE CAPTIONS

Figure 1-1: Position of Akutan Island within the Aleutian Arc. Dots represent volcano locations along the arc.

Figure 1-2: ERTS-LANDSAT image #2413-21234-7 1 taken March 10, 1976, showing Akutan Island and vicinity.

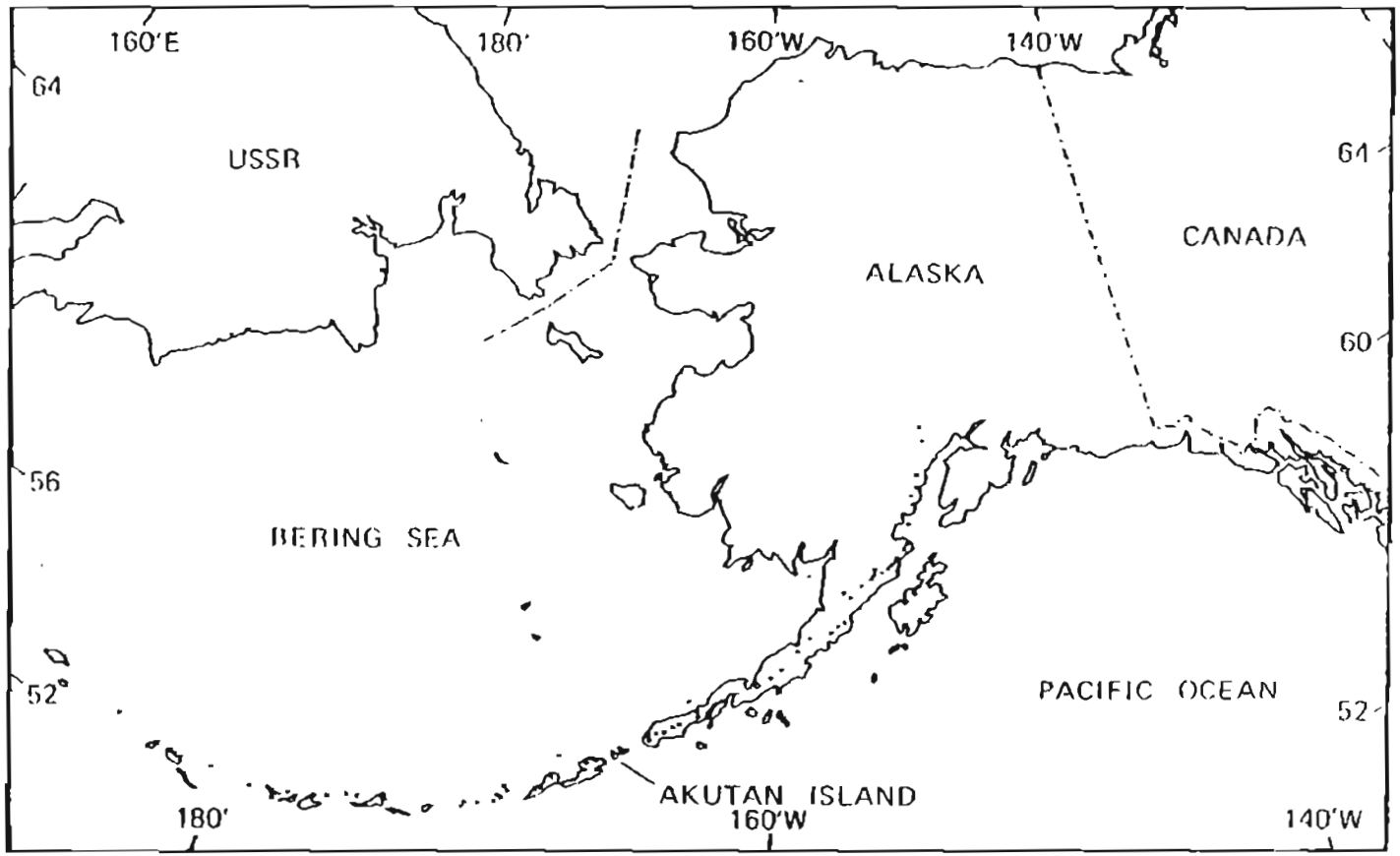
160°E
180°
160°W
140°W
64
USSR
61
CANADA
ALASKA
60
56
BERING SEA
52°
PACIFIC OCEAN
52
AKUTAN ISLAND
180°
160°W
140°W

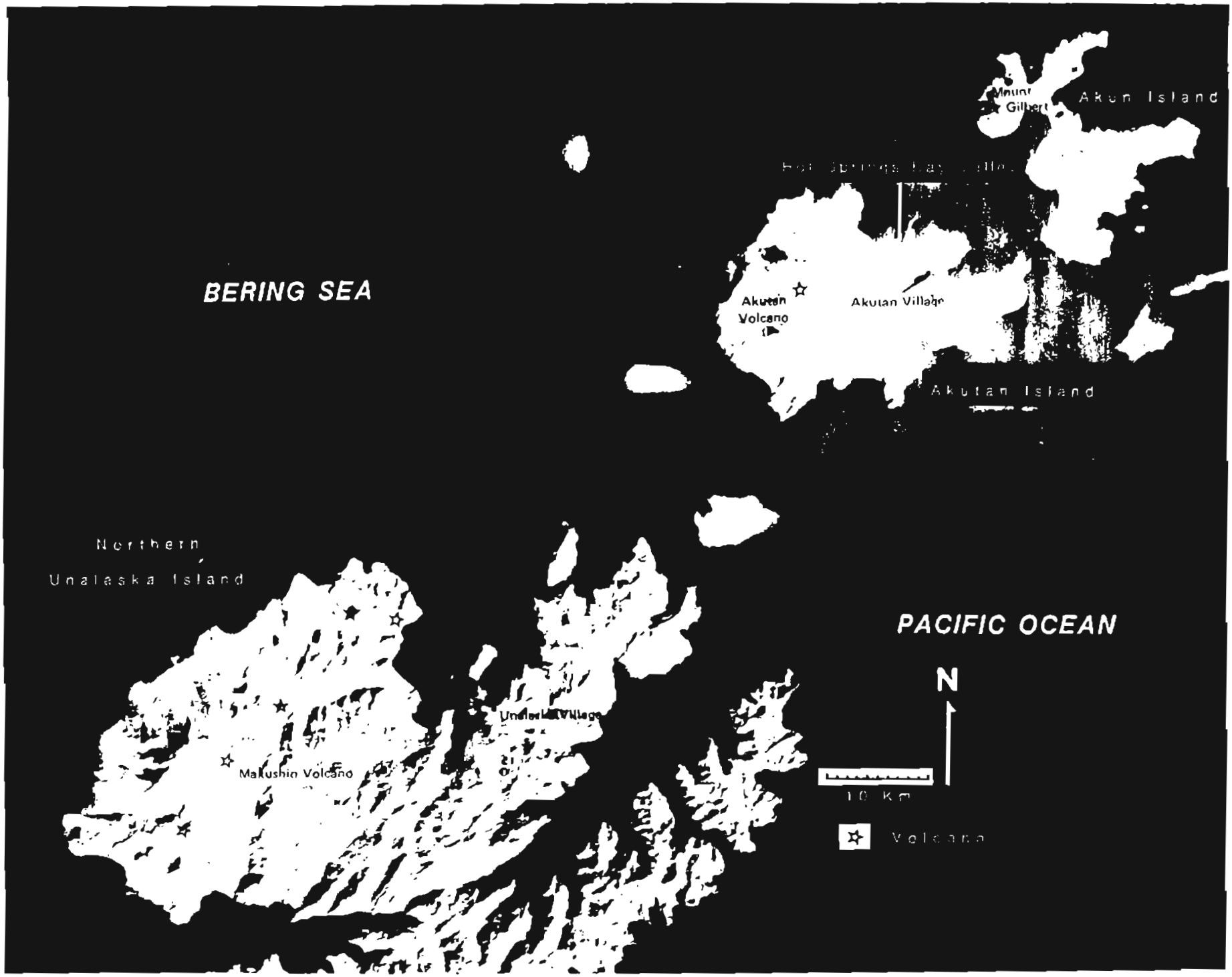
BERING SEA
Akun Island
Akutan Volcano
Akutan Village
Akutan Island
Northern
Unalaska Island
PACIFIC OCEAN
N
Makushin Volcano
10 Km
Volcano

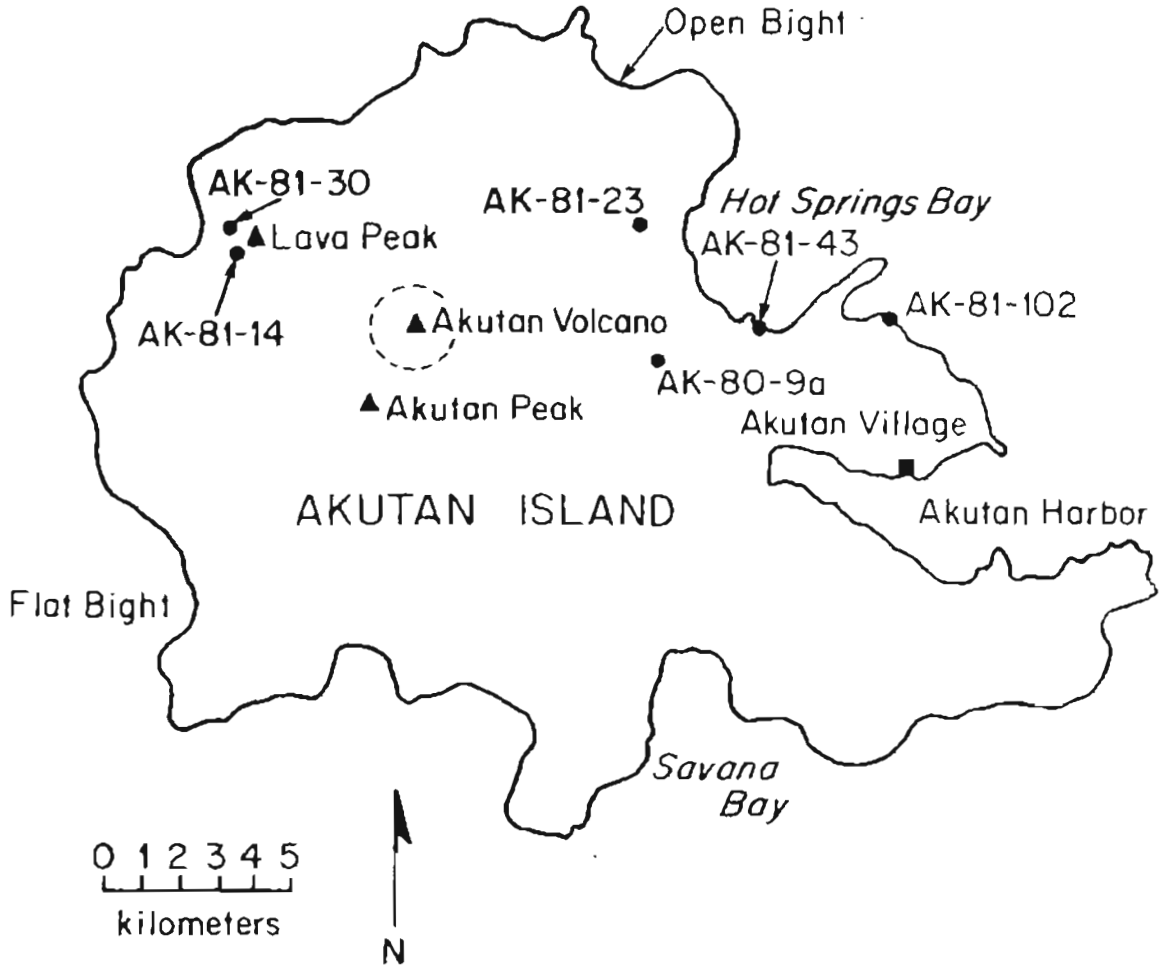
Open Bight
AK-81-30
Lava Peak
AK-81-23
Hot Springs Bay
AK-81-43
AK-81-102
AK-81-14
Akutan Volcano
AK-80-9a
Akutan Peak
Akutan Village
AKUTAN ISLAND
Akutan Harbor
Flat Bight
Savana Bay
0 1 2 3 4 5
kilometers
N

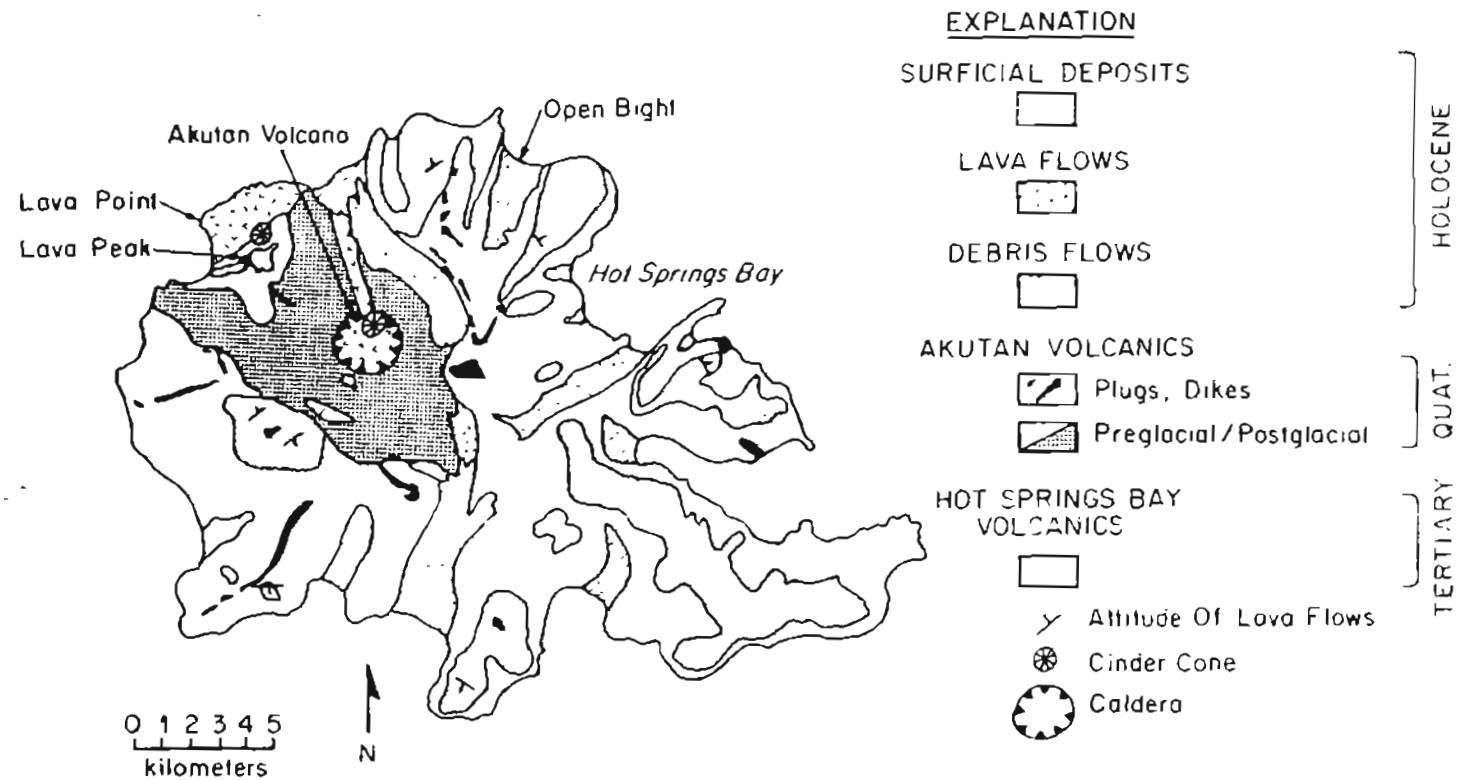
Akutan Volcano
Open Bight
Lava Point
Lava Peak
Hot Springs Bay
0 1 2 3 4 5
kilometers
N
EXPLANATION
SURFICIAL DEPOSITS
LAVA FLOWS
DEBRIS FLOWS
HOLOCENE
AKUTAN VOLCANICS
Plugs, Dikes
Preglacial/Postglacial
QUAT.
HOT SPRINGS BAY VOLCANICS
TERTIARY
Attitude Of Lava Flows
Cinder Cone
Caldera

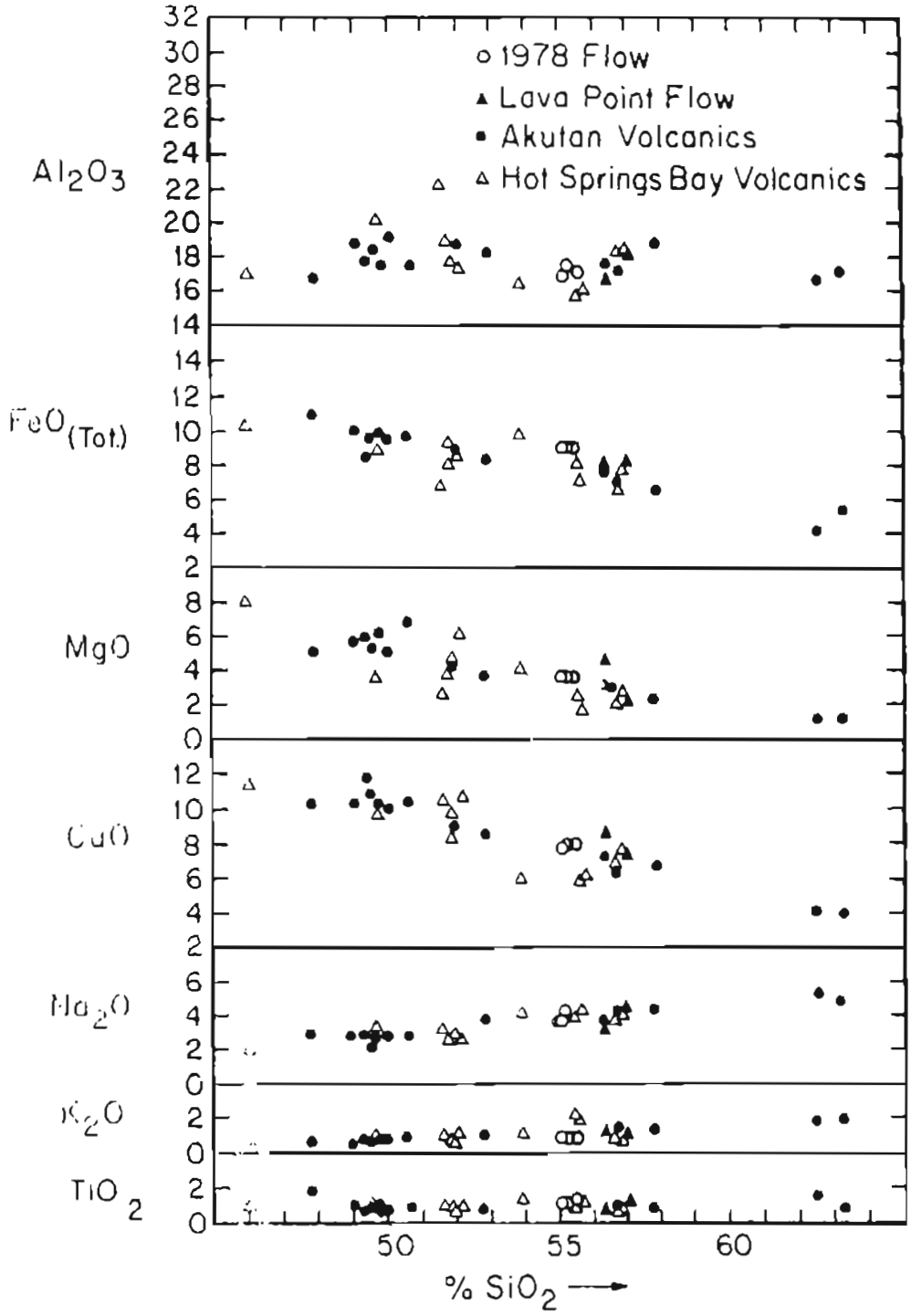
o 1978 Flow
▲ Lava Point Flow
• Akutan Volcanics
△ Hot Springs Bay Volcanics
Al_2O_3
$FeO_{(Tot.)}$
MgO
CaO
Na_2O
K_2O
TiO_2
% SiO_2 ⟶

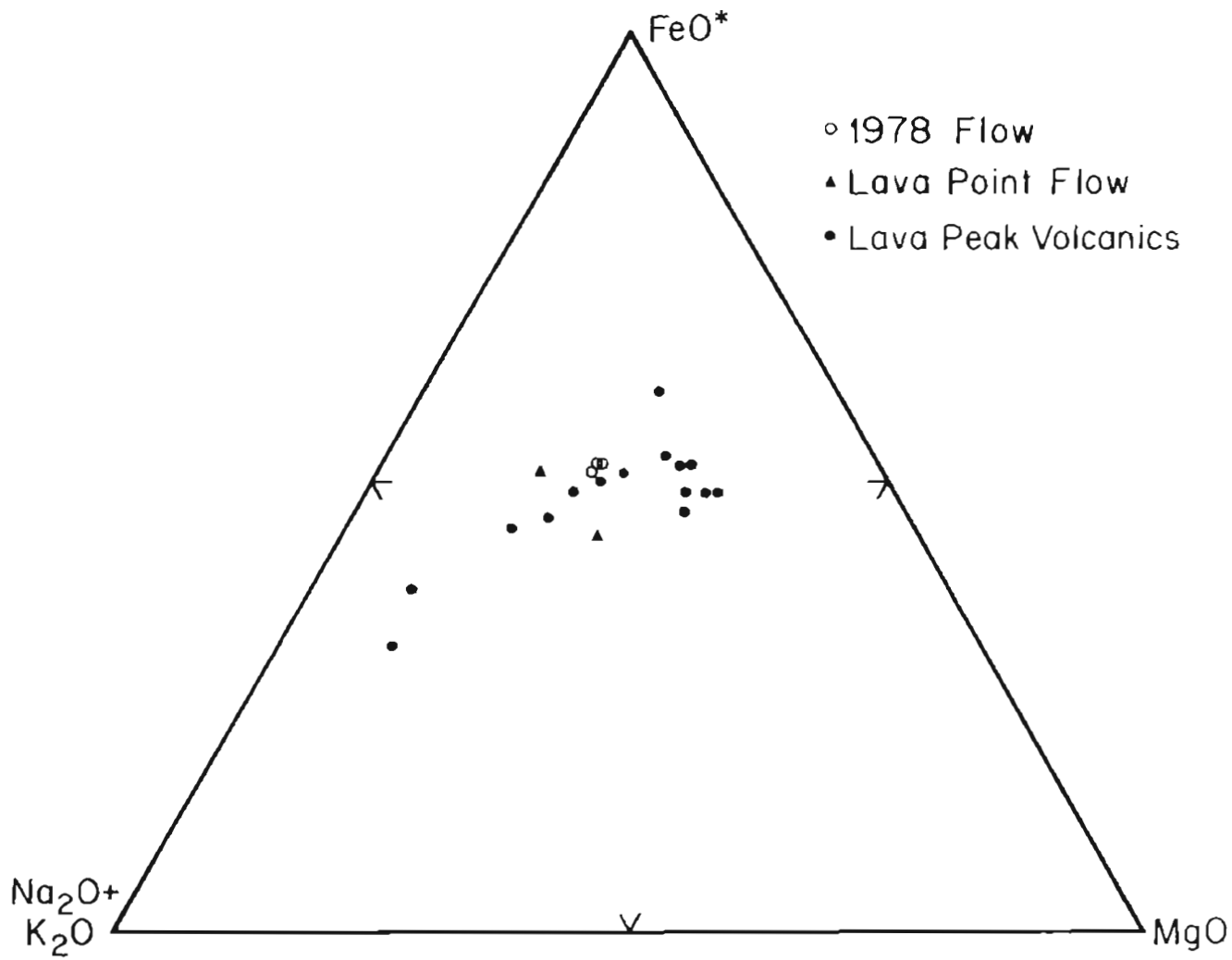
FeO*
1978 Flow
Lava Point Flow
Lava Peak Volcanics
Na2O+
K2O
MgO

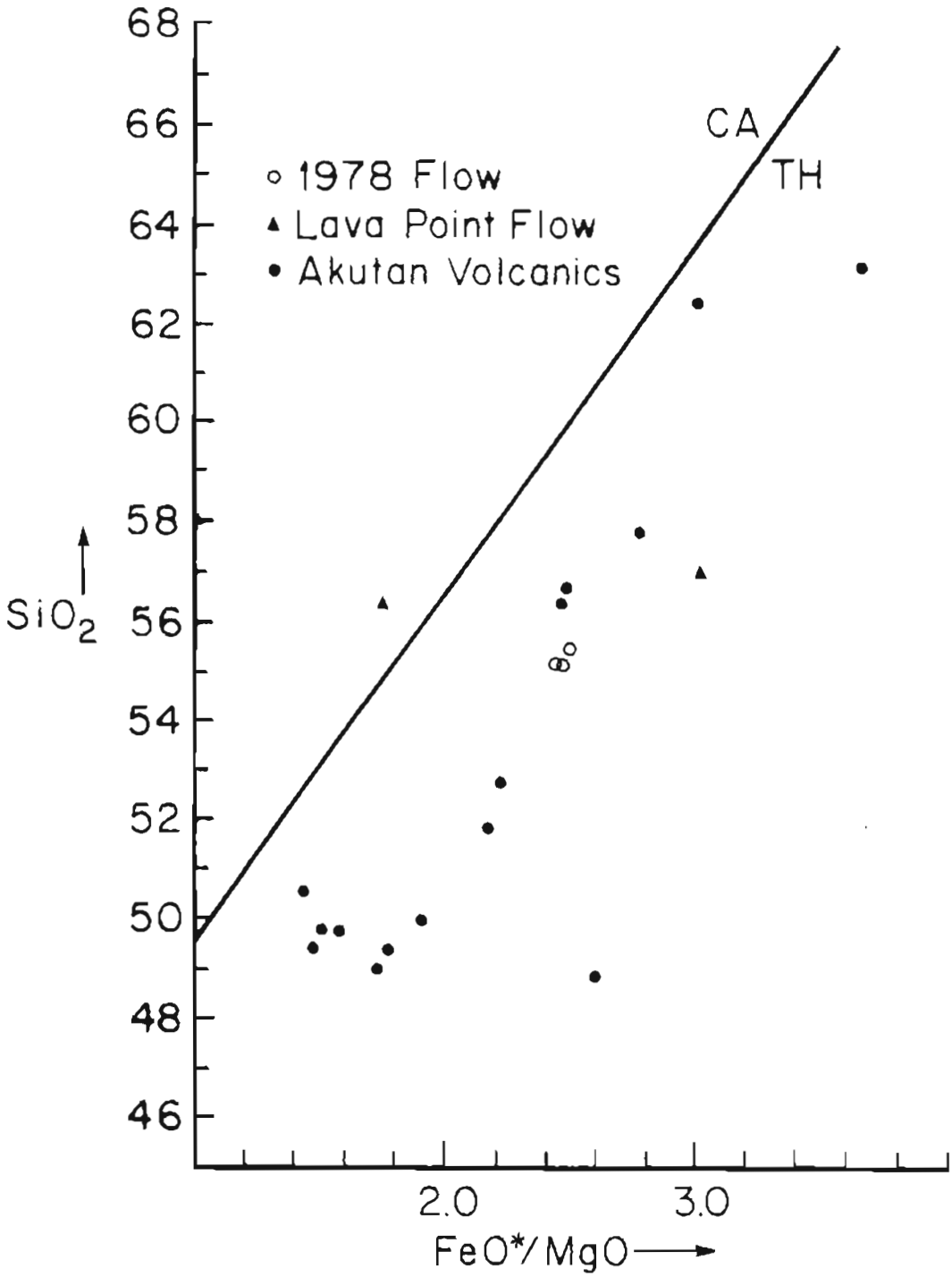
68
66
64
62
60
58
56
54
52
50
48
46
SiO2
CA
TH
1978 Flow
Lava Point Flow
Akutan Volcanics
2.0
3.0
FeO*/MgO

CHAPTER 2

GEOLOGY OF NORTHERN AKUTAN ISLAND

by

Samuel E. Swanson[1] and Jay D. Romick[2]

[1]Geophysical Institute, University of Alaska, Fairbanks, Alaska 99701
[2]Alaska Division of Geological and Geophysical Surveys*, 794 Unviersity Avenue, Basement, Fairbanks, Alaska 99701

*Current address: Department of Geological Sciences
Cornell University
Ithica, N.Y. 14853

INTRODUCTION

Akutan Island is located in the eastern Aleutian chain at 54°05' latitude and 165°55' longitude, about 45 km northeast of Unalaska Island. The island is 29 km long, 21 km wide, and is oriented roughly east-west (fig. 2-1). It is dominated by Akutan Volcano, a 1,300 m high composite volcano. Central and eastern Akutan consists of steep ridges separating glacially scoured valleys which predate the formation of Akutan Volcano. The radial drainage pattern of these valleys suggests an old topographic high in the same area that is now occupied by Akutan Volcano. Western Akutan has gentle topography dissected by streams flowing off the west flanks of the volcano.

The summit of Akutan Volcano is capped by a 2 km diameter caldera. Within the caldera is a cinder cone, which existed prior to 1931 (Finch, 1935), and a small lake. The caldera is breached on the north side. Northwest of Akutan Volcano are two small eruptive centers, an old eroded volcanic center consisting primarily of lava flows (Lava Peak), and a cinder cone (near Lava Point) which developed sometime before 1870 (Byers and Barth, 1953).

Very little geologic information about Akutan Island has been published. Russians visited the island in the 1850's. R.H. Finch conducted the first scientific exploration of the island in 1931, and briefly described the geology and topography of the island (Finch, 1935). Finch noted that Dr. T.A. Jaggar had visited the island in 1907 and 1927 and had made some correlations between the volcaniclastic units on Akutan and those on the Alaska Peninsula, but nothing was published regarding that correlation.

Byers and Barth conducted field work on Akutan Island in 1948 as part of the U.S. Geological Survey study of the Aleutian Islands after World War II,

but no official report was issued. They prepared a geologic map of Akutan Island, which is in the U.S. Geological Survey archives in Menlo Park. Byers and Barth (1953) published some information on Akutan Island in a paper discussing both Akutan and Akun islands, but their major emphasis was on the recent 1947 and 1948 eruptions and not past volcanic activity or geology.

Motyka and others (1981) briefly described Akutan geology in their report on the geothermal resources of the island. Perfit and Gust (1981) published some isotope and microprobe analyses of samples from Akutan Island, and discussed their results relative to other Aleutian Islands. McCulloch and Perfit (1981) published isotope and rare earth element data for Akutan lavas.

Much of the geology and petrology described here is summarized from Romick, 1982. Readers interested in detailed descriptions of the analytical methods used and of the mineralogy and geochemistry of Akutan volcanic rocks are referred to Romick's original work.

GENERAL GEOLOGY

Figure 2-2 is a map of the general geology of Akutan Island modified from Byers and Barth (1948 unpublished map). Akutan Island consists of volcaniclastic debris flows interbedded with subordinate lava flows which are overlain in places by younger volcanic deposits associated with Akutan Volcano. The volcaniclastic material and flows are exposed principally on central and eastern Akutan Island and are here referred to informally as Hot Springs Bay volcanics. They consist primarily of volcaniclastic deposits locally in excess of 700 meters thick (Motyka and others, 1981). The Hot Springs Bay volcanics are slightly to moderately altered to chlorite and carbonate. The volcaniclastic rocks contain numerous dikes, especially near

Hot Springs Bay. Dikes located around Hot Springs Bay Valley strike primarily northwest, while those located to the west of Hot Springs Bay Valley are oriented primarily northeast; however dike orientations span 180 degrees. Small gabbroic bodies intrude the Hot Springs Bay volcanics. The orientation and arrangement of several small curvilinear intrusions exposed south of Open Bight (fig. 2-2) suggest that they may be ring dikes associated with an older caldera system. Bedding attitudes (fig. 2-2) also suggest an older center of volcanic activity near Open Bight (Byers and Barth, unpublished data).

On northwestern Akutan Island a high ridge, here called Lava Peak, is made up of at least 19 flows and 7 dikes. Eleven almost flat-lying flows of the Hot Springs Bay volcanics are unconformably overlain by eight or more flows which dip to the west. East of the peak a baked, autobrecciated zone appears to be the core of an eroded volcanic center.

Dikes intrude the lower eleven flows and are only exposed on the north side of the Lava Peak. A large dike exposed east of Lava Peak also intrudes the lower 11 lava flows, but is truncated by the upper sequence of flows. The dike is the backbone of the ridge to the east of Lava Peak and may have been a feeder dike from Akutan Volcano. There are several flows to the south of Lava Peak which are topographically lower than the Lava Peak rocks and are mantled by recent tephra deposits from Akutan Volcano.

The Hot Springs Bay volcanics are unconformably overlain by a unit, here called the Akutan volcanics, which is dominantly composed of basalt and andesite flows. These flows are generally unaltered and cap ridges between Pleistocene valleys as well as forming the relatively uneroded flanks of Akutan Volcano. These flows are in places overlain by Holocene volcanic deposits.

North of Lava Peak is a cinder cone and lava flow (Lava Point flow) which may have formed in 1852 (Simkin and others, 1981). The cone is approximately 100 m high and 300 m across at the base. The lava flow is about 4 km^2 in area, and forms Lava Point (fig. 2-2).

Recent volcanic deposits include several historic flows, the most recent of which formed in 1978, and pyroclastic deposits. The 1978 lava flow followed two stream drainages down the north flank of the volcano and came to within one kilometer of the coast. Ash eruptions interspersed with these flows have mantled some of the deposits on western Akutan Island, and have occasionally reached Akutan Village on the east side of the island (Finch, 1935; Byers and Barth, 1953). Volcanic activity, documented on Akutan Island since 1790 is listed in table 2-1.

IGNEOUS ROCKS

Hot Springs Bay Volcanics

The oldest rocks exposed on Akutan Island, here informally referred to as the Hot Springs Bay volcanics, underlie most of the island and are exposed on about half the island (fig. 2-2). The base of the section is not exposed, but the unit is, in places, at least 700 m thick. Typical exposures of these rocks are found in the sea cliffs surrounding Hot Springs Bay and most of our data from this unit are taken from these outcrops.

Volcanic Breccia

Volcanic breccia is the dominant lithology, but dikes of porphyritic

basalt and andesite are also found within this unit. Outcrops of the breccia are limited to the sea cliffs; on land, the breccia forms rounded, grass-covered slopes. The dikes are more resistant and often form outcrops on an otherwise grassy hillside.

The volcanic breccia of the Hot Springs Bay unit is a poorly sorted and poorly stratified rock composed of fragments of basalt and andesite. Internal bedding is lacking, but individual layers (flows?) are marked by slight breaks in slope or erosional surfaces. Angular to rounded blocks up to 3 m in diameter are enclosed in a matrix as-fine-as clay-sized. There is no evidence, such as baked contacts or bread crust bombs, to indicate the breccias were hot at the time of emplacement. We interpret these breccias as mudflow deposits. Carbonate and chlorite alteration is pervasive throughout the breccias.

Dikes

Vertical dikes intrude the volcanic breccias. The dikes range in thickness from 0.3 to 10 m, but nesting of dikes-within-dikes locally produces thicknesses up to 13 m. Contact metamorphism of the enclosing breccias by the dikes is limited to a zone of baking 1 - 4 cm wide adjacent to the dikes. Strike of the dikes is generally to the northwest, but the attitudes are quite variable; individual dikes can change strike over 90° in a single outcrop. Flow-banding, defined by mineralogical layering and/or vesicule alignment is common in some of the dikes and is parallel to the margins of the dikes.

Porphyritic basalt is the dominant lithology found in the dikes. Phenocrysts of plagioclase set in a fine-grained matrix of plagioclase, chlorite and carbonate (altered clinopyroxene) is the most common mineralogy.

There are also phenocrysts of olivine, clinopyroxene and, rarely, hornblende in the dikes, but the common alteration of mafic minerals makes recognition of these phases difficult. Phenocrystic and groundmass olivine and augite are often replaced by fine-grained carbonate and/or chlorite. This replacement is so complete in many samples that plagioclase is the only recognizable primary phase. Carbonate-filled amygdules are also common in the dikes. The alteration pattern is similar to that found in the host volcanic breccias and probably represents a single alteration event.

Age

The Hot Springs Bay volcanics are the oldest rocks exposed in the study area. A marked unconformity separates the volcanic breccias and dikes of the Hot Springs Bay volcanics from the overlying Lava Peak flows. Dikes of the Hot Springs Bay volcanics exposed in the sea cliffs between Sandy Cove and Hot Springs Bay are also truncated by an unconformity and overlain by Lava Peak flows.

The Hot Springs Bay volcanics of Akutan Island are similar and may be equivalent to the Unalaska Formation (Drewes and others, 1961) on Unalaska Island. Volcaniclastic sediments with minor lava flows characterize both the Unalaska Formation and the Hot Springs Bay volcanics. Dikes and other intrusives cut both units and Quaternary lavas unconformably overlie both units.

Intrusive Rocks

Three phaneritic intrusive igneous rocks were sampled on Akutan Island.

One of the intrusions is a 150 m wide plug exposed in Sandy Cove. This mass shows columnar jointing and one side of the plug intrudes along a bedding surface in the Hot Springs Bay volcanics in a sill-like fashion. A smaller plug of gabbro, intrusive into the Hot Springs Bay volcanics, is located on the coast about 4 km northwest of Hot Springs Bay Valley. The third sample is a small block of diorite collected from the 1978 tephra deposits near Lava Peak.

The gabbro is an equigranular rock consisting of ophitic plagioclase and clinopyroxene about 2 - 4 mm in diameter. The diorite block from the 1978 tephras is also composed of augite and plagioclase, but has a cumulate texture and a smaller grain size (1 - 2 mm). The Sandy Cove plug is composed of phenocrysts of augite and plagioclase in a holocrystalline groundmass of plagioclase, augite and opaque minerals.

The gabbroic and dioritic rocks from Akutan are similar in texture and mineralogy to some of the mafic phases of plutons on Unalaska Island (Drewes and others, 1961; Perfit and others, 1980). The plug at Sandy Cove is more similar to the dikes in the Akutan volcanics.

A whole-rock K-Ar age determination on the plug in Sandy Cove yields an age of 1.1 ± 0.1 m.y. (table 2-2). This age is identical, within experimental error, to ages of both lava flows and dikes in the Lava Peak volcanics, indicating affiliation with the younger volcanics.

Akutan Volcanics

A series of lava flows, informally referred to as the Akutan volcanics, unconformably overlies the Hot Springs Bay volcanics. Resistant ridge-capping lava flows dominate the Akutan volcanics. Individual flows either rest

directly on other flows or are separated by thin layers of volcanic breccia. The lava flows form steep slopes with good exposure. Dikes are also found within the Akutan volcanics, but are not as abundant as in the Hot Springs Bay volcanics.

Flows

Lava flows of the Akutan volcanics range in thickness from 2 to 31 m. Top and bottom surfaces of the lava flows are often brecciated and the bases of many flows have baked contacts. Flow banding, defined by vesicules and phenocrysts, is found in some of the flows. Columnar jointing, oriented perpendicular to the flow surface, is developed in some lava flows. Within thicker flows, columnar jointing is only developed in the upper portion of the flows.

The Akutan volcanics consist of porphyritic basalt and andesite. Most of the rocks contain over 10 percent phenocrysts set in a holocrystalline groundmass, but at least one lava flow near Akutan Village contains only rare phenocrysts of plagioclase. Plagioclase is the most abundant phenocryst phase and is found in all of the samples examined. Other phenocryst phases, in decreasing order of abundance, include augite, olivine, and hypersthene and opaque minerals set in a groundmass of plagioclase, augite, and opaques. Feldspars in the groundmass are often aligned to form a trachytic texture.

Intrusions

Dikes and small plugs intrude the lava flows of the Akutan volcanics (fig. 2-2). The dikes range in thickness from 0.5 - 15 m and plugs up to 0.5

km in diameter intrude the lava flows. Some thicker dikes in the Lava Point area show columnar jointing with the columns oriented perpendicular to the walls of the dike. Flow banding defined by oriented vesicules and phenocrysts parallels the margins of some dikes.

Porphyritic olivine basalt is the most common lithology found in the dikes, but about 1/3 of the dikes do not contain any olivine. Common phenocryst phases include plagioclase, augite, and olivine set in a matrix of plagioclase, augite, and opaque minerals. Minor quartz, calcite, and chlorite veinlets are found in dikes south of Open Bight.

Dikes and plugs that are believed to be correlative with the intrusions in the Lava Peak volcanics are found in the breccias of the Hot Springs Bay volcanics (fig. 2-2). These intrusions are distinguished from those of the Hot Springs Bay volcanics by a general lack of alteration and a finer grain size.

Byers and Barth (1948) believed the circular outcrop pattern shown by some of these intrustions (cf. southwest of Open Bight) is related to a ring-dike structure. This pattern is most apparent east of Akutan Volcano where series of disconnected dikes form a semi-circular pattern about the present summit caldera (fig. 2-2). Another series of dikes form ridges that radiate from Akutan Volcano to the south, southwest and west (fig. 2-2). The radial dike pattern may also be related to an earlier caldera-forming event.

Alteration

Alteration is uncommon in the western Akutan volcanics, but is more prevalent on the eastern side of Akutan Island. Alteration in the samples from western Akutan is confined to oxidation of some olivine phenocrysts. On

eastern Akutan Island, chlorite and/or carbonate are sometimes found in the groundmass. Some olivine on eastern Akutan is partially replaced by chlorite.

Age

The Akutan volcanics unconformably overlie the Hot Springs Bay volcanics and are dissected by at least one major period of glaciation. Exposures in the sea cliffs southeast of Hot Springs Bay and dikes in the Hot Springs Bay volcanics are truncated by an unconformity which is, in turn, covered by lava flows of the Akutan volcanics. There is little relief on the unconformity and the lava flows above appear to parallel the crude bedding in the underlying breccias.

The lack of widespread alteration and the stratigraphic position suggest that the Akutan volcanics are significantly younger than the Hot Springs Bay volcanics. Radiometric ages measured by the K-Ar method on whole-rock samples from the Akutan volcanics range from 1.1 ± 0.2 to 1.5 ± 0.1 m.y. (table 2-2). Near Lava Peak a lava flow near the base of the section is dated at 1.1 ± 0.1 m.y. A lava flow west of Hot Springs Bay that overlies breccias of the Hot Springs Bay volcanics yields an age of 1.4 ± 0.2 m.y., which is consistent with the results from Lava Peak.

Holocene Volcanics

Lava Point

A cinder cone developed in 1852(?) just northeast of Lava Peak. A lava

flow erupted from the base of the cone, covering about 4 km^2, and makes up what is called Lava Point (Byers and Barth, 1953). The lava flow is very blocky, and has two lobes which flowed into the sea. Erosion has exposed numerous lava tubes on the northern border of the flow which have developed into spectacular bridges and caves along the coastline. The rock is very vesicular, and contains plagioclase phenocrysts, with few mafic minerals, in a glassy groundmass. The groundmass contains flow-aligned plagioclase laths, some opaque minerals, and a great deal of brown glass.

Akutan

In 1978 a lava flow erupted in the summit caldera, flowed down the north flank of Akutan Volcano in two lobes, and came within 1 km of the coast. The flow consists of very blocky (aa) lava ranging from vesicular to very glassy in texture. In hand specimen, the rocks are aphanitic with occasional plagioclase phenocrysts. In thin section, plagioclase makes up about 32 percent of the rock, while clinopyroxene, olivine, and opaque minerals make up less than 7 percent. The groundmass has a tachytic texture and consists of plagioclase laths and brown glass.

There have been several other historic lava flows from Akutan (table 2-1) and the relatively uneroded shape of most of the volcano indicates that a large portion of the modern edifice is Holocene.

GEOMORPHOLOGY AND SURFICIAL DEPOSITS

Glacial Landforms

Glacial landforms are very prominent on the higher slopes of the central part of Akutan Island. There are U-shaped valleys, cirques and aretes of various sizes. The bottoms of major valleys formed by glacial action have been modified by stream erosion and the deposition of postglacial volcanic debris flows. Stream erosion in the upper reaches of the glaciated valleys has produced incised, V-shaped stream channels over 150 m in depth. Lower portions of the major valleys are filled with volcaniclastic debris.

Only one small glacier exists on Akutan. This glacier covers about 1 km^2 between 1,100 m (3,600 ft) and 825 m (2,700 ft) elevation on a pinnacle on the rim of the caldera.

There are several well-defined cirques on Akutan Island. Major valleys, such as those behind Open Bight or Hot Springs Bay Valley, are headed by cirques. Smaller valleys, such as the one behind Sandy Cove, are also headed by small cirques. Cirques on Akutan island are confined to elevations higher than 365 m (1,200 ft), similar to those on Unalaska Island (Drewes and others, 1961), indicating a snowline of 365 m (1,200 ft) at the time of glaciation.

Glacial till was not identified during the course of the present study. However, Byers and Barth (1948) identified a small moraine associated with the glacier on Akutan Peak. The extensive deposits of recent tephra and volcaniclastic debris that fill most of the valleys would conceal any till that might be present. Morphology of the major valleys suggests the valley glaciers must have terminated offshore from the present coastline and thus terminal moraines for these glaciers are not found.

Stream Erosion and Deposits

Postglacial stream erosion has produced V-shaped canyons up to 150 m in

depth on the rugged upper slopes of Akutan Island. Stream channels choked with large boulders completely cover the canyon bottoms. Terrace remnants of outwash gravels are found along the stream channels where the stream gradient rapidly decreases. In the lower portion of the major valleys, streams meander in response to a gentle gradient and expose volcaniclastic valley-fill debris in the stream banks (Swanson and others, this report).

Marine Deposits

Beach deposits ranging from boulders to sand are common around Akutan Island. Steep cliffs immediately adjacent to the shoreline promote boulder beaches that are only exposed at low tide. Further removed from the cliffs, beach deposits range from cobbles to sand. Bars and spits are found across the mouths of some bays (for example, Hot Springs Bay and Open Bight) thus isolating lagoons or lakes from the sea.

Eolian Deposits

Dunes have formed behind some of the sand beaches, such as at Hot Springs Bay. The presence of dunes is controlled by the availability of sand. Dunes reach a height of 10 m and are stabilized by a lush growth of grasses.

Volcaniclastic Deposits

Layers of volcanic ash and lapilli with occasional bombs are widespread on the Western half of Akutan Island. Thickness of the deposits is quite variable and ranges from 0 on steep slopes to over 30 m in some valley bot-

toms. Thick accumulations of volcaniclastic debris in valleys are probably material from adjacent slopes that was remobilized by fluid mudflows. Bedding is crudely developed within these deposits, but local channeling does betray fluvial reworking of the deposits. Older, but postglacial, volcaniclastic deposits with some cementation are found in Hot Springs Bay Valley (Swanson and others, this report).

GEOCHEMISTRY

Major oxide analyses for over 30 samples of Akutan lava flows, dikes and plugs are available (Romick, 1982). Figure 2-3 shows a silica variation diagram of the major oxides for samples from the Hot Springs Bay and Lava Peak volcanics plus the historic lava flows on Akutan. Silica ranges from 49 to 63 weight percent on Akutan. Samples of lava flows and intrusions from the Akutan volcanics show a well-defined fractionation trend that includes the historic lavas on Akutan. FeO* (FeO + 0.899 Fe_2O_3), Mg, and Ca decrease with increasing Si, while Na and K increase. Aluminum decreases slightly with increasing fractionation and Ti remains unchanged over the observed range of Si contents. The Hot Springs Bay volcanics show a similar pattern of chemical variation, but the scatter is much greater than the Akutan trend (fig. 2-3). The variable alteration to calcite, chlorite and clays of the Hot Springs Bay volcanics results in scatter in the Al, Fe, Mg, and Ca contents of these rocks. Further discussions of the mineralogy and petrology will not deal with the Hot Springs Bay volcanics because the rocks are extensively altered making recognition of primary mineralogic and geochemical trends difficult, and because these rocks are old and are thus unrelated to the current magmatic/geothermal system.

Akutan volcanic rocks have been characterized as tholeiitic (Perfit and Gust, 1981; McCulloch and Perfit, 1981; Kay and others, 1982). Rather weak Fe-enrichment is found in the Akutan volcanic rocks (fig. 2-4). The increase in FeO^* (total Fe)/MgO ratios with increasing SiO_2 (fig. 2-5) is similar to the tholeiitic trend described by Kay and others (1982) for other Aleutian volcanoes.

Patterns of chemical variation (figs. 2-3, 2-4, and 2-5) permit the interpretation that the Lava Peak volcanics and the recent lava flows at Lava Point and from Akutan Volcano are comagmatic. The relatively smooth curvilinear patterns of variation are typical of the trends produced by fractionation in crystal-liquid systems. This relatively simple pattern of chemical variation is consistent with the apparently simple volcanic plumbing system of one central vent (Akutan Volcano) and one satellite vent (Lava Point).

INTERPRETATION

The rather simple pattern of chemical variation (fig. 2-3 and 2-4) can be explained by the extraction of phases rich in Ca, Fe, and Mg, resulting in a decrease in these components with increasing Si. The removal of the commonly observed phenocryst assemblage plagioclase + olivine + augite could produce this pattern of variation in the Akutan lavas. Hypersthene replaces olivine in the phenocryst assemblage in bulk compositions with more than 52 weight percent SiO_2. This change in phenocryst mineralogy does not change the overall pattern of fractionation (decreasing Ca, Fe, Mg; increasing Si), but it may explain a discontinuity in the pattern of MgO variation at about 52 weight percent SiO_2 (fig. 2-3).

Phase equilibria studies in a haplobasalt system ($CaAl_2Si_2O_8$ - $CaMgSi_2O_6$ - Mg_2SiO_4 - SiO_2) have revealed a crystallization sequence similar to that found in the volcanic rocks of Akutan (Presnall and others, 1978). Low pressure, one atmosphere, experimental studies show that bulk compositions low in Si will initially crystallize some combination of plagioclase, olivine and augite (clinopyroxene). Increasing fractionation in the experimental systems results in a reaction of olivine (in the presence of plagioclase and augite) with the silicate liquid to produce hypersthene (orthopyroxene).

Compositional and textural data from the phenocrysts are consistent with low pressure fractionation. The phenocrysts show a very restricted range of compositions, especially in comparison to other andesitic systems (Gill, 1978). Such a restricted compositional range argues for a simple, near-surface crystallization history. Zones of glass inclusions within Akutan plagioclase were formed as a result of the fast growth of plagioclase at a somewhat undercooled temperature. Such dramatic temperature fluctuations within a crystallizing magma chamber also indicate a near-surface environment.

Shallow-level fractionation of the Akutan lavas suggests the existence of a shallow-level magma chamber under Akutan Volcano. Partial draining of such a magma chamber could explain the small caldera on Akutan Volcano as well as the compositional and mineralogic trends within the lavas. High heat flow associated with a shallow magma may produce the thermal anomalies on Akutan that are removed from the active volcanic vents.

REFERENCES CITED

Byers, F.M., Jr., and Barth, T.F.W., 1948, Geology of Akutan Island, unpublished geologic map and field notes: U.S. Geological Survey Archives, Menlo Park, California.

Byers, F.M., Jr., and Barth, T.F.W., 1953, Volcanic Activity on Akun and Akutan Island: Proceedings, 5th Pacific Science Conference, 1949, New Zealand, v. 2, p. 382-397.

Drewes, H., Fraser, G.F., Snyder, G.L., and Barnett, H.F. Jr., 1961, Geology of Unalaska Island and adjacent insular shelf, Aleutian Islands, Alaska: U.S. Geological Survey Bulletin, v. 1028-S, p. 583-676.

Finch, R., 1935, Akutan Volcano: Zeitschrift fur Vulkanologie, Bd. XVI, p. 155-160.

Kay, S.M., Kay, R.W., and Citron, G.P., 1982, Tectonic controls on tholeiitic and calc-alkaline magmatism in the Aleutian arc: Journal of Geophysical Resources, v. 87, p. 4051-4072.

McCulloch, M., and Perfit, M., 1981, $^{143}Nd/^{144}Nd$, $^{87}Sr/^{86}Sr$ and trace element constraints on the petrogenesis of the Aleutian island arc magmas, Earth Planetary Science Letters, v. 56, p. 167-179.

Miyashiro, A., 1974, Volcanic rock series in island arcs and active continental margins: American Journal of Science, v. 247, p. 321-355.

Motyka, R.J., Moorman, M.A., and Liss, S.A., 1981, Assessment of thermal spring sites Aleutian Arc, Atka Island to Becherof Lake - preliminary results and evaluation: Alaska Division of Geological and Geophysical Surveys Open-file Report 144, 173 p.

Perfit, M.R., Brueckner, H., Lawrence, J.R., and Kay, R.W., 1980, Trace element and isotopic variations in a zoned pluton and associated rocks, Unalaska Island, Alaska: A model for fractionation in the Aleutian calc-alkaline suite: Contributions to Mineralogy and Petrology, v. 73, p. 69-87.

Perfit, M.R., Gust, D.A., 1981, Petrochemistry and experimental crystallization of basalts from the Aleutian Islands, Alaska: (abs), 1981 IAVCEI Symposium, Arc Volcanism, Tokyo and Hokane, Japan, p. 288-289.

Presnall, D.C., Dixon, S.A., Dixon, J.R., O'Donnell, T.H., Brenner, N.L., Schrock, R.L., and Dycus, D.W., 1978, Liquidus phase relations on the join diopside-forsterite-anorthite from 1 atm to 20 kbar: Their bearing on the generation and crystallization of basaltic magma: Contributions to Minerology and Petrology, v. 66, p. 203-220.

Romick, J.D., 1982, The igneous petrology and geochemistry of northern Akutan Island, Alaska: Master's thesis, University of Alaska, Fairbanks, 151 p.

Simkin, T., Siebert, L., McCelland, L., Bridge, D., Newhall, C., and Latter, J., 1981, Volcanoes of the World: The Smithsonian Institution, Hutchinson Ross Publishing Co., Stroudsburg, Pennsylvania, 232 p.

Table 2-1: Volcanic activity on Akutan Island since 1790.

Date	Type of Eruption	Location
1790	Smoking	
1828	Smoking	
1838	Smoking	
1845	Smoking	
March 1848	Small explosive eruption	
1852	Parasitic cone eruption	NW of Summit
1862	Smoking	
1865	Glow seen from Unimak Pass	
1867	?	
1883	Small steam and ash eruption	
1887	Lava flow	
1892	?	
1896	Glowing	
1907	Continuously active	
Feb. 22, 1908	Lava flow	
1911	Ash fell on Akutan Village	
1912	Smoking	
1928	Smoke and "flaming"	
May 1929	Explosive eruption and lava flow	
1931	Explosive eruption	
1946-47	Lava flow and explosive eruption	
1948	Explosive eruption	
Oct. 1951	Explosive eruption	
1953	?	

1972	Explosive eruption	
1974	Parsitic cone, ash eruption and lava flow	West flank?
1976-77	Explosive eruptions	
Sep. 25, 1978	Lava flow and ash eruptions	
1980	Explosive eruption	

Sources: Finch (1935), Byers and Barth (1953), and Simkin and others (1981).

Table 2-2. K-Ar Ages for Akutan Lavas

Sample No.	Material Dated	Map Unit	% K wt %	rAr^{40} mole/g	% rAr^{40}	Age_6 ($\times 10^6$ yrs)
AK-81-14*	lava flow	Akutan volcanics	0.691	0.0133	8.5	1.1 ± 0.2
	whole rock					
AK-81-30*	dike	Hot Springs Bay volcanics	0.648	0.0175	23.8	1.5 ± 0.1
	whole rock					
AK-81-23*	lava flow	" " "	1.23	0.0305	10.0	1.4 ± 0.2
	whole rock					
AK-80-9a*	lava flow	" " "	0.806	0.0159	13.6	1.1 ± 0.1
	whole rock					
AK-81-102*	plug	" " "	0.731	0.0141	7.4	1.1 ± 0.1
	whole rock					

*Sample location is shown on figure 2-1. $\lambda_e + \lambda_{e'} = 0.581 \times 10^{-11}\ yr^{-1}$; $\lambda_B = 4.962 \times 10^{-10} yr^{-1}$; $^{40}K/K_{total} = 1.167 \times 10^{-4}$ mol/mol; R.L. Armstrong, University of British Columbia, analyst.

Figure Captions

Figure 2-1. Map of Akutan Island showing location of radiometrically dated samples (Table 1).

Figure 2-2. Generalized geology of Akutan Island modified from Byers and Barth (1948).

Figure 2-3. Harker variation diagram for Akutan volcanic rocks.

Figure 2-4. AFM diagram for Akutan volcanic rocks.

Figure 2-5. FeO*/MgO vs. SiO_2 diagram for Akutan volcanic rocks. (FeO* = FeO + 0.899 Fe_2O_3). Calc-alkaline (CA)/tholeiitic(TH) dividing line is after Miyashiro (1974).

CHAPTER 3

GEOLOGY OF HOT SPRINGS BAY VALLEY

AKUTAN ISLAND, ALASKA

by

Samuel E. Swanson,[1] Donald L. Turner,[1] Jay D. Romick,[2*]

and Roman J. Motyka[2]

[1]Geophysical Institute, University of Alaska, Fairbanks, Alaska 99701
[2]Alaska Division of Geological and Geophysical Surveys*, 794 Unviersity Avenue, Basement, Fairbanks, Alaska 99701

*Current address: Department of Geological Sciences
Cornell University
Ithica, N.Y. 14853

INTRODUCTION

Hot Springs Bay Valley is located on the eastern side of Akutan Island in the eastern Aleutian Islands. The valley is about 4.2 km long and 0.9 km wide and trends approximately NE. Steep valley walls rise almost 500 m above a flat valley floor (pl. 1). Hot Springs Creek meanders over the gently sloping floor of Hot Springs Bay Valley and drains into the sea at Hot Springs Bay. Helicopter and Zodiac raft-supported geologic mapping of Hot Springs Bay Valley has produced a 1:20,000 scale geologic map (pl. 1). The valley walls are composed of volcanic breccia with minor intercalated lava flows. Lava flows are more abundant on the higher slopes. Dikes 15 cm to 2 m thick intrude the layered sequence in the valley walls. Two small gabbroic bodies intrude the flows, along the coast north and south of Hot Springs Bay Valley (pl. 1). Outcrops of valley fill consists of volcanic debris flows, dune sands and contemporary beach deposits.

VALLEY WALLS

Preglacial Debris Flows

Much of the lower valley walls adjacent to Hot Springs Bay Valley are composed of volcanic debris flow deposits of the informally named Hot Springs Bay volcanics (Swanson and Romick, this report). Individual flows lack internal stratification. Bedding attitudes can, however, be determined from occasional layers of pyroclastic material or lava flows. The deposits are unsorted and comprised of angular blocks up to 1 m in diameter in a sand-size matrix. Petrologically, the flows are best termed volcanic breccia.

Different textural varieties of basalt and basaltic-andesite comprise the blocks in the debris flows. Blocks within the debris flows do not show any evidence, such as oxidized rims or radial fractures, that the flows were hot at the time of emplacement. These flows probably represent remobilized debris from the upper slopes of Akutan volcano.

Basalt and Basaltic-Andesite Lava Flows

Lava flows are more abundant on the higher elevations surrounding Hot Springs Bay Valley (pl. 1). The lava flows tend to be more resistant to erosion than the breccias and therefore form caps on ridges. Flows range in thickness from 3.5 to 10 m and some show crudely developed columnar jointing perpendicular to the base. Lava flows dip at shallow (3 - 5°) angles toward the sea.

Phenocrysts of augite, plagioclase and minor olivine in a moderately altered matrix characterize the lava flows in the lower walls of the valley. The groundmass is holocrystalline and plagioclase microlites sometimes define a flow banding, resulting in a trachytic texture. Olivine phenocrysts are partially altered to iddingsite and the augite and the groundmass is often altered to a mixture of carbonate and chlorite. Often, the groundmass plagioclase is unaltered.

Higher in the section the lava flows are less altered and do not contain olivine. Flows that cap the ridge immediately north of the valley (pl. 1) have a very fine-grained matrix and contain about 15% phenocrysts. Plagioclase is the dominant phenocryst phase, followed by augite and hypersthene which also form phenocrysts. Opaque minerals are unusually abundant in these

lavas and constitute about 2 percent of the rocks. Except for rare carbonate amygdules these lavas show no sign of alteration.

The upper flows unconformably overlie the Hot Spring Bay volcanics and are informally referred to as the Akutan volcanics (Swanson and Romick, this report).

Dikes and Other Intrusions

Numerous dikes are exposed in the sea cliffs and hillsides around Hot Springs Bay Valley (pl. 1). The dikes intrude the near-horizontal lava and breccia flows and are often well-exposed because they are more resistant to erosion than the volcanic breccias. Dikes are more abundant in the lower portion of the stratigraphic section. At least one dike exposed in the walls of Hot Springs Bay Valley is truncated against the bottom surface of a lava flow, indicating the lava flows in the upper part of the section post-date at least some of the dikes.

Orientation of the dikes varies considerably, but they generally trend northwesterly to westerly around Hot Springs Bay Valley. Dips of the dikes are variable, but typically at a high angle. Dike thickness ranges from 0.4 - 5.0 meters. Nesting of dikes within dikes has been noted in some localities resulting in an aggregate thickness of up to 13 meters.

Dike rocks are typically fine-grained to aphanitic with occasional phenocrysts of plagioclase and, more rarely, augite, olivine or hornblende. The matrix is sometimes trachytic and usually a holocrystalline mixture of plagioclase, augite and opaque minerals, but glass was noted in the groundmass of some dike samples. Mineral banding exists in some dikes; augite and

olivine are concentrated toward the dike interiors and plagioclase is concentrated near the margins. The banding may be the result of flow differentation during dike emplacement.

Dike alteration in the vicinity of Hot Springs Bay Valley is variable, but generally more pervasive than elsewhere on Akutan Island. Commonly pyroxene and olivine (when present) are at least partially altered to an assemblage of chlorite plus carbonate. Degree of alteration varies greatly both across the width of individual dikes and between adjacent dikes only a few meters apart.

A small plug of augite gabbro is exposed in the sea cliff north of Hot Springs Bay Valley (pl. 1). The rock is fine grained, ophitic, and appears to be a hypabyssal equivalent of many of the dikes.

SURFICIAL DEPOSITS

Sand Dunes

Two parallel sand dunes derived principally from beach deposits are present near the mouth of Hot Springs Bay Valley (pl. 1). A dune about 7 m high is located behind the present beach. This dune is partially overgrown by grass, especially on the landward side, and is still active. A second, older, dune is located about 300 m up-valley from the beach dune and is about 130 m wide and 12 m high. The older dune is completely overgrown with grass. Studies of sea level changes in the Aleutian Islands (R.F. Black, personal commun., 1982; Black, 1982) suggest that the older dune was formed during a period of a 2 - 3 m higher-than-present sea level stand that occurred between 10,000 and 3,000 yr ago. Most of the Hot Springs Bay Valley fill must have

been in place of the time of sea level rise in order to form a platform for construction of the older sand dune. The active coastal dune began forming since 3,000 yr ago as sea level slowly dropped to its present level. Both dunes are cut by Hot Springs Creek.

Postglacial Volcanic Debris Flows

Our geologic mapping shows that the present valley floor is completely covered by a volcanic debris flow of unknown thickness. Similar volcanic debris flows are exposed in several valleys on the western part of the island (Swanson and Romick, this report). These deposits are believed to have formed when water saturated pyroclastic debris from the upper flanks of Akutan Volcano flowed down into the valleys that drain the volcano.

Two stream bank outcrops of debris flow deposits were found on the northwest side of Hot Springs Bay valley, one between springs C and D, (table 3-1) and one up-valley from there. Several shallow auger holes near the center of the valley also encountered the same unit. The unit is highly indurated and gray where fresh and brown where weathered. The matrix is clay-rich and encloses abundant dark-grey to black scoria ranging in size from 1.5 mm to 5 cm.

Numerous holes drilled for the helium soil gas survey in the western part of the valley encountered hard drilling and brought up cuttings of basaltic scoria in a gray, clay-rich matrix, indicating the presence of this unit. Two 2 m-deep seismic shot holes located 500 and 845 m up valley from the older dune also encountered hard drilling and brought up similar cuttings. Both shots blew out large fragments of the massive debris flow unit. These ranged up to 0.7 m across in the southernmost shot hole. The fragments were fresh,

indurated, gray in color and contained abundant dark-gray-to-black basaltic scoria in a clay-rich matrix. Where seen in the shot holes, the unit is megascopically indistinguishable from the unit in the cutbank outcrops described previously.

In order to determine whether or not this volcanic debris flow flowed over the older dune near the mouth of the valley (pl. 1), six 1.2 m deep holes were drilled along a traverse across the dune, spaced about 1 - 2 m apart in elevation. Cuttings and hard drilling indicative of the debris flow were present along the back side of the dune to within about 1.7 m of the top of the dune. Two additional holes were drilled at the seaward edge of the dune and at about 10 m farther seaward. Both holes produced cuttings indicative of the presence of the volcanic debris flow.

This evidence suggests that the debris flow overrode the ancient dune and that the still-fluid deposits then slumped off the top of the dune. An alternate possibility is that the lahar surged through a stream-cut channel in the dune and then flooded the area seaward of the dune. The presence of the deposit seaward of the ancient dune indicates the flow post-dates the sea-level recession of 2,000 - 3,000 yr ago. Valley-dune topography constrains the thickness at the distal end of this debris flow to <3 m.

About 0.3 kilometers up the E-W tributary valley at the head of the main valley (pl. 1), a volcanic debris flow deposit at least 3.6 m thick, is exposed (table 3-2). The deposit is light brown in color, extremely well-bedded, poorly consolidated, and is composed of lapilli and clasts, up to 46 cm in diameter. The absence of draping of beds over large clasts and the lack of depression of underlying beds by these clasts indicate that this is not an air-fall deposit. The following evidence argues against this being a stream-laid deposit:

1. All clasts and matrix grains are sharply angular.
2. There is no cross-bedding or cut-and-fill structure in the entire 4 x 30 m exposure.
3. Bedding is continuous around the large clasts with no evidence of back eddy turbulence.
4. The deposit is very poorly sorted.

The continuous nature of the bedding suggests laminar flow of a wet, mass of dominantly sand-size material containing a few larger clasts. This unit is interpreted as representing a proximal facies of the valley-filling lahar described previously. It appears that this debris flow came down the E-W tributary valley from the flanks of Akutan Volcano and completely covered the floor of Hot Springs Bay Valley, probably flowing over previous debris flow deposits and valley fill alluvium which were deposited prior to the formation of the ancient dune discussed above.

J.W. Reeder (personal commun., 1985) reported finding a similar section in the same vicinity consisting of soil overlain by pyroclastics which in turn are overlain by the volcanic debris flow. Reeder (1983) obtained C-14 dates on the underlying soil layer and on soil layers underlying similar pyroclastics at two other locations on Akutan Island. The three determinations yielded an average age of 5,200 ± 200 rybp. Thus the volcanic debris flow covering Hot Springs Bay Valley is younger than 5,200 rybp, which is consistent with the coastal debris-flow and sea-level change relationships discussed previously.

Beach Deposits

Material on the beaches ranges in size from sand through boulders. On the geologic map (pl. 1) sand and gravel beaches have been mapped separately while boulder beaches have not been distinguished. Sand and gravel beaches typically form an apron leading to dunes behind the beach, thus leaving some of the sand from the beach-dune system exposed, even at high tide. Boulder beaches consist of blocks of volcanic rock derived from the sea cliffs located immediately behind the beach. The boulder beaches are small and typically are only exposed at low tide.

GEOMORPHOLOGY

Recent studies of representative islands in the Aleutians have shown that ice caps covered all major islands in the late Wiconsinan Stage and extended considerable distances over the now submerged Aleutian platform (Gard, 1980; Black, 1981; Black, 1983). Thus, glacier erosion is largely responsible for the serrated ridges radiating from Akutan summit and for the large U-shaped valleys draining the interior of Akutan Island. Retreat of the Wisconsinan ice sheet in the Aleutian Islands is thought to have occurred about 10,000 to 12,000 yr ago, indicating a fairly young age for Hot Springs Bay Valley. The V-shaped lower parts of the western tributary valleys to Hot Springs Bay Valley are apparently due to postglacial downcutting by streams. The present valley floors were formed in part by in-filling of volcanoclastic, glacial-fluvial, and alluvial deposits.

GEOLOGIC HISTORY

The earliest geologic event in the development of Hot Springs Bay Valley was the deposition of the thick sequence of volcanic breccias. These deposits were probably formed by volcanic debris flows from an ancestral Akutan Volcano. The debris flows were cool mudflows that formed from melted snow or rain that remobilized volcanic debris on the upper slopes of the volcano. These earliest deposits could not be dated directly.

A series of near-vertical dikes of basaltic andesite was intruded into the sequence and breccias. The strike of the dikes toward the present summit of Akutan Volcano suggest dike intrusion may be related to some event at the summit, such as caldera formation. Byers and Barth (1953) suggested such a relation in their 1948 reconnaissance of Akutan Island. Small plugs that intrude the lava flows and breccias are probably related to this period of dike emplacement.

An extensive period of erosion followed the dike intrusion in the lower portions of the section. A relatively flat erosion surface was produced resulting in truncation of some dikes in the lower section. Extrusion of a series of early Pleistocene basalt and basaltic-andesite lava flows marked the end of the erosional period.

Wisconsinan glaciation was widespread on Akutan Island. The glaciers heavily dissected the older series of breccias, lavas, and dikes. The glacier that carved Hot Springs Bay Valley probably overflowed the low divide that separates this valley from Akutan Harbor and flowed down that valley as well. Glaciers terminated seaward of the present beach line.

Following retreat of the Wisconsinan glaciers about 10,000 to 12,000 yr ago (Black, 1975), glacial-fluvial deposits, alluvium, and cinder-laden lahars

from the upper slopes of Akutan Volcano began to fill Hot Springs Bay Valley. A general rise in sea level of 3 m resulted in sand dune formation in the lower section of the valley sometime between 10,000 and 3,000 yr ago (Black, 1982, personal commun., 1982). Extensive postglacial valley-filling pyroclastic deposits and debris flows were emplaced in several valleys draining Akutan Volcano and may be related to the formation of Akutan Caldera. Carbon-14 dates obtained by Reeder (1983) shows these deposits are younger than 5,200 rybp. The volcanic debris flow that flowed down Hot Springs Bay Valley was emplaced sometime after sea-level recession began 3,000 yr ago.

REFERENCES CITED

Black, R.F., 1975, Late-Quaternary geomorphic processes: Effects on the ancient Aleuts of Umnaks Island in the Aleutians: Arctic, v. 28, no. 3, p. 159-169.

Black, R.F., 1982, Holocene sea-level changes in the Aleutian Islands: New Data form Atka Island: In Holocene sea level fluctuations, magnitude and causes: D.J. Colquhoun, Organizer, IGCP #61, p. 1-12.

Black, R.F., 1983, Glacial chronology of the Aleutian Islands: In "Glaciation in Alaska": Alaskan Quaternary Center, University of Alaska Museum Occasional Paper No. 2, p. 5-10.

Byers, F.M., Jr., and Barth, T.F.W., 1953, Volcanic activity on Akun and Akutan Island: Pacific Science Congress, 7th, New Zealand, 1949, Proceedings, v. 2. p. 382-397.

Gard, L.M., Jr., 1980, The Pleistocene geology of Amchitka Island, Aleutian Island, Alaska: U.S. Geological Survey Bulletin 1478, 38 p.

Reeder, J.W., 1983, Preliminary dating of the caldera forming Holocene volcanic events for the eastern Aleutian Islands: Abstract, 96th Annual Meeting, Geological Society of America, v. 15, p. 668.

Table 3-1. Section 1, Volcanic debris flow deposit between Spring C and D (location, pl. 1).

		Thickness (centimeters)
1.	Tundra cap, active zone of plant growth	12
2.	Soil, black, sandy	8
3.	Soil, dark-brown, rich in organic matter	3
4.	Soil, dark-grey	7
5.	Soil, brown, clay-rich	4
6.	Soil, very dark-brown, clay-rich	1
7.	Lapilli breccia, gray, clay-rich matrix with black scoriaceous cinders up to 5 cm diameter. Material is poorly sorted and does not show any stratification. Microscopically the matrix consists of about 99% fine-grained clay enclosing plagioclase (0.1 - 0.2 mm diameter). The matrix is well indurated. Base of this unit is not exposed.	150
	Total exposed section	185 cm

Table 3-2. Section 2, Volcanic debris flow deposit in upper tributary of Hot Springs Bay Valley (location, on pl. 1).

		Thickness (centimeters)
1.	Tundra cap, intergrown mass of modern roots	10
2.	Soil, dark-brown to black	19
3.	Soil, moderate olive brown, sandy	4
4.	Soil, gray, sandy	2
5.	Soil, light olive brown, sandy	11
6.	Soil, gray, sandy	2
7.	Soil, light olive grown, sandy	4
8.	Lapilli breccia, light-brown, sand to silt-size matrix with black, angular scoriaceous cinders with some blocks to 46 cm. Planar bedding is not disrupted by the presence of large blocks. No clay-sized particles are present. Base of unit is not exposed.	300
	thickness of exposed section	352 cm

CHAPTER 4

GEOPHYSICAL SURVEYS

by

Eugene M. Wescott, William Witte, Donald L. Turner, and Becky Petzinger

Geophysical Institute, University of Alaska, Fairbanks, Alaska 99701

INTRODUCTION

Geophysical methods were used at Hot Springs Bay valley to determine the thicknesses and physical properties of valley-filling sediments and volcanic debris flows, depth to bedrock, and to locate and delineate possible geothermal reservoirs. As there were no existing data on any of these subjects, several techniques were used to provide as much information as possible.

The near-surface (6 m) earth conductivities measured with a Geonics EM-31 noncontacting conductivity meter have been used elsewhere to map areas of anomalous temperatures (Wescott and Turner, 1981; Turner and Forbes, 1980; Osterkamp and others, 1983). EM-31 readings were taken at 25 m intervals along northwest-southeast grid lines spaced 100 m apart. The grid system is shown on plate 2. The electrical resistivity at greater depths was measured by Schlumberger vertical electrical soundings and by co-linear dipole-dipole sections. The layering of debris flows and sediments and depth to basement was investigated by use of the seismic refraction profile technique. Gravity profiling and VLF measurements were carried out, but these techniques did not produce usable results.

Analysis of the results has produced an integrated model of the lower valley to a depth of about 150 m.

SHALLOW GROUND CONDUCTIVITY MEASUREMENTS

The specific conductances of waters from springs A_2 and D_2 are 1775 and 700 mhos/cm at 25°C, respectively (Motyka and others, 1981). At the actual spring temperatures of 84 and 58.8°C, the reciprocals of the conductances

(the resistivities) of the waters are 2.39 and 8.03 ohm-m respectively, using the relationship that the conductivity at temperature T: $\sigma_T = \sigma_{25}[1 + 0.023 (T - 25)]$. The resistivities of the formations filling the valley are in general much higher, so the presence of hot water near the surface should be apparent by low resistivity (high conductivity).

The Geonics Ltd. EM-31 noncontacting terrain conductivity meter measures the apparent conductivity of the ground with an effective depth of penetration of about 6 m when the coils are horizontal. It operates by transmitting a 9.8 kHz signal into the ground via a self-contained dipole transmitter coil at one end of a boom which induces circular eddy current loops in the ground. The magnitude of these current loops is directly proportional to terrain conductivity in the vicinity of the loop. Each current loop generates a magnetic field proportional to the current in the loop. The receiver coil at the other end of the 4 m boom detects a portion of the induced magnetic field which results in an output voltage proportional to terrain conductivity.

If the ground is homogeneous to about 6 m, the apparent conductivity is the true conductivity. However, if there are layers of different conductivity within the effective depth of penetration, the apparent conductivity will be an intermediate value.

The conductivity of water increases with temperature, and hot water is also likely to contain dissolved salts, further increasing its conductivity compared to cold water (Keller and Frishknecht, 1966).

In our investigations at Pilgrim Springs (Turner and Forbes, 1980), Chena Hot Springs (Wescott and Turner, 1981) and at Manley Hot Springs, (East, 1981), the EM-31 has proved very useful in locating near-surface zones

of anomalous temperatures, even where the salinity of the geothermal water is not high. The correlation between ground temperature and shallow conductivity has proved to be so good that we decided to use the EM-31 to locate areas of near surface temperature anomalies rather than making a more time consuming ground temperature survey.

EM-31 readings were made along the northwest-southeast 100 m grid lines at 25 m intervals, or closer in regions of steep gradients. The results of the survey, converted into resistivity in ohm-m, have been contoured and are shown in figure 4-1. The lowest resistivity zone forms a discontinuous, sinuous pattern near the northwest edge of the valley from about 1,100 m SW to 400 NE. The lowest resistivity, less than 10 ohm-m, forms narrow zones about 10 m wide near the A, C, and D hot springs, and a broad zone on the beach around the E springs.

The sinuous pattern of the anomaly suggests that the hot water may rise to or near the surface via an ancient stream channel which cuts through more impervious volcanic debris flow deposits covering a deeper reservoir (Swanson and others, this report).

Some EM-31 lines, not shown on the grid of figure 4-1, were run across the full width of the valley to determine if any other temperature anomalies existed. In all cases the resistivity was 100 ohm-m or greater all the way to the southeast edge of the valley. The anomalies seem to end at 1,100 m SW, as no low resistivity readings were found further up the valley.

The highest near-surface resistivities were found on the dune formation near 0 SW at greater than 500 ohm-m and also on the recent dune near 400 m NE.

DEEP RESISTIVITY MEASUREMENTS

Schlumberger Vertical Electric Soundings

The Schlumberger vertical electric sounding (VES) technique involves four colinear electrodes in which current is put into the ground at the outermost electrodes A and B while the resulting voltage is measured across a pair of electrodes MN in the center of AB with MN << AB. To make a VES the current electrodes AB are moved outwards while the potential electrodes remain fixed. The larger the spacing AB, the greater the depth of investigation. The apparent resistivity is calculated from the formula:

$$\rho = \pi\left(\frac{AB^2}{MN} - \frac{MN}{4}\right)\frac{V}{I} \qquad (4\text{-}1)$$

where AB and MN are the current electrode and potential electrode separations, V is the voltage across MN and I is the current (Keller and Frischknecht, 1966). The apparent resistivity vs 1/2 AB is plotted on log-log paper for interpretation by comparison with sets of theoretical curves or by computer modelling to give true resistivity vs depth. The interpretation model assumes horizontal layers of uniform resistivity.

We carried out four Schlumberger vertical electric soundings, with 1/2 AB spacings ranging from 0.68 m to 316 m located as shown in figure 4-2.

VES #1 (fig. 4-2) was run northeast-southwest along the same line as seismic profile B-B' (see fig. 4-10). It was centered at 0 NW, 400 m SW, and was carried out to a ½ AB spacing of 316 m. The data are plotted on log-log paper in figure 4-3 along with a true resistivity-true depth model calculated by means of an automatic curve fitting program (Zhody, 1974). The program

uses various numbers of layers to approach a best fit. In the case of the model, the model VES curve is shown as well as the true resistivity vs depth, with the spacing scale serving as depth in meters. The model indicates that a low resistivity layer begins at a depth of 52 m where the resistivity drops to 12 ohm-m, and is 42 m thick. An even lower resistivity layer of 7 ohm-m starting at a depth of 148 m is suggested by the data.

VES #2, (fig. 4-2) was run parallel to and 75 m northwest of VES #1 and centered at 75 m NW, 275 m SW. It was carried out to a 1/2 AB spacing of 136 m. The location was chosen to sample the resistivity of the volcanic debris flow deposits, evident as a dry terrace and identified by shallow auger holes and a trench in the terrace bank (Swanson and others, this report). Figure 4-4 shows the observed apparent resistivity values, a model apparent resistivity curve and true resistivity vs. depth, with a depth scale equal to the 1/2 AB spacing scale. The model uses six layers to make a good fit to the data.

The volcanic debris flow unit has a resistivity of 181-517 ohm-m to a depth of 1 m, below that the resistivity decreases to 45 m at a depth of 20 m. An underlying low resistivity layer has a resistivity of 10.5 ohm-m, a thickness of 40 m and starts at a depth of 20 m. The resistivity of the underlying probable bedrock unit is much higher, 1,524 ohm-m, and begins at 60 m.

VES #3, was run on the stream terrace northwest of Hot Springs Creek between springs C and D (fig. 4-2). Owing to space limitations the maximum 1/2 AB spacing was only 68 m. Figure 4-5 shows the observed apparent resistivity values, and a model using eight layers. In this situation the conditions for a one-dimensional interpretation are clearly violated in that

the steep hillside with high resistivity bedrock begins about 10 m northwest of the array, and the high resistivity probably extends steeply beneath the array. Nevertheless, the interpretation via a horizontal layered model is valid for the near surface layers and is probably also indicative of the deeper layering. There is a thin near-surface layer of resistivity 2.9 ohm-m indicated, and deeper layers of 6.1-4.2 ohm-m with a combined thickness of 23 m starting at a depth of 13.5 m. The fourth VES was also run in the vicinity of one of the springs, the A group (fig. 4-2). Figure 4-6 shows the observed apparent resistivities, and a model with seven layers. The interpretation suggests a low resistivity layer of 2.2 ohm-m starting at a depth of 9.1 m, underlain by a layer of 9.8 ohm-m. As the array could only be extended to 68 m the resolution of the deepest layer is not very certain.

Deep Resistivity Profiling

Deep electrical resistivity measurements were made using a Zonge Engineering and Research Organization GDP-12 induced polarization/resistivity receiver system. A Geotronics FT-4 transmitter capable of a 4 ampere square wave signal was used as the signal source. The Zonge system uses a pair of microprocessors to process the field data (stacking and averaging), to improve the signal-to-noise ratio and calculate the resistivity and phase shift. The system can be used with 16 different frequencies from 1/125 to 256 Hz to produce a complex resistivity curve, but due to the time available we ran 1/4 Hz as the standard measurement on both Schlumberger and dipole-dipole measurements.

As shown in figure 4-2 three dipole-dipole profiles were run along and across the valley. We used 100 m dipoles and generally extended each

receiving spread out to n = 5. Figure 7 shows the dipole-dipole resistivity survey electrode configuration. The whole array can be moved horizontally to sample depth vs. horizontal distance. The results are usually presented as a pseudo-section, where the apparent resistivity values are plotted at the intersections of lines drawn at 45° from the horizontal between the center of the transmitter and the center of the receiver locations.

Apparao and Roy (1973) have defined the depth of investigation for homogeneous ground to be that depth which contributes the maximum to the signal measured at the ground surface. For the co-linear dipole-dipole configuration their model studies indicate the depth of investigation as: 0.195 (n+2)a, where a is the dipole length. In our case the depth of investigation at n=5 would be 137 m. However, the effects of deeper layers are seen in model studies and the data can be interpreted.

In common practice the nominal depth of investigation is usually assumed to be about 1/2 the distance between the transmitting and receiving dipoles. Thus the survey at n=5 is assumed to have sampled to about 300 m depth, yet features of a few tens of meters could be distinguished.

Figure 4-8 shows all three pseudo-sections plotted to show where they intersect each other. There is a sharp resistivity discontinuity at a pseudo-depth of 150 m in all three pseudo sections, where the resistivity decreases from values in the 10's of ohm-m to lower values. The longest pseudo-section #2 shows some very interesting effects. The inland dune which runs across the valley has a topographic high centered at 0 m SW. Such a topographic feature will produce a type of anomaly which has been modelled for homogeneous ground by Fox and others (1978). The effect would be to produce a small zone of higher resistivity beneath station 0 with two zones of lower resistivity sloping down at 45° away from station 0. In fact, the

resistivity decreases generally towards the northeast. The minimum value is at a pseudo-depth of 200 m between station 0 and 100 m NE. To the southwest of the dune there is a clear break in resistivity at a pseudo-depth of 150 m, with a low resistivity layer indicated below the upper layers. Keller and Frischknecht (1966) have published two-layer tables for plotting a set of two-layer interpretation curves for the dipole-dipole array. Using the apparent resistivity vs. pseudo-depth at 400 m SW as typical, the curve fitting for two layers suggests an upper layer 40 m thick of resistivity 100 ohm-m underlain by a layer of 11 ohm-m. The resistivity increases with depth below the second layer, indicating a third layer, higher in resistivity. This simple interpretation agrees fairly well with our VES #1 interpretation (fig. 4-3). As the resistivity decreases towards the northeast and the zone becomes apparently thicker, it is reasonable to suggest that the low resistivity layer increases in thickness towards the northeast, and/or the overlying resistive layer thins towards the northeast.

The interpretation of dipole-dipole pseudo-sections is not simple or straightforward except in simple horizontal layering situations. Two or three dimensional resistivity configurations can be modelled to produce pseudo-sections for comparison with the observed data. For dipole-dipole 1, which extends completely across the valley (figs. 4-2 and 4-8), the situation is essentially two-dimensional, and we have made a number of two-dimensional model calculations using the computer code developed by Dey and Morrison (1975). This modelling program uses an array of discrete resistivity values. Owing to the very large size of this array and the cost of computer runs for such a large program, we restricted the array to 113 x 16 elements. The smallest feature we modelled is a resistivity element 10 m deep x 20 m wide. Numerous models were run. Those which had a fair fit to the data showed the

same basic structure: a resistive cap layer of 40 to 70 m thickness underlain by a layer of low resistivity thinning out to the southeast and underlain by a more resistive basement. An exact fit to the observed psuedo section was not obtained, perhaps because we did not incorporate topography (the valley walls). Figure 4-9 shows the observed data, a model pseudo-section and the model cross section with no vertical exaggeration.

Summary of Deep Resistivity Measurements

The two VES measurements VES #1 and #2 were far enough away from the valley edges to give a reasonable idea of the resistivity vs depth of the valley subsurface between springs B and C. Both show an upper layer of about 10 m thickness of moderate resistivity, about 120 ohm-m, underlain by layers of decreasing resistivity. VES #2, which is closer to the NW valley side where the springs reach the surface, indicates a low resistivity zone of 10.5 ohm-m extending to a depth of 60 m. VES #1 nearer the center of the valley shows slightly lower resistivity, which may well be influenced by the higher resistivity in the same layer towards the SE side of the valley.

The dipole-dipole measurements require 3-dimensional modelling for detailed interpretation, but by two layer curve matching and 2-dimensional modelling the same general picture is found. The uppermost layer has a model resistivity of about 100 ohm-m and a thickness of 40 - 70 m. The low resistivity layer may have a resisitivity as low as 3 ohm-m towards the northwest side of the valley and 100 ohm-m towards the southeast side. The underlying basement rocks model with 1,500 ohm-m.

SEISMIC REFRACTION PROFILING

Methods Used

The seismic refraction method can produce data on the velocities, thicknesses, and attitudes of layers beneath a survey line. This is true if the velocities of each distinct layer increase with depth, and if distinct layers are thick enough - otherwise they may not be detected at all and the calculated depths be in error. The hidden layer problem is a serious drawback to the seismic refraction method, and there is evidence that our seismic data are affected by this problem. Analysis of the first arrival times can also distinguish faults or other structural relief on a refractor boundary.

We used two Geometrics Nimbus ES-1210F portable seismographs to investigate the structure of the valley. The Nimbus-12 seismograph is a 12 channel analog-to-digital recorder, with memory storage for stacking multiple shots or hammer strokes for signal-to-noise enhancement and post-shot variation of output amplitude for optimum traces. Twenty four seismometers were laid out in a line with a 15 m spacing. Sixty percent seismic dynamite in 2 to 3 m holes served as the shot energy source. In the first shots, both seismographs were triggered by the same blaster, to produce a 24 channel record with a single shot. We found several instances where the seismographs did not trigger simultaneously, and all the later shots were single 12 channel spreads.

In order to detect dipping refractors, seismic spreads must be shot in both directions and this was done in Hot Springs Bay Valley. Figure 4-10

shows a map of Hot Springs Bay Valley with the locations of three seismic refraction profile lines. B-B', the longest, ran northeast-southwest along the 0 baseline from 50 SW to 670 SW. Seven shots were used to obtain reversed travel times. We used a multi-layer dipping seismic refractor program (Campbell, 1981) to analyze the travel time curves. This program assumes: that the velocity in all layers is constant within the layer; that all refractor interfaces are planar; and that there are no hidden layers. In reality velocities may show variations laterally and with depth, interfaces are often curved or show some topography, and there may be hidden layers.

Results

Figure 4-11 shows the travel time curves and the calculated cross section for profile B-B'. Note that where the refractor interfaces are shown dashed there are no data at all due to the fact that there the angle of incidence is less than the critical angle, and the energy is either reflected and shows up as a second arrival, or is refracted downward. There are three major refractors evident in the data. The top unit varies in thickness from 45 m at 50 m SW to 31 m near 670 m SW, and has a velocity of about 1,630 m/s. The upper portion of this unit was observed to be a volcanic debris flow with apparent low porosity and permeability (Swanson and others, this report).

The second major unit has a velocity varying between 3,240 and 3,505 m/s. This intermediate velocity zone is of interest because it coincides with a low resistivity layer found from the Schlumberger vertical electric soundings and dipole-dipole traverses. The depth to the base near the northeast end of the profile is about 135 m. The base slopes up the valley at about 7°, with a depth of 78 m near 495 SW. The reversed shots 8, 9, and

10 covered a spread of only 165 m, which was not long enough to reach the bottom of the 3,505 m/sec layer.

Beneath the low resistivity layer the velocity increases to 4,900 m/sec. We have labeled the base layer as probable volcanic bedrock.

Profile A-A' was run along 108 m SW, perpendicular to profile B-B' (fig. 4-10). Figure 4-12 shows the first arrival travel time curves. The data are very clean, showing the presence of a thin low velocity layer of 1,250 m/sec, 4 to 6 m thick with two deeper layers indicated by the breaks in slope. The basal refractor appears to slope towards the center of the valley.

The velocity of the second layer is 1,960 m/s, which corresponds to the top volcanic debris flow unit in profile B-B' of 1,610 m/s. By the dipping refractor program (Campbell, 1981) the third layer would have a velocity of 4,550 m/s and the interface would dip at about 10° which would correspond to the volcanic basement. However, there is reason to suspect this analysis due to the hidden layer problem discussed previously. There is no indication of the intermediate layer of v = 3,240 m/s to 3,505 m/s seen in profile B-B'. This layer can be hidden even though its velocity is intermediate between the 1,960 m/s and 4,900 m/s if it is not thick enough to show up on the first arrival travel time curve. It may thin towards the valley edges even though it was seen in B-B'.

By ray tracing techniques we have calculated that a blind zone can exist with a thickness of about 45 m if we use the velosities of 3,240 and 4,900 m/s observed in profile B-B' near the intersection of AA' and BB'. The interpreted cross section, using these assumptions, is shown at each end of the cross section. The dotted line indicates the location of the interface if the hidden layer was missing. The layer thickness and velocities where profile B-B' intersects profile A-A' are shown. The agreement in depth is

not perfect but is reasonable. The apparent slope suggests that the 1,950/3,240 m/s interface may slope towards the center of the valley at about 7°, but it might be more nearly horizontal because the hidden layer problem makes the slope uncertain. The refractor interfaces are shown with shorter dashed lines where no seismic data are possible due to the ray path.

Profile C-C' starts at 500 m SW, 50 m SE of profile B-B', and runs southwest parallel to B-B' (fig. 4-13). Again the data seem very clean with only two major layers indicated as in Profile A-A'; the v = 3,240 m/s layer is missing (fig. 4-13). By ray tracing and use of hidden layer nomographs (Hawkins and Maggs, 1961) we found that a 17 m thick layer of the intermediate velocity could be hidden, and, due to our 15 m seismometer spacing, perhaps as much as 25 m thickness of the layer could possibly be present. This is less than projected from B-B', but we would expect less due to the dip towards the center of the valley seen in A-A' (fig. 4-12). The interpreted profile at the bottom of figure 4-13 shows the more conservative nomograph model. The dotted lines near each end of the profile indicates the zero thickness hidden layer interface solution. Also shown by shorter dashes on the interface lines are the limits of seismic data due to the ray path.

Discussion of Seismic Results

The first arrivals indicative of a particular refractor are the waves that are critically refracted along the surface of the layer. Therefore, no information is available from deeper in the layer. For instance, inspection of the material from seismic shot holes and a trench shows that the upper portion of the layer with velocity ranging between 1,630 and 1,960 m/sec is a volcanic debris flow. The entire thickness of the 1,630 - 1,960 m/sec layer

may be composed of several debris flows or might have layers of sediments of similar velocity.

The next unit has a velocity about twice that of the top unit, and its upper surface is possibly an erosional surface as it appears to slope up the valley and also up towards the center of the valley. It is interpreted as a hidden layer in profiles A-A' and C-C'. It has low resistivity extending from the northwest valley side to near the valley center, and probably is a reservoir for hot or saline waters. The velocity is at the upper 80 percent fiducial limit for sandstones and shales, and falls at the center of the velocity distribution characteristic of limestone and dolomite but is less than the 80 percent fiducial limit of granites and metamorphics (Grant and West, 1965). Thus it would appear to be a fairly rigid rock. It has a velocity slightly lower than found by Wescott and others for the Unalaska formation under Summer Bay valley on Unalaska (unpublished data).

The basal layer with a velocity of 4,900 m/s is obviously a much more solid rock than those lying above it. The resistivity data show that the basal unit is higher in resistivity than the low resistivity unit. Its velocity falls near the center of the velocity distribution of granitic and metamorphic rocks (Grant and West, 1965). The basal layer could also be an intrusive rock, a volcanic flow, a pyroclastic flow, or a well-cemented volcanic debris flow. Kienle (personal commun.) investigated seismic velocities on Augustine Volcano, Alaska, and found a unit with a similar velocity to be a sedimentary rock cemented with zeolites, presumably from hydrothermal activity.

SUMMARY AND DISCUSSION OF GEOPHYSICAL SURVEYS

Figure 4-14 shows three-dimensional perspective cross sections of the lower valley and presents a composite model of the seismic and resistivity data.

The near-surface conductivity (reciprocal resistivity) measurements show a narrow sinuous pattern about 1,500 m long near the northwest side of the valley. Assuming that there is excellent correlation between conductivity and temperature, the anomaly pattern shows where hot water rises to near the surface. No other zones of anomalous near-surface conductivity were found further up the valley or towards the southeast part of the valley. The surface layer seen in the valley, particularly southwest of the dune near 0 m SW, is composed of a volcanic debris flow with low porosity and permeability.

For hot water to rise through this impermeable cap layer there must be a zone of higher porosity/permeability or a fracture system. The sinuous form of the near-surface conductivity anomaly suggests the high porosity/permeability zone could be a buried stream channel.

Deeper electrical resistivity measurements with Schlumberger vertical electric soundings have led to a resistivity model. There is a near surface layer of 2 to 10 m thickness of moderate resistivity (120 ohm-m), underlain by a thicker layer 12 to 55 m in thickness, increasing in thickness towards the center of the valley. This is underlain by a layer of low resistivity (4.2 to 12 ohm-m) with a depth to basement ranging from 36 m near springs C and D to 94 m near the northeast-southwest O baseline. The basement layer has a resistivity ranging from 514 to 1,524 ohm-m.

Motyka and others (this report) present evidence that the thermal spring waters are derived from a shallow reservoir where cold meteoric waters are mixing with thermal waters that are ascending from deeper levels. The temperature of the parent thermal water is estimated at 170 - 190°C while that of the cold water fraction at 10°C. The zone of mixing is inferred to be the region of low resistivity underlying the northwest corner of the valley with the resulting mixed reservoir water having temperatures of 120 to 135°C. The reservoir is shown by cross hatching in figure 4-14. The higher resistivity of the southeast side of this layer may be due to cold water entry from that side.

By the general form of Archies Law, the fractional porosity of a rock can be estimated by:

$$\phi = (\rho_w/\rho_a)^{\frac{1}{2}} \qquad (4\text{-}2)$$

(Telford, 1976), where ρ_w is the resistivity of the formation water and ρ_a is the apparent resistivity of the bulk rock. Using the 25°C resistivity of hot spring A water, 5.63 ohm-m (Motyka and others, this report) we calculate the resistivity at the mixing reservoir temperature of 135°C to be 1.53 ohm-m. Using the reservoir layer resistivity values from VES #1 and #2, the estimated porosity of the layer ranges from 37 to 48 percent. These estimates do not include the possible contribution to the resistivity of clay minerals, which would lower the calculated porosity. Keller and Frischknecht (1966) show the normal range of post-Paleozoic clastic volcanics as 10 to 60 percent porosity. The other important factor, permeability, cannot be estimated from the available data.

For the basement rock, using 1.53 ohm-m for the hot water resistivity, and a resistivity of 514 to 1,5000 ohm-m, we estimate a porosity of three to five percent.

The 100 m dipole-dipole survey produced a similar model differing somewhat in depths and resistivity. One and two-dimensional interpretations suggest a cap rock of resistivity about 100 ohm-m and thickness 40 to 70 m underlain by a reservoir layer of resistivity 3 ohm-m and perhaps having a base 150 m deep in the center of the valley. The basement resistivity was modelled using a value of 1,500 ohm-m.

Although no computer models were produced for the long northeast-southwest pseudo-section #2 it appears that the reservoir layer thickens toward the northeast and thins up the valley to the southwest. From the geophysical measurements we cannot determine whether this is an effect of the reservoir layer becoming thicker in that direction or whether there is saltwater intrusion from the ocean. R.F. Black (personal commun., 1982) argues for hot water to produce the zone of low resistivity, stating that "In the Aleutians, in general, sufficient precipitation occurs and enough hydraulic head is available to keep salt water out of most valleys."

The basement layer, presumed to be an extension of the Hot Springs volcanic sequence exposed in the valley walls, has a high resistivity and also a surface which dips towards the center of the valley and also to the northeast towards the mouth of the valley. This suggests that the basement surface was glaciated into a U-shape prior to filling the valley with glacial till, glacial-fluvial deposits, debris flows and sediments.

The seismic refraction profiling agrees fairly well with the resistivity data although the interpretation is complicated by the hidden layer problem.

There are three basic layers. The uppermost, disregarding the weathering layer, has a range in velocity from 1,610 to 1,960 m/s and a thickness ranging from 31 to 45 m. This corresponds to the upper layer of medium resistivity seen by the resistivity measurements. The second layer, which is inferred as a hidden layer in two of the profiles, has a velocity of 3,240 to 3,505 m/s corresponds to the low resistivity reservoir layer. Bedrock, with the relatively high velocity of 4,900 m/s could be composed of volcanic debris flows or volcanic flows, instrusive rock, or possibly a well-cemented sedimentary or pyroclastic unit. The possible occurrence of hydrothermal cementation is consistent with a higher temperature reservoir beneath the basement interface predicted by water geochemistry (Motyka and others, this report).

The geophysical data cannot delineate a conduit system bringing the hot water up into the reservoir layer. Although the expression of near-surface hot water is a sinuous pattern, suggesting a buried stream channel, the hot water may be entering the reservoir elsewhere. The pattern of helium soil gas and mercury anomalies (Wescott and others, this report) tends to show high values further out into the valley than the near surface conductivity.

REFERENCES CITED

Al'pin, L.M., Berdichevskii, M.N., Vedrintsev, G.A., and Zagarmistr, A.M., 1966, Dipole methods for measuring earth conductivity, translated by G.V. Keller, Consultants Bureau, New York, p. 11-37.

Apparao, A., and Roy, A., 1973, Field results for direct-current resistivity profiling with two-electrode array: Geoexploration, v. 11, p. 21-44.

Campbell, D.L., 1981, Four or fewer dipping seismic refractors: Interpretation, in manual of Geophysical Hand Calculator Programs, HP volume: Society of Exploration Geophysics, SE 15 13-C.

Dey, A., and Morrison, H.F., 1975, Resistivity modelling for arbitrarily shaped two dimensional structures: Engineering Geoscience and Lawrence Berkeley Laboratory, University of California, p. 1-54.

East, J., 1982, Preliminary investigations at Manley Hot Springs, Alaska: University of Alaska, Geophysical Institute Report UAG R-290, p. 56-59.

Fox, R.C., Hohmann, G.W., and Rijo, L., 1978, Topographic effects in resistivity surveys, UURI report IDO/78-1701.b.3.2.1, p. A30-A38.

Grant, F.S., and West, G.F., 1965, Interpretation theory in applied geophysics: McGraw-Hill Book Co., New York, p. 8.

Hawkins, L.V., and Maggs, D., 1961, Nomograms for determining maximum errors and limiting conditions in seismic refraction survey with a blind-zone problem: Geophysical Prospecting, v. IX(4), p. 526-532.

Keller, G.V., and Frischknecht, F.C., 1966, Electrical methods in geophysical prospecting: Pergamon Press, New York, p. 492-493.

Motyka, R.J., Moorman, M.A., and Liss, S.A., 1981, Assessment of thermal spring sites, Aleutian Islands, Atka Island to Becherof Lake: Preliminary results and evaluation, Alaska Division of Geological and Geophysical Surveys Open-file Report 144, 175 p.

Osterkamp, T.E., Kawasaksi, K., and Gosink, J.P., 1983, Shallow magnetic induction measurements for delineating near-surface hot groundwater sources in Alaskan geothermal areas, Journal of Energy Resources Technology, v. 105, (2), p. 156-161.

Telford, W.M., Geldart, L.P., Sheriff, R.E., and Keys, D.A., 1976, Applied Geophysics: Cambridge University Press, London, p. 445.

Turner, D.L., and Forbes, R.B., 1980, eds., A geological and geophysical study of the geothermal energy potential of Pilgrim Springs, Alaska, Report UAGR-271, Geophysical Institute, University of Alaska, Fairbanks, Alaska, p. 113-135.

Wescott, E.M., and Turner, D.L., 1981, A geological and geophysical study of the Chena Hot Springs geothermal area, Alaska, Report UAG R-283, Geophysical Institute, University of Alaska, Fairbanks, Alaska, p. 31-42.

Zhody, A.R., 1974, A computer program for the automatic interpretation of Schlumberger sounding curves over horizontally stratified media, U.S. Geological Survey Report GD-74-017, p. 232.

FIGURE CAPTIONS

Figure 4-1. Map of Hot Spring Bay Valley, Akutan Island, Alaska, with superposed near-surface (6 m) electrical resistivity contours from a ground conductivity survey. We assume from past experience that the resistivity values are inversely related to anomalously high ground temperatures. Zones of less than 10 ohm-m are cross hatched.

Figure 4-2. Map of Hot Springs Bay Valley, Akutan Island, Alaska, with locations of four vertical electric soundings (VES) made using the Schlumberger array and three dipole-dipole profiles.

Figure 4-3. VES #1 plot of apparent resistivity vs. 1/2 AB spacing - observed data, asterisks and computed model, curved solid line. The true resistivity vs. depth of the model is shown by straight line segments.

Figure 4-4. VES #2 on the volcanic debris flow terrace. See figure 3 for explanation.

Figure 4-5. VES #3 plot near hot springs C and D. See figure 3 for explanation.

Figure 4-6. VES #4 plot, near hot springs A. See figure 3 for explanation.

Figure 4-7. Dipole-dipole resistivity electrode configuration.

Figure 4-8. 100 m dipole-dipole resistivity pseudo-sections plotted to show where the northwest-southeast sections intersect the northeast-southwest section. The sections generally show a medium resistivity cap layer 40 to 70 m thick overlying a low resistivity layer which is underlain by bedrock. The pseudo-depth scale is identical to the horizontal scale. Apparent resistivity values are in ohm-m.

Figure 4-9. Pseudo-section plots of dipole-dipole 1 profile across Hot Springs Bay Valley. The upper figure shows the pseudo-section produced from the observed data. The bottom figure is a two-dimensional resistivity model cross-section with its corresponding pseudo-section shown above. No vertical exaggeration.

Figure 4-10. Map of Hot Springs Bay Valley, Akutan Island, Alaska, showing the locations of three seismic refraction profile lines.

Figure 4-11. Top: First arrival travel time curves. Bottom: Interpreted cross section, profile B-B' parallel to valley. The layer with velocity 3,240-3,505 m/s corresponds to the low resistivity layer. The interface where dashed indicates the zones where no information is available from the refracted seismic energy. The intersection of cross valley profile A-A' with depths to corresponding seismic refractors is shown in the cross section.

Figure 4-12. Top: First arrival travel time curves for seismic profile A-A'. Bottom: Interpreted cross section. The v = 3,240 m/sec layer is inferred as a hidden layer which could not be seen in the first arrival travel time

curves. Because it is a hidden layer the 1,960/3,240 m/s inferred interface might be closer to horizontal. The steep dip of the 3,200/4,900 m/s interface suggests a glaciated surface.

Figure 4-13. Top: First arrival travel-time curves for seismic profile C-C' parallel to B-B'. Below: Interpreted cross section. The v = 3,505 m/s layer is inferred as hidden layer which could not be detected in the first arrival travel time data. The dotted lines near each end of the profile show the zero thickness hidden layer interface.

Figure 4-14. Composite cross sections showing the proposed shallow geothermal reservoir (cross-hatched) based on the combination of electrical resistivity and seismic data.

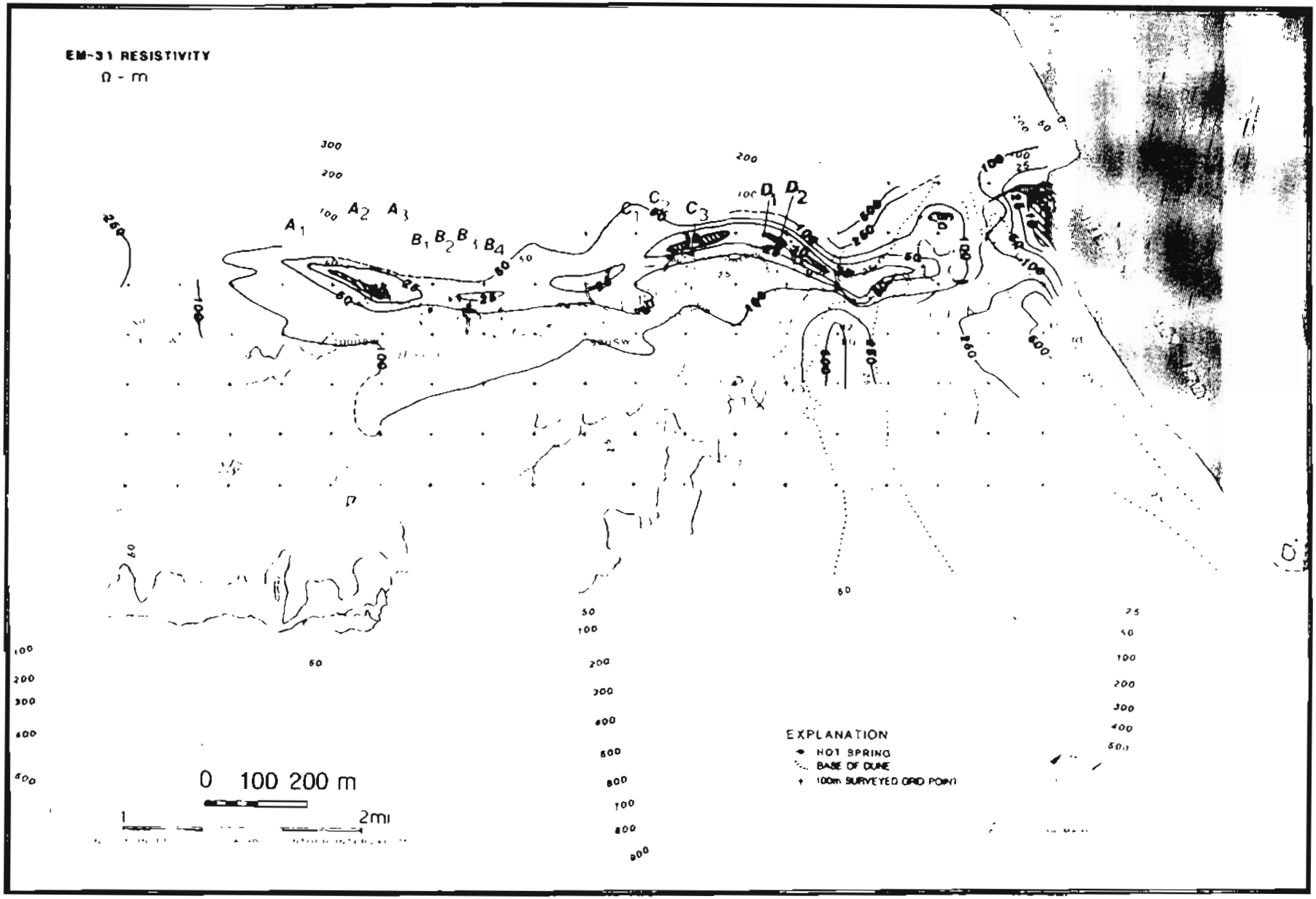
EM-31 RESISTIVITY
Ω - m
A1
A2
A3
B1
B2
B3
B4
C1
C2
C3
D1
D2
0 100 200 m
1 2mi
EXPLANATION
HOT SPRING
BASE OF DUNE
100m SURVEYED GRID POINT

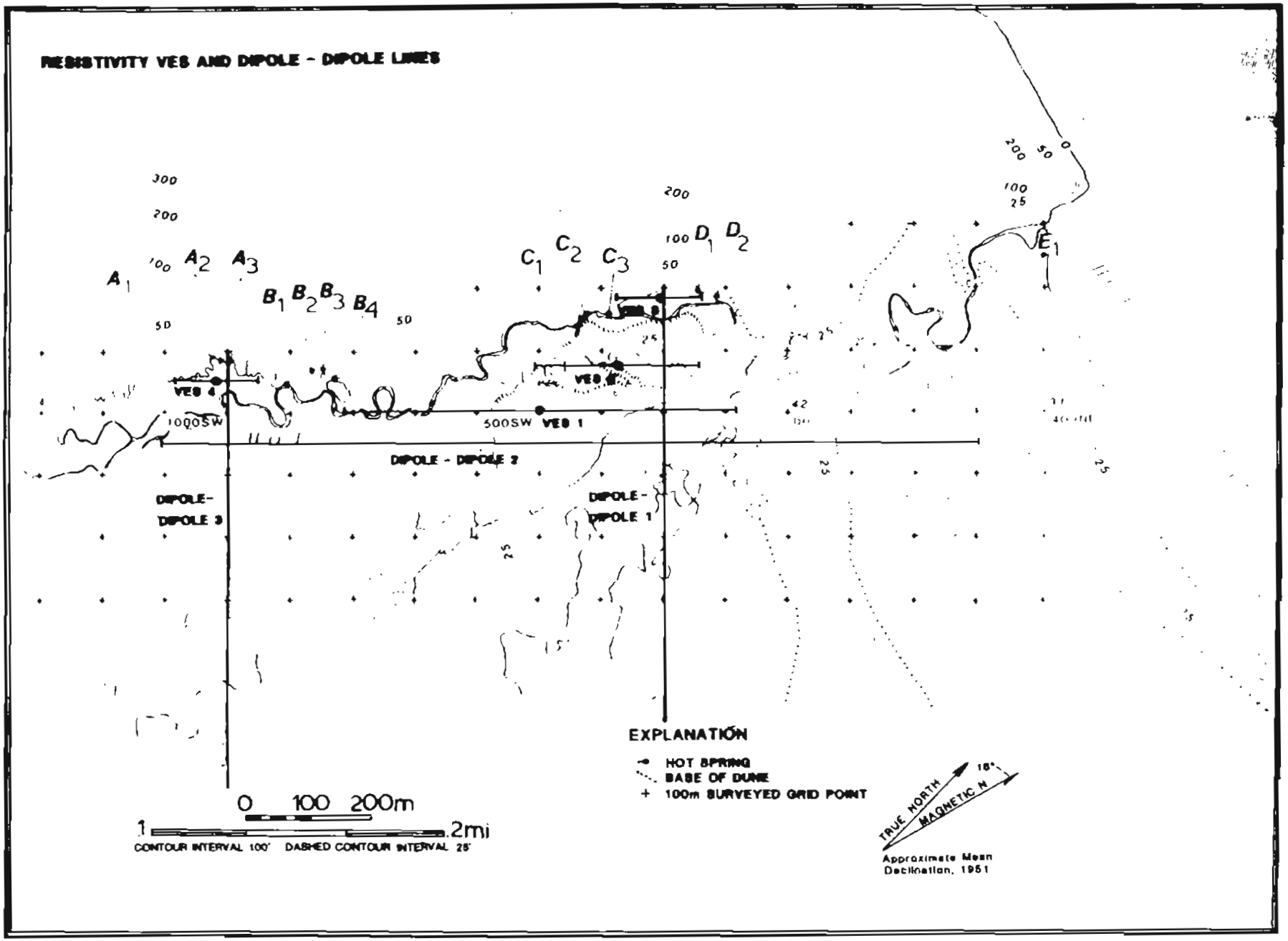
RESISTIVITY VES AND DIPOLE - DIPOLE LINES
A1
A2
A3
B1
B2
B3
B4
C1
C2
C3
D1
D2
E1
VES 4
VES 3
VES 2
VES 1
1000SW
500SW
DIPOLE - DIPOLE 2
DIPOLE-
DIPOLE 3
DIPOLE-
DIPOLE 1
EXPLANATION
HOT SPRING
BASE OF DUNE
100m SURVEYED GRID POINT
0 100 200m
1 .2mi
CONTOUR INTERVAL 100' DASHED CONTOUR INTERVAL 25'
TRUE NORTH
MAGNETIC N
16°
Approximate Mean
Declination, 1951

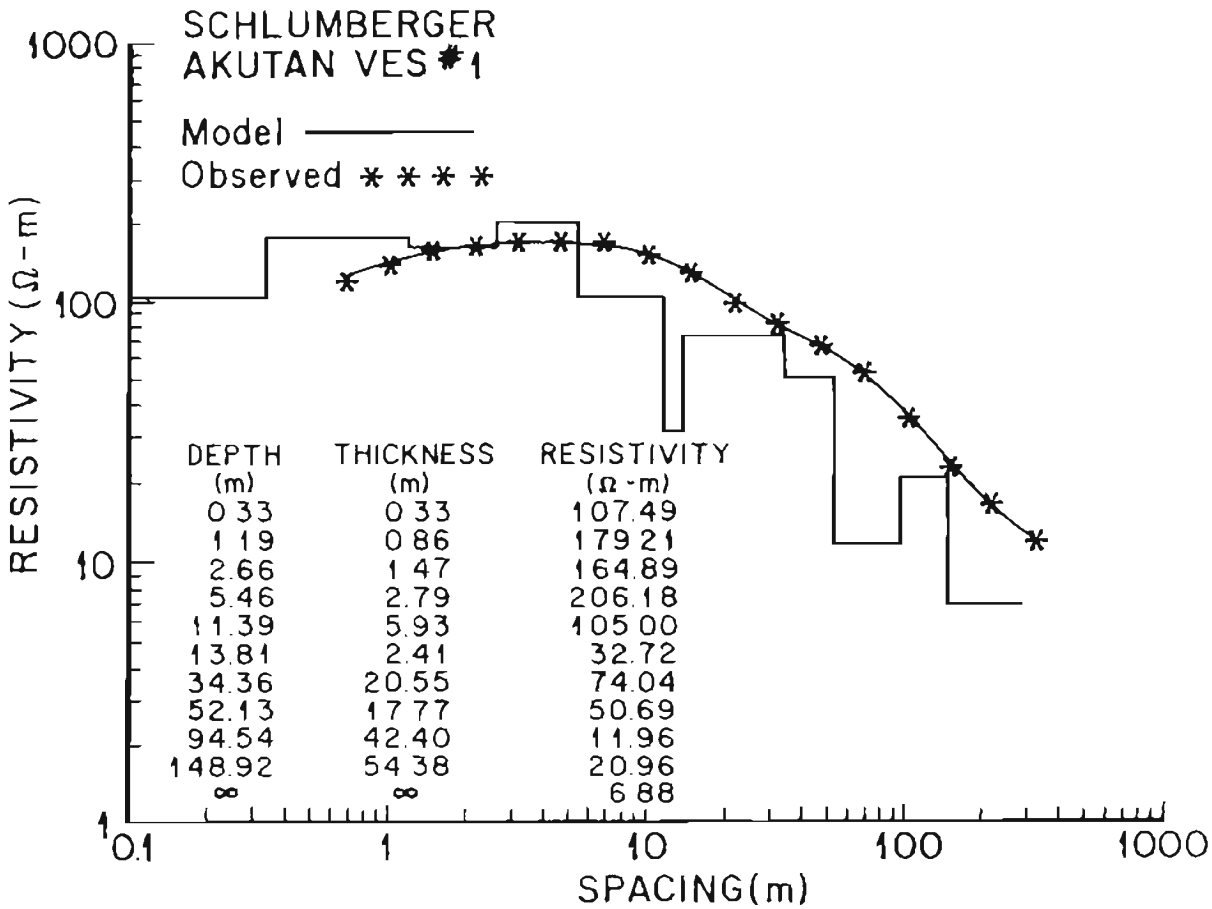
SCHLUMBERGER
AKUTAN VES #1
Model
Observed * * * *
RESISTIVITY (Ω-m)
1000
100
10
1
0.1
1
10
100
1000
SPACING(m)
DEPTH (m) | THICKNESS (m) | RESISTIVITY (Ω-m)
0.33 | 0.33 | 107.49
1.19 | 0.86 | 179.21
2.66 | 1.47 | 164.89
5.46 | 2.79 | 206.18
11.39 | 5.93 | 105.00
13.81 | 2.41 | 32.72
34.36 | 20.55 | 74.04
52.13 | 17.77 | 50.69
94.54 | 42.40 | 11.96
148.92 | 54.38 | 20.96
∞ | ∞ | 6.88

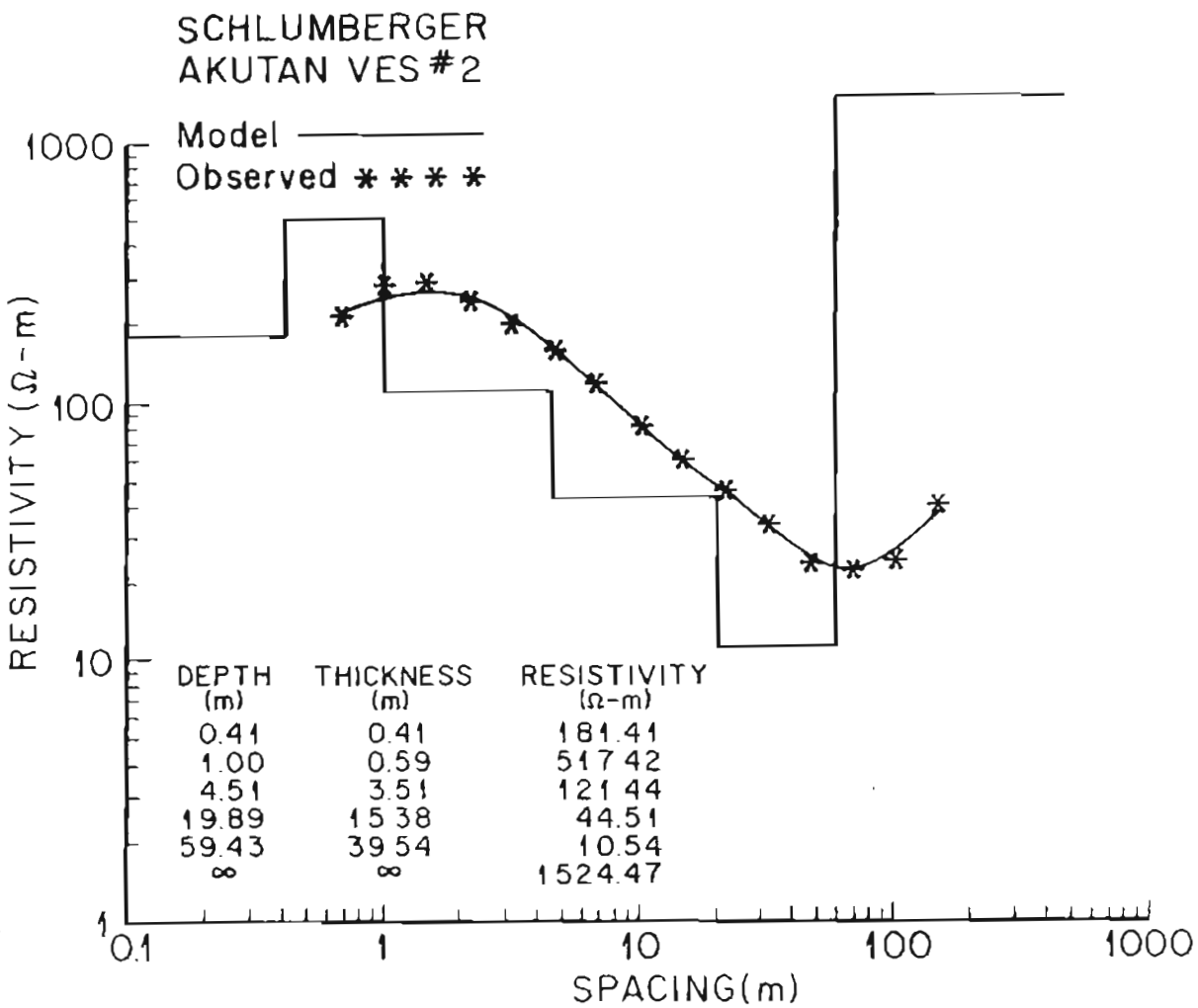
SCHLUMBERGER
AKUTAN VES #2
Model
Observed * * * *
1000
100
10
1
RESISTIVITY (Ω-m)
0.1
1
10
100
1000
SPACING(m)
DEPTH (m) | THICKNESS (m) | RESISTIVITY (Ω-m)
0.41 | 0.41 | 181.41
1.00 | 0.59 | 517.42
4.51 | 3.51 | 121.44
19.89 | 15.38 | 44.51
59.43 | 39.54 | 10.54
∞ | ∞ | 1524.47

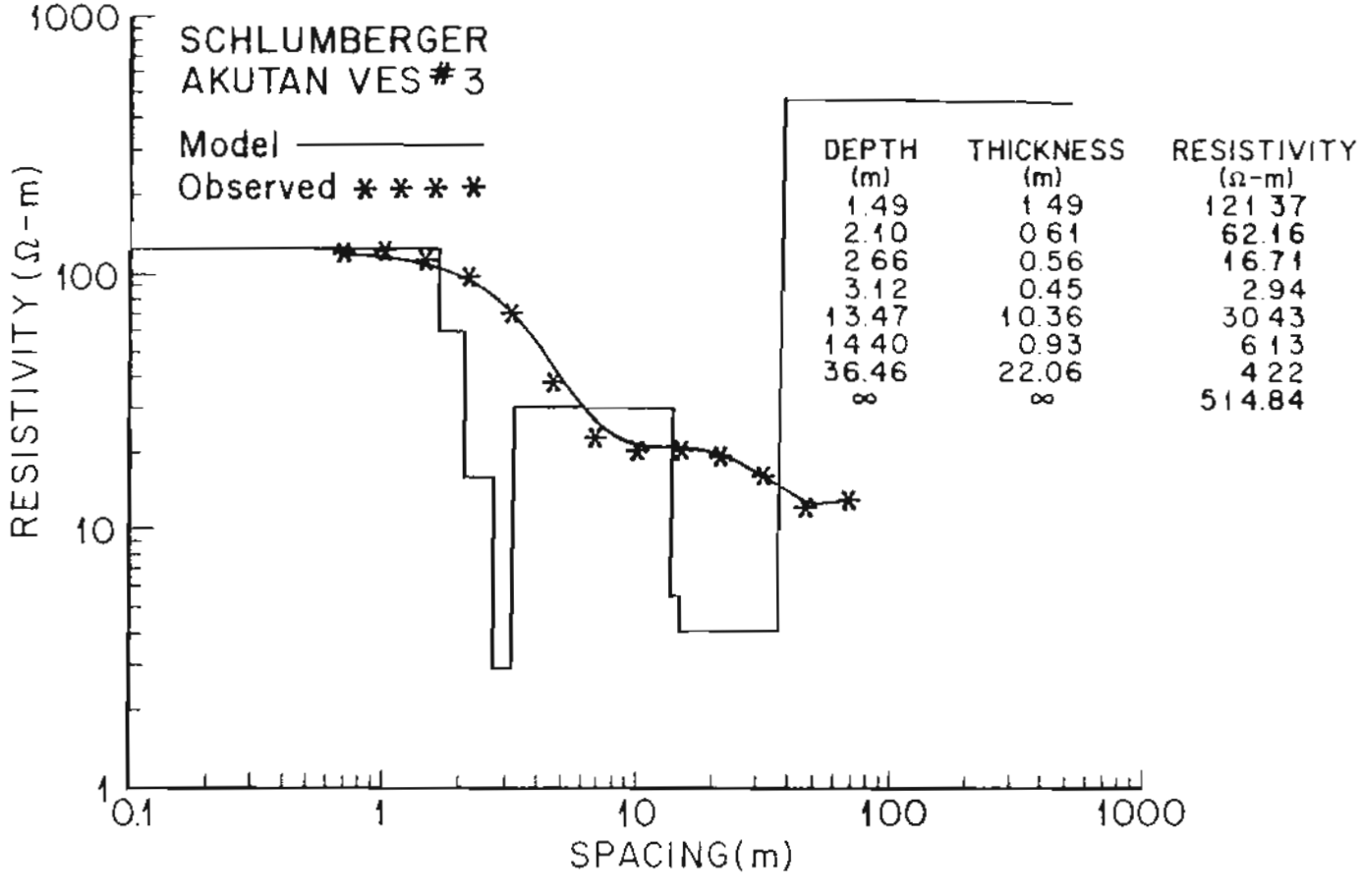
SCHLUMBERGER
AKUTAN VES#3
Model
Observed * * * *
DEPTH (m)
THICKNESS (m)
RESISTIVITY (Ω-m)
1.49 1.49 121.37
2.10 0.61 62.16
2.66 0.56 16.71
3.12 0.45 2.94
13.47 10.36 30.43
14.40 0.93 6.13
36.46 22.06 4.22
∞ ∞ 514.84
RESISTIVITY (Ω-m)
1000
100
10
1
0.1
1
10
100
1000
SPACING(m)

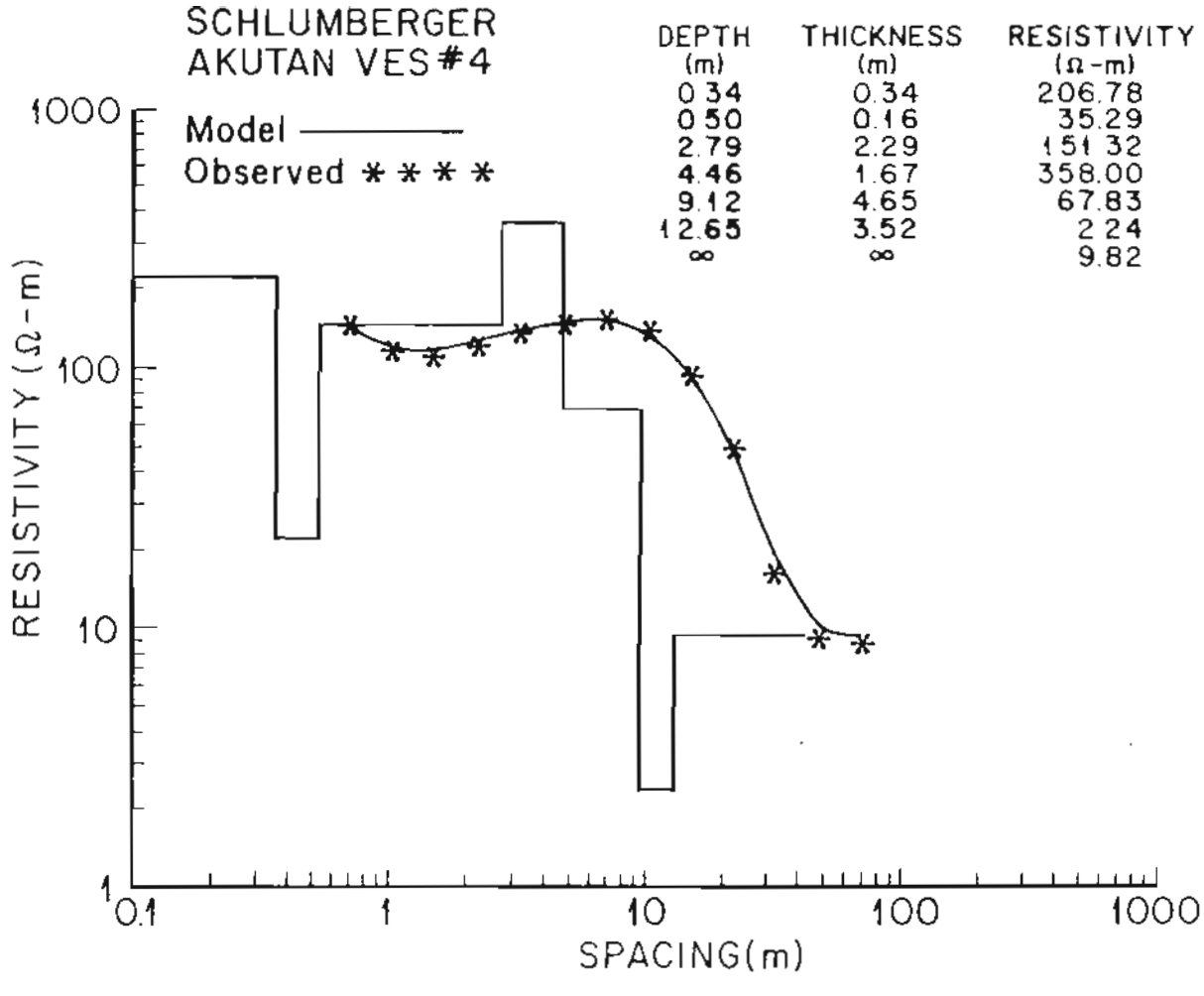
SCHLUMBERGER
AKUTAN VES#4
Model
Observed * * * *
DEPTH (m)
THICKNESS (m)
RESISTIVITY (Ω-m)
0.34 0.34 206.78
0.50 0.16 35.29
2.79 2.29 151.32
4.46 1.67 358.00
9.12 4.65 67.83
12.65 3.52 2.24
∞ ∞ 9.82
RESISTIVITY (Ω-m)
1000
100
10
1
0.1
1
10
100
1000
SPACING(m)

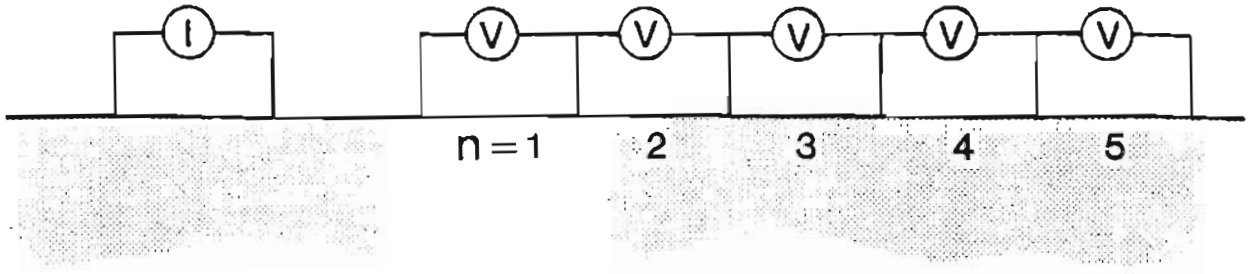
I
V
V
V
V
V
n = 1
2
3
4
5

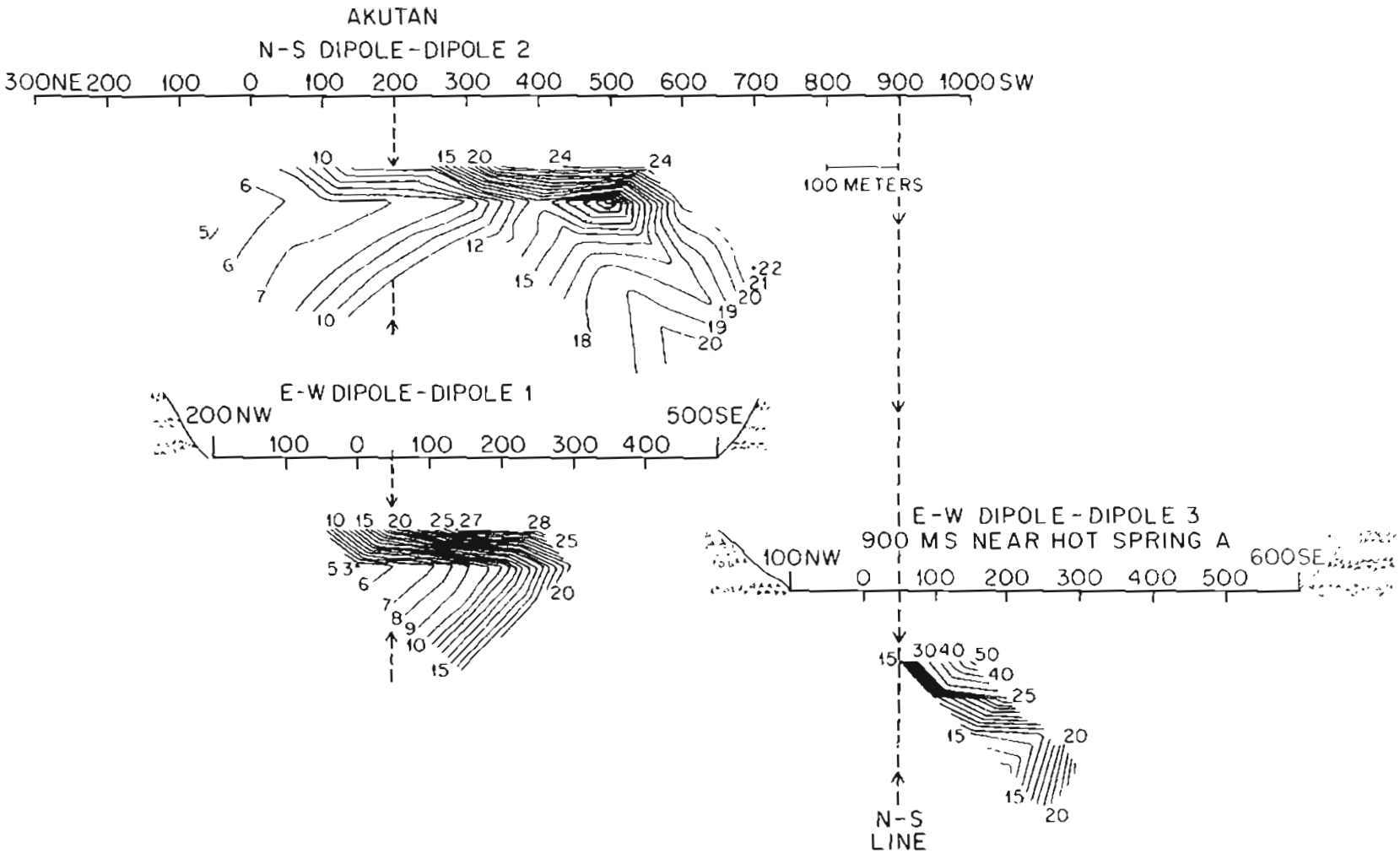
AKUTAN
N-S DIPOLE-DIPOLE 2
300NE 200 100 0 100 200 300 400 500 600 700 800 900 1000 SW
100 METERS
E-W DIPOLE-DIPOLE 1
200 NW
500 SE
100 0 100 200 300 400
E-W DIPOLE-DIPOLE 3
900 MS NEAR HOT SPRING A
100 NW
600 SE
0 100 200 300 400 500
N-S
LINE

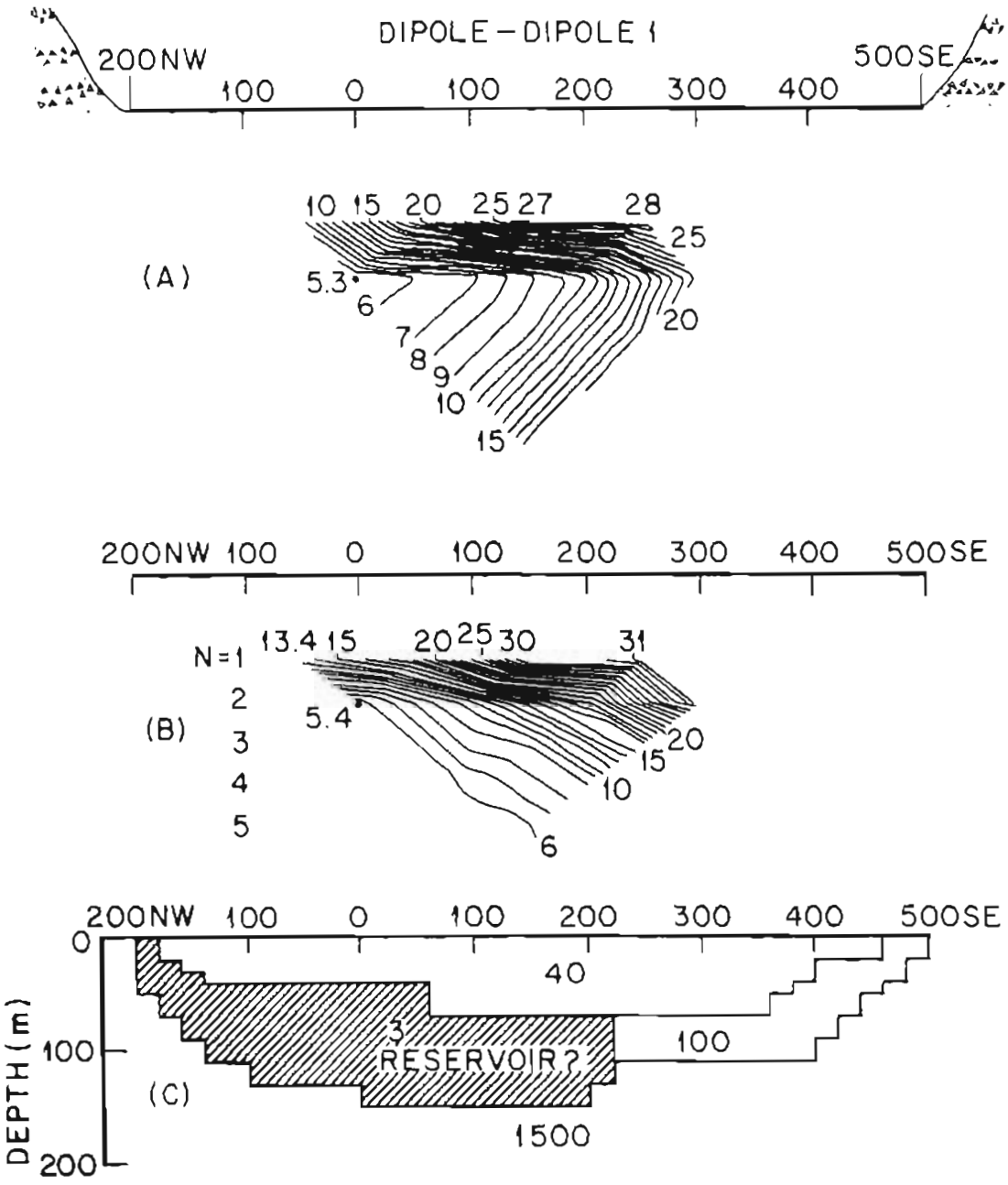
DIPOLE – DIPOLE 1
200NW
500SE
100 0 100 200 300 400
(A)
10 15 20 25 27 28
25
5.3
6
7
8
9
10
15
20
200NW 100 0 100 200 300 400 500SE
N=1
2
3
4
5
(B)
13.4 15 20 25 30 31
5.4
20
15
10
6
200NW 100 0 100 200 300 400 500SE
0
100
200
DEPTH (m)
40
3
RESERVOIR?
100
(C)
1500

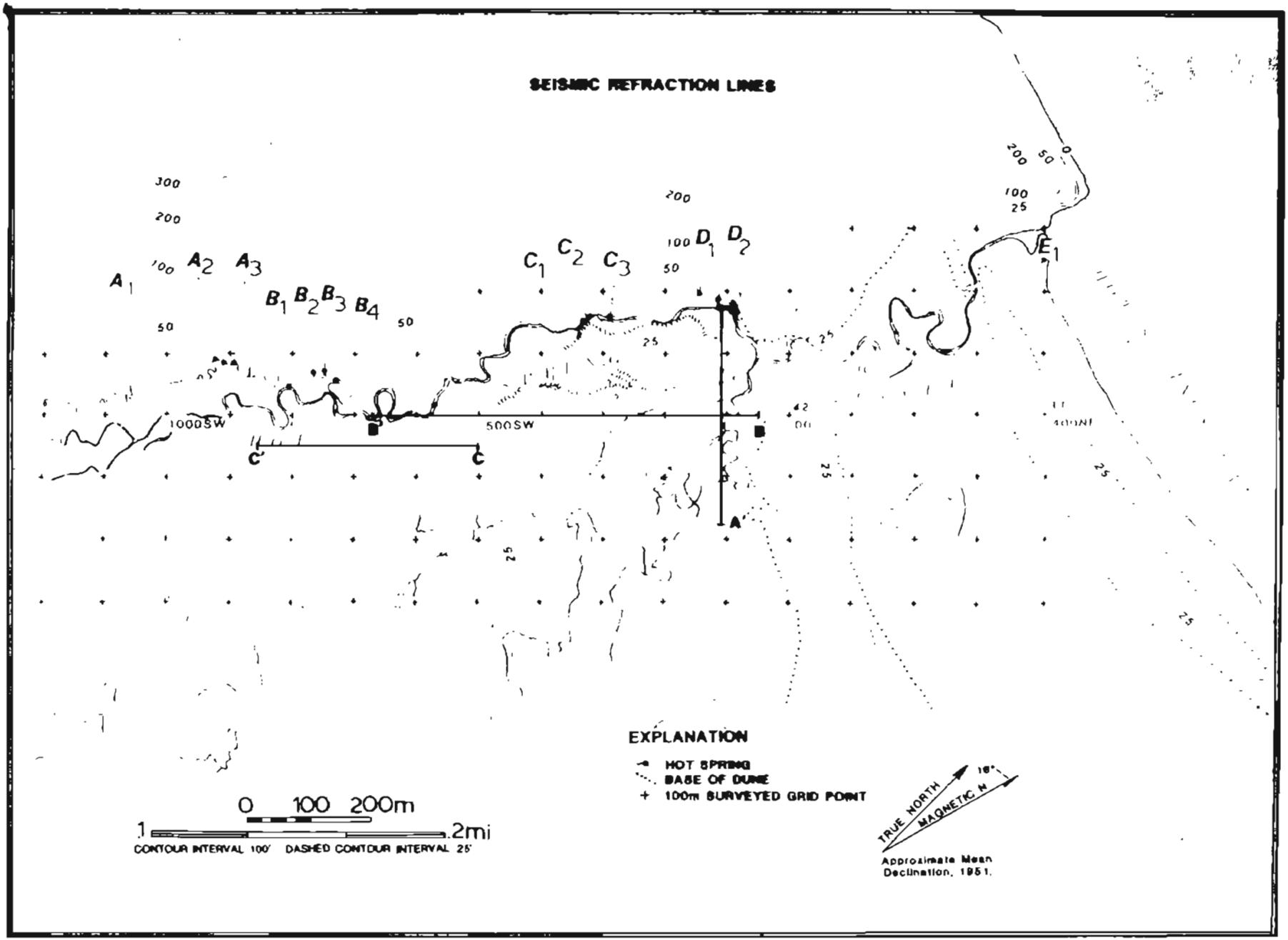
SEISMIC REFRACTION LINES
A1
A2
A3
B1
B2
B3
B4
C1
C2
C3
D1
D2
E1
1000SW
500SW
400NE
A
B
B
C
C
EXPLANATION
HOT SPRING
BASE OF DUNE
100m SURVEYED GRID POINT
0 100 200m
1 .2mi
CONTOUR INTERVAL 100' DASHED CONTOUR INTERVAL 25'
TRUE NORTH
MAGNETIC N
16°
Approximate Mean
Declination, 1951.

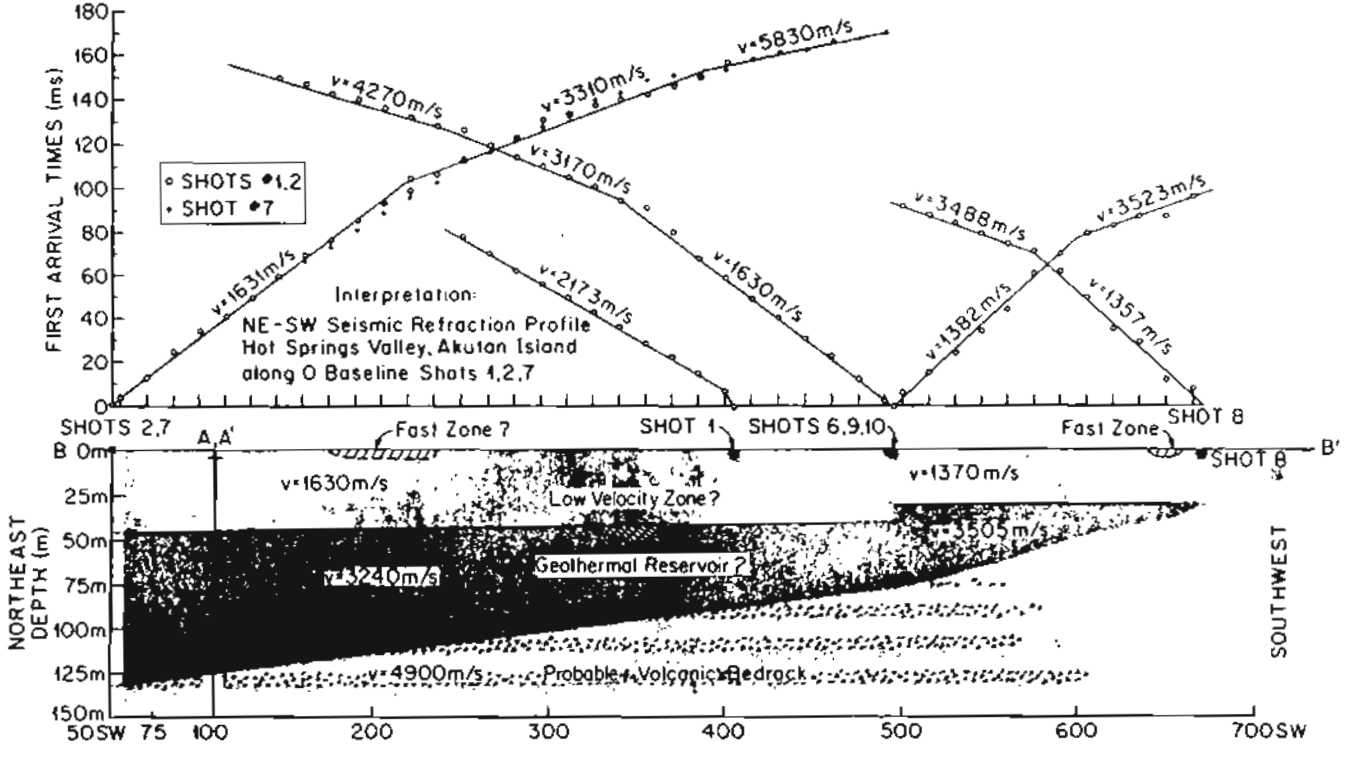
FIRST ARRIVAL TIMES (ms)
180
160
140
120
100
80
60
40
20
0
o SHOTS 1,2
• SHOT 7
v=1631m/s
v=4270m/s
v=3310m/s
v=5830m/s
v=3170m/s
v=1630m/s
v=2173m/s
v=3488m/s
v=3523m/s
v=1382m/s
v=1357m/s
Interpretation:
NE-SW Seismic Refraction Profile
Hot Springs Valley, Akutan Island
along O Baseline Shots 1,2,7
SHOTS 2,7
A
A'
Fast Zone ?
SHOT 1
SHOTS 6,9,10
Fast Zone
SHOT 8
B
B'
0m
25m
50m
75m
100m
125m
150m
v=1630m/s
Low Velocity Zone?
v=1370m/s
v=3505m/s
v=3240m/s
Geothermal Reservoir ?
v=4900m/s
Probable Volcanic Bedrock
NORTHEAST
DEPTH (m)
SOUTHWEST
50SW
75
100
200
300
400
500
600
700SW

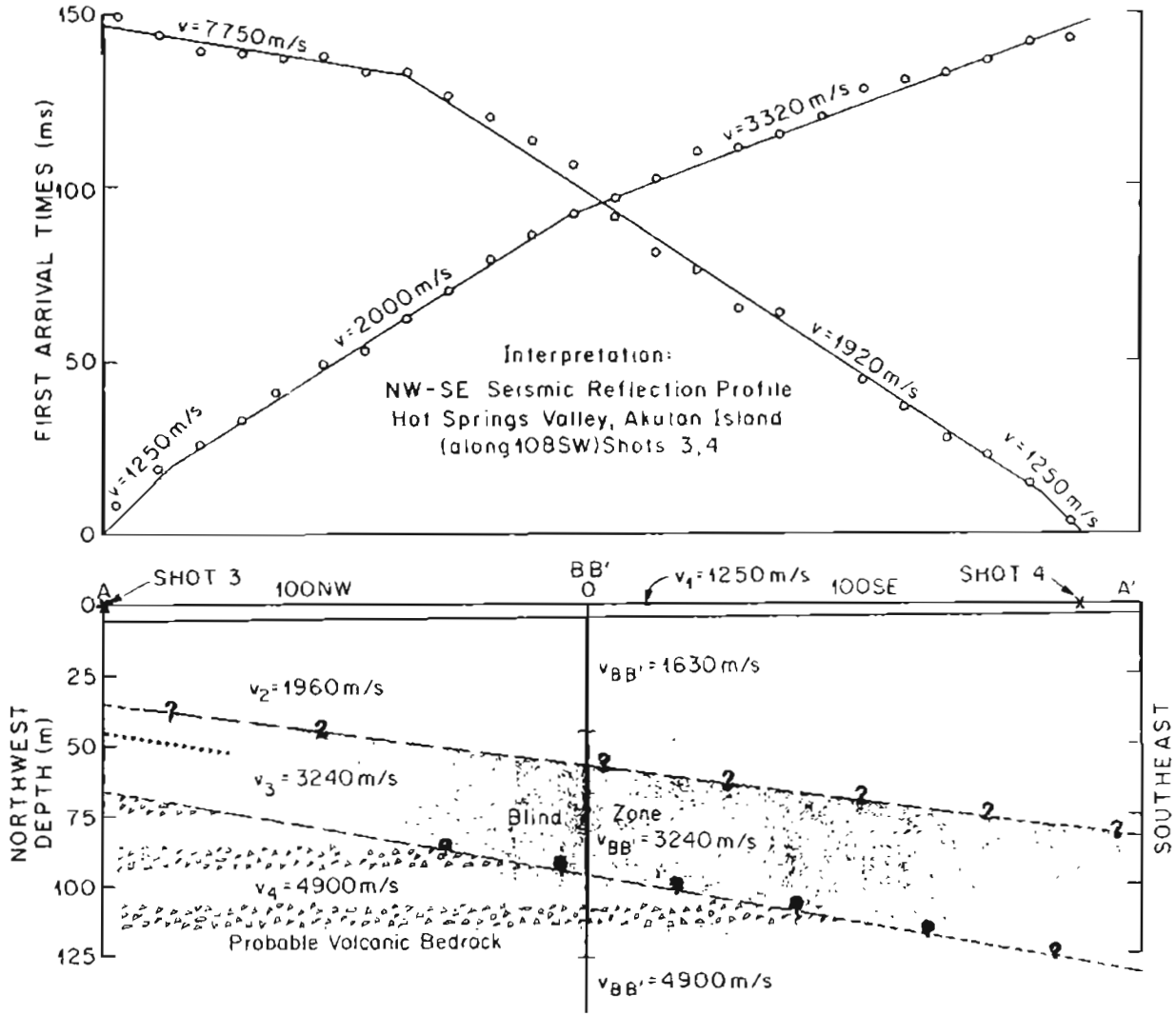
FIRST ARRIVAL TIMES (ms)
150
100
50
0
v=7750m/s
v=3320m/s
v=2000m/s
v=1250m/s
v=1920m/s
v=1250m/s
Interpretation:
NW-SE Seismic Reflection Profile
Hot Springs Valley, Akutan Island
(along 108SW) Shots 3, 4
A
SHOT 3
100NW
BB'
0
v_1=1250m/s
100SE
SHOT 4
A'
NORTHWEST
DEPTH (m)
0
25
50
75
100
125
v_2=1960m/s
v_3=3240m/s
v_4=4900m/s
Blind Zone
$v_{BB'}$=1630m/s
$v_{BB'}$=3240m/s
$v_{BB'}$=4900m/s
Probable Volcanic Bedrock
SOUTHEAST

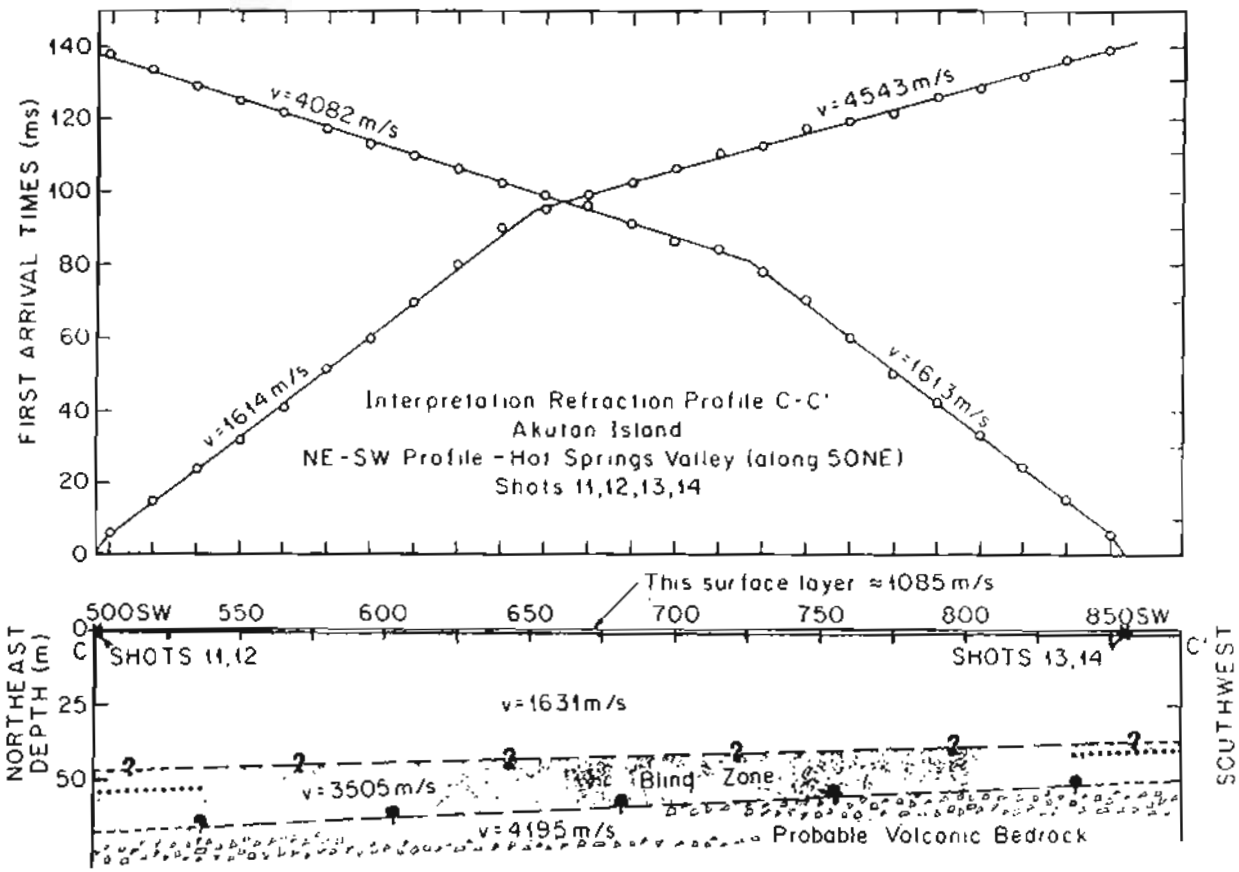
FIRST ARRIVAL TIMES (ms)
140
120
100
80
60
40
20
0
v=4082 m/s
v=4543 m/s
v=1614 m/s
v=1613 m/s
Interpretation Refraction Profile C-C'
Akutan Island
NE-SW Profile - Hot Springs Valley (along SONE)
Shots 11,12,13,14
This surface layer ≈1085 m/s
500SW
550
600
650
700
750
800
850SW
NORTHEAST
DEPTH (m)
0
C
SHOTS 11,12
SHOTS 13,14
C'
SOUTHWEST
v=1631 m/s
25
50
v=3505 m/s
Bling Zone
v=4195 m/s
Probable Volcanic Bedrock

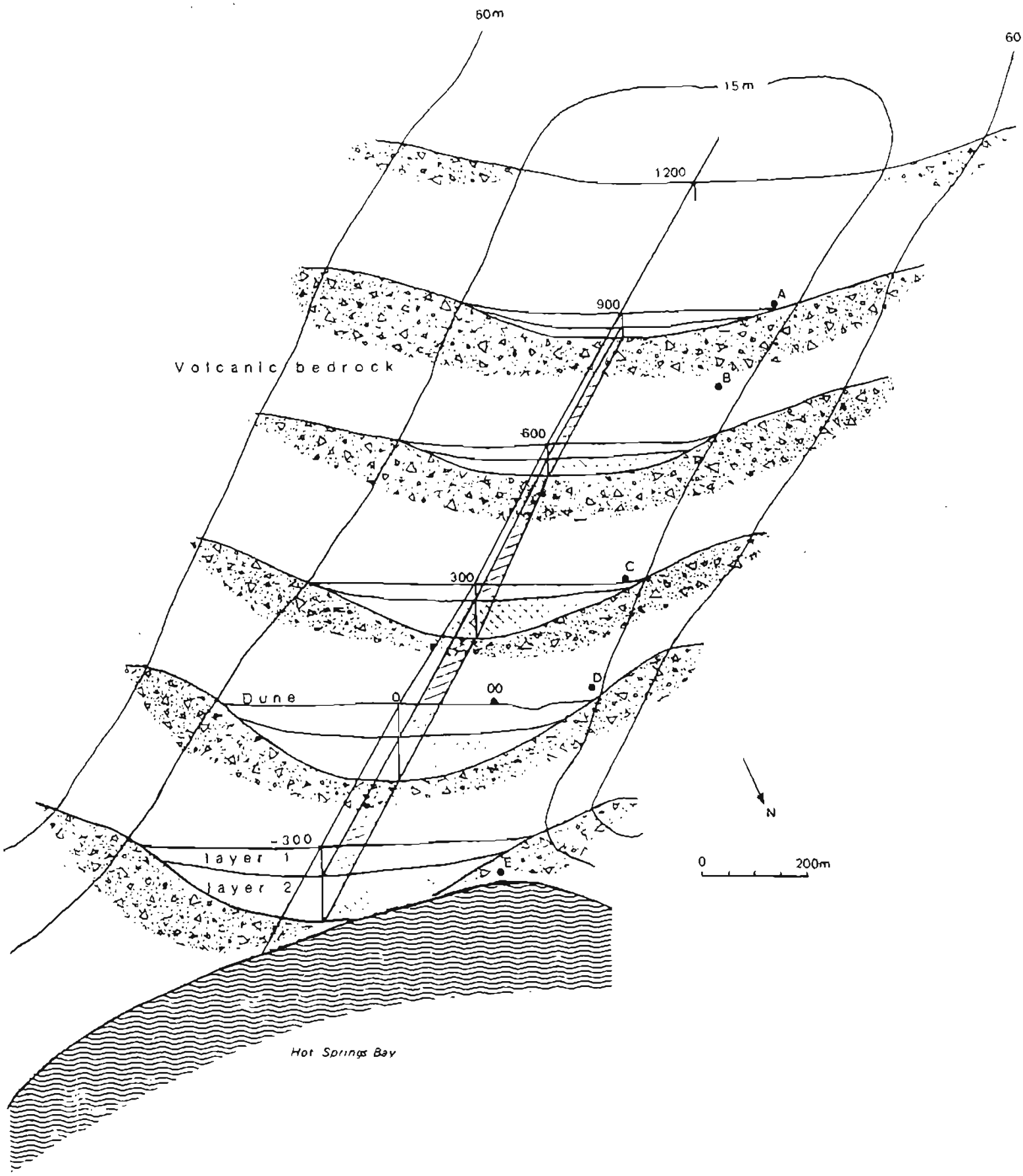
60m
60
15m
1200
900
A
Volcanic bedrock
B
600
300
C
Dune
O
00
D
N
-300
layer 1
layer 2
E
0
200m
Hot Springs Bay

CHAPTER 5

HELIUM AND MERCURY SOIL SURVEYS

by

Eugene M. Wescott, Donald L. Turner, William Witte,

and Becky Petzinger

Geophysical Institute, University of Alaska,

Fairbanks, Alaska 99701

INTRODUCTION

The concentrations of helium and mercury in soil and in water have been shown to be useful indicators of geothermal resources [Roberts, (1975); Roberts, et al., (1975), Bergquist, (1980); Matlick and Buseck, (1975)]. In Alaska, helium and mercury surveys in the Chena Hot Springs area (Wescott and Turner, 1981a), at Pilgrim Springs (Wescott and Turner, 1981b), Summer Bay Warm Springs, Unalaska Island (Wescott and Turner, 1982a) (Republic Geothermal Inc., 1983) and Manley Hot Springs, (East, 1982) have shown excellent correlations with areas of upwelling of geothermal waters.

HELIUM SURVEY

The radioactive decay of uranium and thorium is the source of helium in the earth. Helium is chemically inert, physically stable, and quite soluable in ground water at depth, but sparingly soluable under ambient conditions. It's practically nonabsorbable, highly mobile and therefore able to penetrate thousands of meters of overburden. Helium is present in the atmosphere at a spatially and temporally low constant abundance level of 5.239 ppm (Gluekauf, 1946; Pogorski and Quirt, 1981). The solubility of helium in water increases with temperatures above 30°C, making geothermal waters efficient scavengers of helium (Mazor, 1972). As the geothermal waters rise towards the surface, helium is released due to cooling and de-pressurization.

Helium occurs in soil in several ways: a) trapped in the crystal lattice of soil grains; b) as gas in macro or intercrumb pore space; c) dissolved in the water film on soil grains; d) in micro or crumb pore spaces; e) in gas bubbles in the soil fluid; and f) dissolved in water. Helium in macro or

intercrumb pore spaces was sampled by driving a hollow collection tube about 75 cm into the ground and drawing off a gas sample in a syringe. The gas was then introduced into a small evacuated steel 'CO_2' cartridge and sealed. This technique only works well where the soil is fairly dry and free of rocks.

Helium in water films on soil grains, in micro or crumb pore spaces and in bubbles in water-filling pore spaces was sampled by augering a soil core sampler about 75 cm into the ground, placing the bottom soil core in a steel can and sealing it.

Water samples were collected in a 500 ml sample bottle to 85% of volume, capped immediately with an air tight cap equipped with a septum. The bottle was shaken vigorously for 30 seconds to allow the helium dissolved in the water to equilibrate with the air space above the water, then a gas sample was drawn off by syringe through the septum and inserted into an evacuated steel cartridge as in the soil gas sampling technique. In the case of soil samples, a gas sample is drawn off from the head space in the can after sufficient time has elapsed to allow the helium in the soil to equilibrate with the air in the head space.

The helium analysis was done at Western Systems, Inc., Morrison, Colorado, by mass spectrometry with a precision of 10 ppb.

Research in the past few years has shown that we cannot simply relate the helium concentration values derived from the three separate sampling methods. The 'water' samples are usually much higher than the soil head space or soil gas values. Soil head space values must be corrected for a number of parameters to derive a pore space concentration including: soil and air temperature, barometric pressure at the time of collection, and water content and soil density. In addition, it is important to also measure and

correct for light hydrocarbons, some of which may be generated in the soil by bacterial action after canning. Only raw uncorrected values were used in the survey of Hot Springs Bay Valley. We know from our recent research that anomalously high raw helium values represent valid anomalies regardless of whether or not the corrections discussed above are made.

The average atmospheric concentration of helium is 5.239 ppm (Gluekauf, 1946). Depending on the production rate, transport, and trapping in the soil, the background pore space He concentration may vary somewhat from that value.

The Aleutian basaltic and basaltic-andesite rocks are likely to contain much less uranium and thorium than the more acidic igneous and metamorphic rocks of the interior Alaska and Seward Peninsula hot springs areas. Telford and others (1976) list the average basalt to have 13% Th and 15% U of the average granite. Thus we would expect Aleutian helium anomalies to be less pronounced. It is of interest to compare the values obtained from 4 Akutan hot spring water samples with samples from Manley Hot Springs in the Alaskan interior. The Akutan water samples are about 22% above the atmospheric background: 6.56, 6.41, 6.57 and 6.05 ppm. In comparison, water samples from Manley Hot Springs at 30 ppm are 573% above background, consistent with the higher He production rate in the acidic plutonic and metamorphic rocks of that area (East, 1982). This result supports our suggestion that significant He anomalies on Akutan should be of less absolute value than at Manley Hot Springs or other similar Alaskan geothermal areas.

Figure 5-1 shows an enlarged portion of Hot Springs Bay Valley with the helium soil concentrations and the 25 and 10 ohm-m near-surface EM-31 resistivity contours. Soil gas samples are not shown because the two types of helium sample data cannot be directly compared.

To allow for the dispersion of duplicate soil measurements, the variations in sampling conditions, and correction factors not included in this analysis, we have chosen a soil He value of 5.40 ppm and above as anomalous. Compared to other Alaskan localities with higher U and Th backgrounds this is a conservative value. As can be seen in figure 5-1, most of the samples are anomalous by this criterion. Several are greater than 6.0 ppm. Note that the anomalous He values extend several hundred meters towards the center of the valley away from the hot springs and the near-surface low resistivity contours.

The pattern of helium anomalies is probably distorted by the production of other gases in the organic-rich marsh. There are three samples which are below the atmospheric concentration of 5.24 ppm, one as low as 4.84 ppm. Friedman (personal communication, 1981) has found similar anomalously low helium values in other surveys, and has ascribed this phenomenon to dilution of the helium content of the soil gas by other gases such as CH_4 and CO_2. Thus, since we know some sample sites show anomalously low values below the atmospheric value of 5.24, others which are above 5.24 may have also been lowered by this effect. Because the sample analysis did not include other gases, such as CO_2 and CH_4, we cannot correct for this effect. However, the effect of such a correction would only increase the size of the observed anomalies.

MERCURY SURVEY

Mercury content in soils has also been reported as a possible indicator of geothermal resources (Matlick and Buseck, 1975). They confirmed a strong association of Hg with geothermal activity in three of four areas tested

(Long Valley, California; Summer Lake and Klamathe Falls, Oregon). Mercury deposits often occur in regions containing evidence of hydrothermal activity, such as hot springs (White, 1967).

Mercury is highly volatile. Its high vapor pressure makes it extremely mobile, and the elevated temperatures near a geothermal reservoir tend to increase this mobility. The Hg migrates upwards and outwards away from the geothermal reservoir. Such aureoles are typically larger in area than a corresponding geothermal helium anomaly.

We collected 15 soil samples about 10 cm below the organic layer. The samples were air dried in the shade and sized to -80 mesh using a stainless steel sieve. The -80 portions were stored in airtight glass vials for later analysis. The Hg content of the sample was determined by use of a Jerome Instrument Corp., model 301 Gold Film Mercury detector with sensitivity of better than 0.1 ng of Hg. A standard volume of -80 mesh soil (0.25 cc) was placed in a quartz bulb and heated for one minute to volatalize absorbed Hg which was collected on a gold foil. Heating of the gold foil releases the Hg for analysis as a gas in the standard manner. Calibration is accomplished by inserting a known concentration of Hg vapor with a hypodermic syringe.

The background concentration of Hg in soils varies widely from area to area, and must be determined from a large number of samples. It is generally on the order of 10 parts per billion. We calculated a mean value of 139 ppb for the 15 samples collected at Hot Springs Bay Valley and used that as an anomaly level.

Republic Geothermal conducted a mercury soil survey on Makushin Volcano, Unalaska Island, as part of their exploration for geothermal drilling sites (Republic Geothermal, 1983). They found an analytical range of 230 soil samples between 8 and 31,450 ppb, with an average value of 454 ppb, a median

value of 60 ppb and a mode of 36 ppb. On their map they used 36 ppb as the background value, and contoured 3 x background (108 ppb), 5 x background (180 ppb), and 7 x background (324 ppb).

Figure 5-2 shows a map with the Akutan mercury values plotted on our grid system. One of the largest values of 395 ppb us at 0 NW, 100 S, several hundred meters away from the near-surface temperature anomalies. As we did not sample the complete grid system, we cannot make a definitive statement regarding the mercury pattern. We note, however, that practically all of our samples are above the Makushin background, and three are greater than seven times the Makushin background.

DISCUSSION AND CONCLUSIONS

Compared to other areas where we have investigated He and Hg soil concentrations in geothermal areas, values in Hot Springs Bay Valley would be considered anomalously high. From the water sampling the He values are low compared to continental hot springs areas, which makes the He soil anomalies even more significant. The mercury values were not really numerous enough to draw many conclusions, but in terms of the Makushin Volcano surveys (Republic Geothermal, 1983) the values would be significant anomalies.

Both He and Hg values are high toward the center of the valley, away from the hot springs and the sinuous near-surface, low resistivity patterns. Wescott and others (this report), have suggested the sinuous pattern represents a buried stream channel of high porosity and permeability which allows hot water to come up through the volcanic debris flow capping a geothermal reservoir. The He and Hg data are the only data which might indicate where the hot water is coming up into the reservoir from below.

Data suggests the reservoir may be fed from a conduit system further out into the valley than the buried stream channel. This suggests that a more complete and detailed mercury soil sampling survey might be useful in choosing a drilling site to locate the conduit system bringing hot water up into the reservoir, where mixing with colder water may occur.

REFERENCES CITED

Bergquist, L.E., 1980, Helium: An exploration tool for geothermal sites, Geothermal Resources Council Transactions, v. 3, p. 59-60.

East, J., 1982, Preliminary investigations at Manley Hot Springs, Alaska, U. of Alaska, Geophysical Institute Report UAG R-290, p. 52-65.

Glueckauf, E., 1946, A micro-analysis of the helium and neon contents of air; Proceedings of the Royal Society of London, V185, p. 98-119.

Matlick, J.S., III, and P.R. Buseck, 1975, Exploration for geothermal areas using mercury: a new geochemical technique, in Proceedings, Second United Nations Symposium on the Development and Use of Geothermal Resources, v. 1, p. 785-792.

Mazor, E., 1972, Paleotemperatures and other hydrological parameters deduced from noble gases dissolved in groundwaters; Jordan Rift Valley, Israel, Geochimica et Cosmochimica Acta, v. 36, p. 1321-1326.

Pogorski, L.A., and G. Stewart Quirt, 1981, Helium Emanometry in exploring for hydrocarbons: Part 1, Unconventional Methods in Exploring for Petroleum and Natural Gas II, Benjamin M. Gottlieb, ed., SMU Press, Dallas, Texas, p. 124-135.

Republic Geothermal, 1983, The Unalaska Geothermal Exploration Project, Phase 1B, Final Report, Alaska Power Authority, v. 1, p. 29-36.

Roberts, A.A., 1975, Helium surveys over known geothermal resource areas in the Imperial Valley, California: U.S. Geological Survey Open-file Report, p. 75-427, 6 pl.

Roberts, A.A., I. Friedman, T.J. Donovan, and E.H. Denton, 1975a, Helium survey, a possible technique for locating geothermal reservoirs, Geophysical Research Letter, 2 (6), p. 209-210.

Wescott, E.M., and D.L. Turner, 1981a, A geological and geophysical study of the Chena Hot Springs geothermal area, Alaska, University of Alaska, Geophysical Institute Report UAG R-283, p. 54-61.

Wescott, E., and D.L. Turner, eds., 1981b, Geothermal reconnaissance survey of the central Seward Peninsula, Alaska, University of Alaska, Geophysical Institute Report UAG R-284, p. 37-59.

Wescott, E., and D.L. Turner, 1982a, Geothermal energy resources assessment of parts of Alaska, Final report to the Division of Geothermal Energy of USDOE, under cooperative agreement DE-FC07-79-EI-27034, p. 44-46.

White, D.E., 1967, Mercury and base-metal deposits with associated thermal and mineral waters, in Barnes, H.L., ed., Geochemistry of hydrothermal ore deposits, New York, Holt, Rinehart, and Winston, p. 575-631.

FIGURE CAPTIONS

Figure 1. Map of Hot Springs Bay Valley with helium soil sample concentrations. The contours are 25 ohm-m and 10 ohm-m near-surface resistivity values from Wescott and others (this report). Note the presence of anomalously high He values near the valley center, away from the hot springs.

Figure 2. Map of Hot Springs Bay Valley with mercury soil concentrations. The contours are 25 ohm-m and 10 ohm-m near-surface resistivity values from Wescott and others (this report). Note the anomalously high Hg values extending out into the valley away from the hot springs and low resistivity patterns.

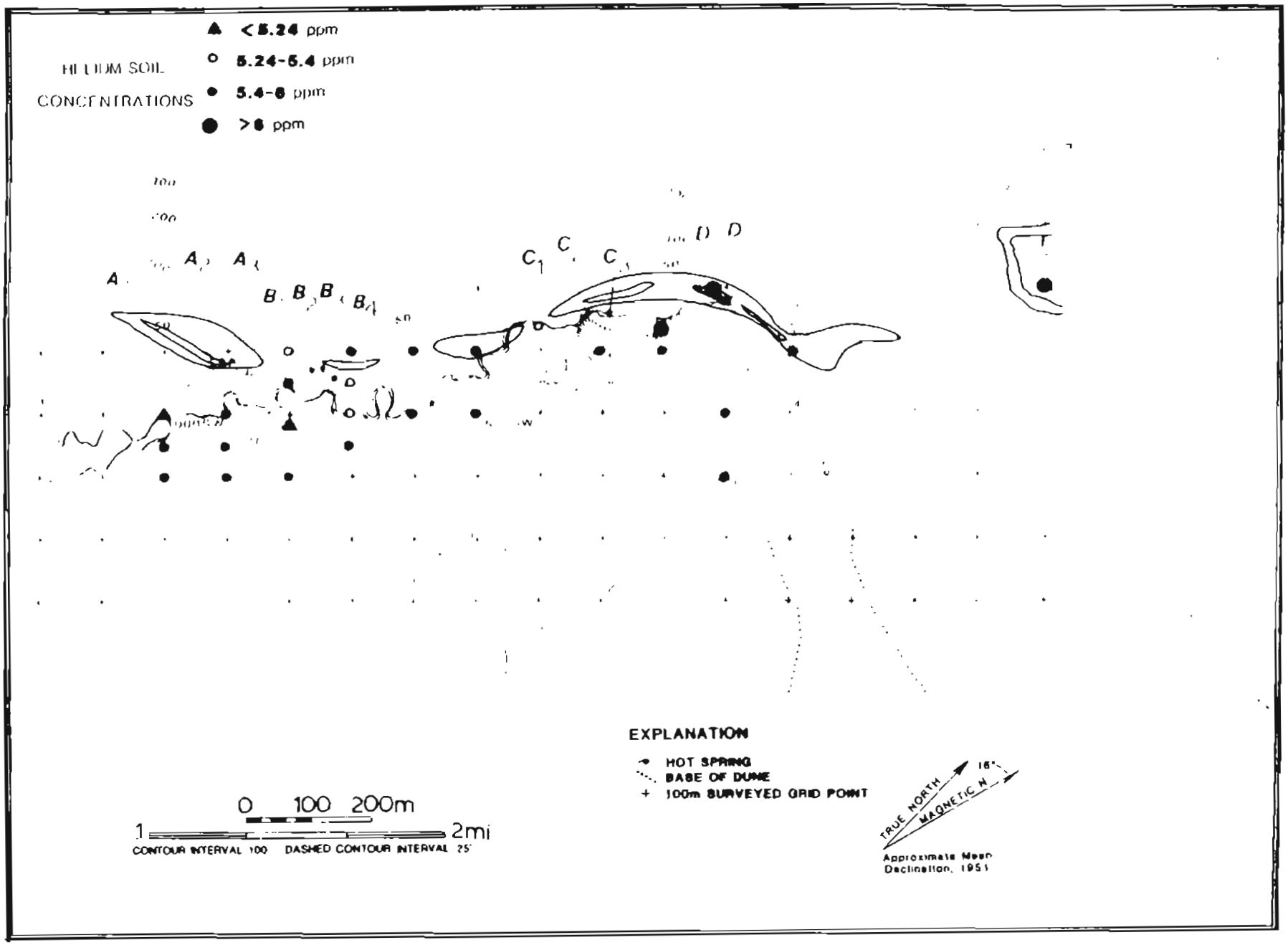
HELIUM SOIL CONCENTRATIONS
< 5.24 ppm
5.24-5.4 ppm
5.4-6 ppm
> 6 ppm
A
A1
A2
B
B1
B2
B3
C
C1
C2
C3
D
D1
EXPLANATION
HOT SPRING
BASE OF DUNE
100m SURVEYED GRID POINT
0 100 200m
1 2mi
CONTOUR INTERVAL 100 DASHED CONTOUR INTERVAL 25'
TRUE NORTH
MAGNETIC N
16°
Approximate Mean Declination, 1951

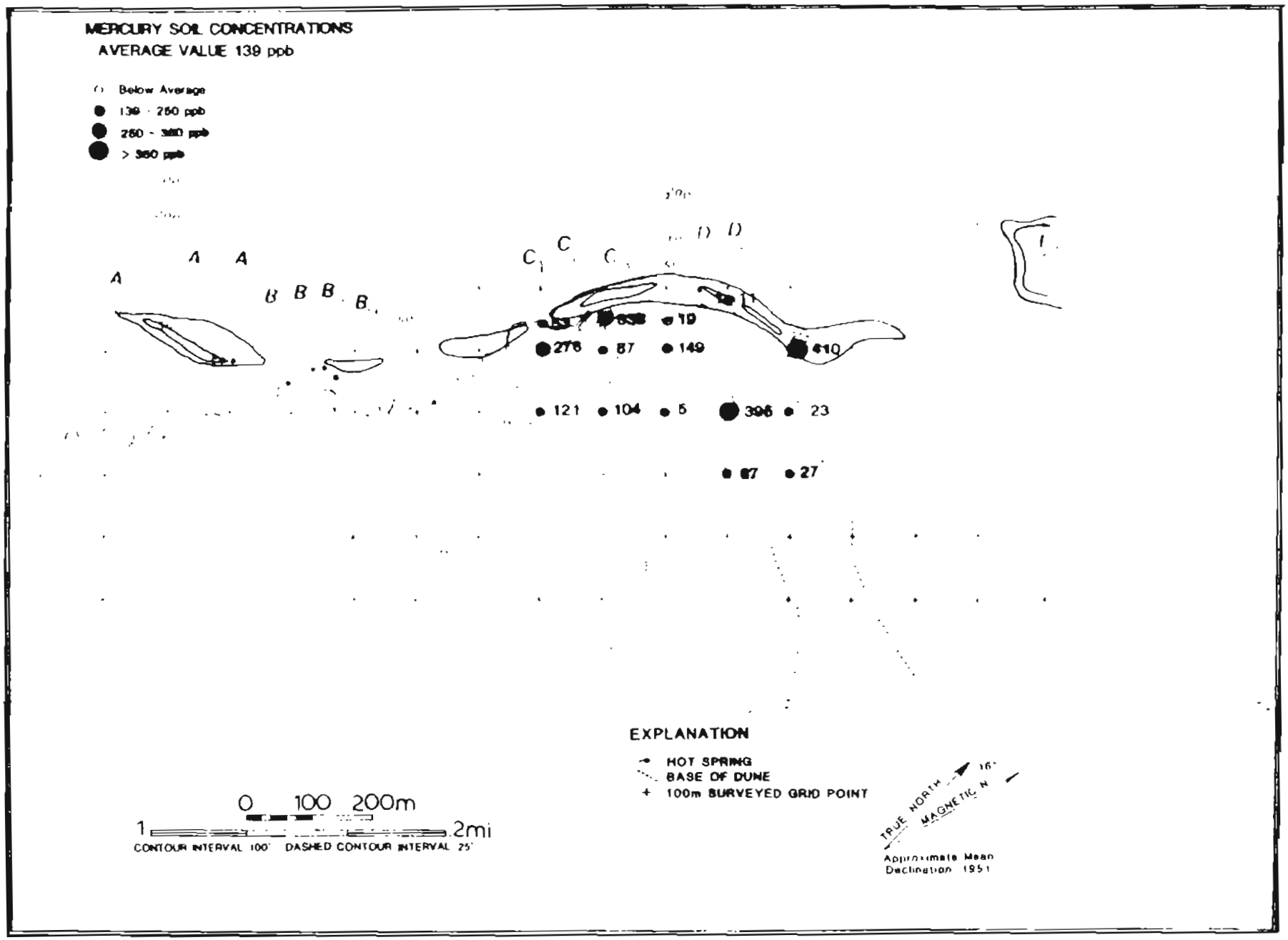
MERCURY SOIL CONCENTRATIONS
AVERAGE VALUE 139 ppb
Below Average
139 - 280 ppb
280 - 360 ppb
> 360 ppb
A A A
B B B B
C C C
D D
19
276
87
149
410
121
104
5
396
23
87
27
EXPLANATION
HOT SPRING
BASE OF DUNE
100m SURVEYED GRID POINT
0 100 200m
1 2mi
CONTOUR INTERVAL 100' DASHED CONTOUR INTERVAL 25'
TRUE NORTH
MAGNETIC N
Approximate Mean Declination 1951

CHAPTER 6

GEOCHEMISTRY OF THERMAL SPRINGS AND FUMAROLES, HOT SPRINGS BAY VALLEY AKUTAN ISLAND, ALASKA

by

Roman J. Motyka[1], Mary A. Moorman[1], and Robert J. Poreda[2]

[1]Alaska Division of Geological and Geophysical Surveys, Fairbanks, Alaska
[2]Scripps Institute of Oceanography, La Jolla, California

INTRODUCTION

Investigations of fluids associated with the thermal springs and fumarole field located in Hot Springs Bay Valley were undertaken to help assess the nature and extent of the underlying hydrothermal system, and to provide estimates of reservoir temperatures. Reconnaissance visits of the springs were made by Byers and Barth (1953), Baker and others (1977), and Motyka and others (1981). The latter study provided the impetus for selecting Akutan for the more detailed geothermal exploration which was carried out in July, 1981. The springs and fumaroles were sampled once again during a one-day visit to the site on August 31, 1983.

The results of the analyses and geothermometry discussed below provide evidence that the thermal spring waters are derived in part from hot water reservoirs with temperatures of 170-190°C. Upon ascent from the reservoirs, the thermal waters are first cooled by mixing with meteoric waters at shallow levels, probably below a capping volcanic debris flow layer. The waters then further cool conductively before emerging at the surface. Thermal spring water chemistry and mixing models suggest the reservoirs contain fairly dilute NaCl waters with Cl levels of ~600 ppm. The similarity of stable isotopic composition of the thermal spring waters to surface stream waters indicate the reservoir is charged by local meteoric waters.

Fumaroles at the head of the valley are probably fed by gases and steam boiling off from a hot water reservoir at deeper levels. Gas geothermometry suggests a reservoir temperature of ~190°C. The carbon isotope ratios in CO_2 and CH_4 and the large proportion of CH_4 present in the gases collected from the fumaroles and hot springs indicate thermogenic breakdown of organic sediments as one of the sources of carbon in the system. The relatively heavy

carbon 13 composition of fumarolic carbon dioxide and the $^{3}He/^{4}He$ ratios of 6.5-7.0 reflect a probable magmatic influence on the hydrothermal system.

THERMAL AREAS

The Akutan hot springs are located in lower Hot Springs Bay Valley, about 4 km northwest of Akutan Harbor and 10 km northeast of Akutan Volcano (fig. 6-1, plates 1 and 2). Five separate groups of thermal springs emanate along Hot Springs Creek in a 1.5 km long zone at the base of the west valley wall. The thermal spring waters issue from fissures in travertine cemented volcanic debris-flow deposits exposed in stream banks (groups A, C, and D), from pools in the valley floor (A, B, and D), and through beach sands (E). Temperature measurements made in creek-bed gravels and increases in chemical concentrations of stream waters show that thermal waters are also discharging directly into Hot Springs Creek and its western tributary below A.

The hottest springs are the southern most, group A, with temperatures as high as 85°C. Temperatures at B, which consists of several shallow pools, range from 38.5 to 50°C. Vent temperatures at C range from 40 to 75°C. Warm temperatures were measured in an adjacent gravel bar indicating discharge of thermal waters directly into the stream. Vent temperatures at site D vary from 26 to 54°C. Elevated temperatures were measured in stream gravels and bars indicating direct discharge of thermal waters into the stream here also. The most northerly group, E, occurs on the shores of Hot Springs Bay in the intertidal zone east of the mouth of Hot Springs Creek (fig. 6-1). Temperatures greater than local surface waters were found at depths of 10 cm or more in the sands over a 2,500 m^2 area of intertidal beach. The highest temperatures (63°C) are adjacent to the outflow channel of Hot Springs Creek.

In addition to the lower valley thermal springs, a solfatara field occurs at an elevation of 350 m (1150 ft), near the head of Hot Springs Bay Valley (Plate 1). The field consists of a series of low to moderately pressurized fumaroles, mildly steaming ground, and boiling acid-sulfate springs covering an area of about 5,000 m^2. Temperatures of the fumaroles and pools are at or near atmospheric boiling point. An aureole of argillic alteration surrounds the solfatara field.

A reconnaissance was made of the rest of the island and visible thermal activity elsewhere appears restricted to the active Akutan Caldera and a still-warm 1978 andesitic lava flow on the north flank of the volcano.

THERMAL WATERS

Water Chemistry

Samples of thermal spring waters were collected as close to the issuing vent as possible, then filtered through 0.45 micron filters. The sample suite normally consisted of 1 liter each of filtered untreated and filtered acidified (HCl) waters; 100 ml 1:10 and 1:5 diluted samples for silica determinations; and 30 ml samples for stable isotope determinations. In addition, raw untreated samples were collected for field determinations of HCO_3, pH, and H_2S. At spring A3, 1 liter of filtered water was collected and treated with formaldehyde for $\delta^{18}O$, H_2O-SO_4 geothermometry, and 1 liter of untreated water was collected for tritium analysis. Representative stream and cold spring waters were also collected.

HCO_3, pH, and H_2S concentrations were determined in the field following methods described in Presser and Barnes (1974). The remaining constituents

were analyzed at the DGGS Geothermal Fluids Laboratory in Fairbanks except as noted in tables 6-1 and 6-2. Major and minor cation concentrations were determined using a Perkin-Elmer atomic absorption spectrometer following standard procedures. Sulfates were determined by the titrimetric (thorin) method; fluorides by specific ion electrode; Cl by Mohr titration; bromide by hypochlorite oxidation and titration; and boron by colormetric carminic acid method. Silica concentrations were determined by the molybdate blue method.

Stable isotope ratios ($^{18}O/^{16}O$ and D/H) were analyzed at Southern Methodist University, Dallas, Texas, and at U.S. Geological Survey, Menlo Park, California. Tritium concentrations were determined at the University of Miami, Miami, Florida.

Results of the chemical analyses of the thermal spring waters are given in table 6-1; those for stream and cold spring waters are in table 6-2. Thermal spring waters from A through D are moderately concentrated sodium-chloride-bicarbonate waters with significant levels of boron. Thermal waters from E are much more saline, reflecting probable mixing with seawater in the intertidal zone. Stream and cold springs, as expected, are much more dilute but several of the samples exhibited relatively high levels of silica. These latter samples generally were taken below thermal spring sites and probably reflect influx of thermal waters.

The percentage cation content of Hot Springs Bay Valley thermal and surface meteoric waters are plotted in figure 6-2. The seawater dilution of springs E (No. 6) is readily apparent as is the dilution of thermal waters at Springs D with colder surface waters (cf. No. 5 to No. 16). The Na + K trend in meteoric waters reflects the sampling of valley stream waters above, near, and below site A respectively.

Thermal waters associated with the fumarole field at the head of the valley are highly acidic and appear to be locally derived surface waters heated by condensing steam and volcanic gases. The constituents in these thermal waters were probably leached from local rocks by the hot acid waters. The silica content of 220 ppm in one of the acid pools reflects the breakdown of silicates and equilibration of the waters to amorphous silica.

Stable Isotopes

Stable isotope compositions of the sampled waters are given in tables 6-1 and 6-2 and plotted in figure 6-3. Also plotted are Craig's (1961) meteoric water line and the Adak precipitation line (Motyka, 1982). Several distinctive features are noted. The first is the marked difference between the 1980 and 1981 isotopic compositions. Except for 15, both surface and thermal spring waters sampled in 1980 plot to the right of the meteoric water lines. No δD analysis is available for A3, 1980 (#1) but the $\delta^{18}O$ is similar to these samples. Waters sampled in 1981 are lighter and all plot left of the meteoric water lines. The differing compositions may reflect seasonal effects or perhaps some variation in average annual meteoric water composition.

A second feature is that the thermal spring waters are isotopically indistinguishable from the surface waters for each year. Thermal waters from hot water systems (T>150°C) are commonly found to have $\delta^{18}O$ positively shifted with respect to local meteoric waters by 1 to 5 mils through high-temperature exchange with silicates (Truesdell and Hulston, 1980). For example at the Makushin geothermal area on neighboring Unalaska Island, reservoir waters with temperatures of 190°C show a shift of 1.5 to 2 mil (Motyka and others, 1985). The lack of a detectable shift in $\delta^{18}O$ in Akutan thermal spring waters

indicates the waters are being diluted with meteoric water or the reservoir temperatures are insufficient to produce significant exchange. Geothermometry and evidence for mixing discussed later supports the former case.

A third feature of the isotope geochemistry is the distinctly heavier composition of spring E water which probably reflects the influence of seawater mixing.

Not plotted in figure 6-2 is the isotopic composition of waters from a fumarole field acid-sulfate pool (table 6-1). Its much heavier composition probably reflects evaporative concentration of heavy isotopes in the pool waters.

Geothermometry

Application of the more commonly used and accepted geothermometers to the Hot Springs Bay Valley thermal spring waters is given in table 6-3. Probable mixing of cold waters discussed below clouds the choice and interpretation of the geothermometers. Those based on ratios such as the cation geothermometers are the least susceptible to mixing problems. Of the Na/K thermometers, the one suggested by Arnorrson (1983) for basaltic terranes is considered the most applicable to the Akutan case. The Na-K-Ca thermometer generally gives a slightly higher or similar temperature. The single water-sulfate oxygen isotope geothermometer for spring A3 of 186°C is consistent with the two cation thermometers. Quartz geothermometers are likely to be affected by dilution and thus predict only minimum temperatures.

The cation and sulfate-water isotope geothermometers generally vary from 170 to 190°C; 185°C is chosen here as the most probable reservoir temperature

based on the average of the Na/K (4), Na-K-Ca (5), and H_2O-SO_4 (8) geothermometer determinations for spring A3.

Mixing

Several lines of evidence indicate that the thermal spring waters are a mixture of cold surface meteoric waters and deeper thermal waters. The strongest indication of mixing is the tritium content of 20.3 T.U. (tritium units) found in a water sample collected from spring A3. Panichi and Gonfiantini (1978) have reviewed the use of tritium as an indicator of age and mixing in geothermal systems. Tritium was introduced into the atmosphere in large quantities during the years of thermo-nuclear weapons testing following 1952. Since the test ban treaty of 1963, tritium in the atmosphere has steadily declined, but still remains at levels much greater than pre-1952. Because of its relatively short half-life (12.3 yrs), tritium provides a good marker for waters of recent age.

As a comparison to the Akutan A-3 waters, the weighted-average tritium content of precipitation in Anchorage in 1980 was 29 T.U., with seasonal variation ranging from the winter minimum of 16 T.U. to the late-spring maximum of 51 T.U. Samples of waters thought to be wholly or partially of recent meteoric origin collected in 1982 from the Makushin geothermal area on Unalaska Island varied from 6 T.U. to 37 T.U. In contrast, thermal reservoir waters collected from the Makushin test well had a tritium content of only 0.10 T.U. (Motyka and others, 1985).

The high tritium content of A3 waters thus means of one of two things: 1) the thermal reservoir waters are extremely young and turn-over time in the reservoir is very short; or 2) the thermal waters are being diluted with a

significant amount of surface meteoric waters. Evidence from Makushin and almost all other investigated hot water systems indicate residence times of waters in geothermal reservoirs are far greater than 25 yrs. Thus the mixing hypothesis is much more probable.

Additional evidence for mixing is the similarity in isotopic composition of surface meteoric waters and thermal spring waters. The presence of magnesium in all the spring waters, particularly D, is also indicative of cold water mixing. Magnesium is usually removed from high temperature waters (T>150°C) through hydrothermal reactions.

Further evidence for mixing comes from consideration of silica and chloride vs. enthalpy trends (figs. 6-4 and 6-5) and geothermometry (table 6-3). Geothermometry predicts reservoir temperatures of 170-190°C but spring temperatures are 85°C or less. Thus the reservoir waters must cool upon ascent either by conduction or mixing. The large flow rates of the springs indicate cooling must at least partially be due to mixing.

The linear trend of SiO_2 in spring waters vs. enthalpy is readily apparent in figure 6-4. The least squares fit (LSF) for the spring data (excluding D), however, intersects the silica axis at 53 ppm which is an improbable concentration for a cold water mixing end member. More probable is that mixing is occurring at deeper levels and the waters then cool conductively before emerging at the surface. Mixing line (M1) is drawn parallel to the LSF but constrained to pass through a point representing a cold water having silica composition of 10 ppm and temperature of 10°C, similar to uncontaminated surface stream waters in the valley. Intersection of M1 with the quartz solubility curve predicts a hot water temperature of ~170°C rather than the most probable estimated reservoir temperature based on cation and sulfate-water oxygen isotope geothermometer of ~185°C. It is

possible that after mixing the waters partially re-equilibrate during ascent to the surface. These trends are illustrated by mixing line M2 and points identified by primed letters. For example, waters emerging at Spring A are a mixture of reservoir cold waters (point A') which then conductively cool from ~135°C to 84°C and in the process lose about 15 ppm of SiO_2.

Although the relative amounts of cooling by mixing and conduction are conjectural, the general features of the preceding mixing model appear consistent with valley geology. The relatively impermeable volcanic debris flow capping the valley would prevent penetration and mixing of cold waters at shallow levels. Mixing would have to occur at intermediate levels perhaps through percolation of meteoric waters along the lateral margins of the valley.

Mixing is also apparent from the chloride-enthalpy diagram (fig. 6-5) but the situation appears more confused than the simple two-component mixing-model illustrated by the silica-enthalpy diagram. The data base is insufficient to adequately constrain the various mixing possibilities but the existence of two different intermediate hot water reservoirs is suggested by the chloride-enthalpy model.

The cold water end member is assumed to have 10 ppm chloride and a temperature of 10°C (pt. S), similar to uncontaminated valley waters. Following the procedures outlined by Fournier (1979), a ray is projected from the cold water point through thermal springs A to a deep thermal water, a. The enthalpy at a is assumed to be that of water at 185°C, the reservoir temperature predicted by cation and water-sulfate oxygen isotope geothermometry. This line passes close to spring B, indicating a common mixing line for these springs which is consistent with their close proximity to each other. Springs D and C plot far off the spring A mixing line indicating water

from more than one reservoir is involved. (Spring E is excluded from the analyses because of its probable seawater contamination.) Furthermore, the silica-enthalpy model predicts conductive cooling as well as mixing is occurring. To account for this latter effect, point A' is chosen as the mixed water which then conductively cools to A. Enthalpy of A' is from mixing line M2 off the silica-enthalpy diagram. A ray from S through A' intersects the 185°C enthalpy line at a' with a chloride concentration of 590 ppm. Although this new A' mixing line can account for springs A, B, and C, it cannot account for spring D, indicating that D is the product of a different mixing trend. In addition the silica model predicts considerably more conductive cooling for spring C than using mixing line A' would allow.

In the chloride-enthalpy diagram, mixing line C' was constructed in a manner analogous to that used for line A', i.e., using the spring C cation geothermometer to define end point c'. Another mixing line could be drawn for spring D but would unnecessarily complicate the diagram. The principal point of the argument is that hot water reservoirs having differing chloride compositions must be called upon to explain the mixing lines and spring compositions. The situation is further complicated by the fact that springs A, B, C, and D all have similar chloride to boron ratios (~40) which suggests a common parent reservoir.

Possible compositions and enthalpies for such parent reservoirs are represented by points X and X'. Point X was determined by the intersection of ray c' and the boiling line, X-a', through point a'. A water X could form C' and D' by mixing with S and form A' and B' by first boiling to point a', then mixing with S. Point X' provides another alternative whereby waters a' are formed by 1) conductive cooling from X'; or 2) mixing from X' to X then boiling to a'; or 3) boiling from X' to a'' then mixing to a'.

The problem with either X or X' is that there are no geothermometric indications of such high temperature fluids. Thus waters at a' and c' would need to remain in these intermediate reservoirs for a substantially long time to allow re-equalibration of cation geochemistry and water-sulfate oxygen isotopes. Furthermore, the only evidence for boiling are the fumaroles at the head of the valley, almost 5 km from the springs.

Thus, although evidence for mixing and conductive cooling of thermal spring waters appears overwhelming, and the existence of different intermediate reservoirs seems probable, the question of the existence and temperature of deeper reservoirs remains unresolved.

Heat Discharge by Spring Flow

Thermal waters from A1, A2, and A3 flow at 40, 51, 118 lpm, respectively, directly into the west fork channel of Hot Springs Creek. The stream bed of the west fork above the outflow basin A1 measured 75.0° to 83.2°C just a few cm below the ground surface, which indicates thermal waters are discharging directly into the cold stream channel. The silica and chloride content of stream waters above and below site A and in the sampled thermal waters provide a means of estimating the cold and hot-water mixing fractions in the stream. Using the equation: $C_m = (1-X)C_h + XC_c$ where C is the concentration of either silica or chloride in the mixed (m), hot (h), and cold (c) fractions, X, the cold water fraction can be calculated. The values from table 6-2, analyses 14 and 15, give a cold-water mixing fractions of 0.922 for Cl and 0.928 for SiO_2. Total water flow in the west fork channel below site A measured 4280 lpm ± 5 percent. The average of the SiO_2- and Cl-determined mixing fractions gives an

estimated total hot-water discharge from site A of 320 lpm. Stream temperatures above and below site A measured 9.8° and 15.4°C, respectively. Substituting these values into the equation $T_m = (1-X)T_h + XT_c$ gives an estimated temperature of 84.5°C for the hot-water fraction, a temperature consistent with the hottest spring vent temperature measured at the site. The heat flux loss represented by this hot-water discharge relative to the stream temperature of 9.8°C is about 1.6 MW.

Measurements of individual spring discharges were not possible at sites other than A. Determination of the total discharge of thermal waters from sites A, B, C plus D was attempted by measuring the stream flow in Hot Springs Creek below D and comparing water chemistries of the stream above A to below D (analyses 8 and 13 respectively in table 6-2). Unfortunately, the thermal water in the stream becomes highly diluted by the large cold water fraction and only a crude estimate of overall heat discharge can be made. The hot water fraction at point 13 based on comparisons of SiO_2, Na+K, and Cl is 0.027, 0.016, or 0.008, respectively. The total stream flow below D was measured to be 52,700 lpm ± 5%, so that the corresponding hot water discharge estimates above this point are 1,420, 840, and 420 lpm. If the hot water fraction is assumed to be 84°C, then the corresponding estimated heat discharges referenced to 10°C are 7.4, 4.4, and 2.2 MW respectively. The estimated flow from group A alone was ~320 lpm so that using Cl concentrations to calculate the hot water fraction below D appears to give too low an estimate, and the more probable heat discharge is between 4.4 and 7.4 MW. A substantial amount of thermal water is probably also discharging at and beyond the beach as evidenced by spring E and the elevated temperatures measured in the surrounding sands.

GAS CHEMISTRY

Gases emanating from the fumarole field and from the lower valley hot springs were collected in 1981; fumarole gases were sampled again in 1983 during a one day reconnaissance visit. Fumarole samples were collected by placing a plastic funnel over a suitably pressurized vent and packing the exterior with mud to prevent air contamination. The funnel was connected to a sodium hydroxide-charged evacuated flask with tygon tubing. The sampling line was purged of atmospheric air, the stopcock in the flask opened and gases allowed to bubble through the sodium hydroxide solution. Carbon dioxide and sulfur gases are absorbed by the sodium-hydroxide allowing trace gases to concentrate in the head space of the flask. Gases from hot springs were sampled in a similar manner except that the funnel was first immersed in a pool over a train of bubbles. The gas sample was taken by allowing the gases to displace water in the funnel then collecting the gas in the evacuated flask.

Gases collected in 1981 were analyzed at the Scripps Institute of Oceanography and at ADGGS, Fairbanks. The 1983 samples were analyzed at U.S. Geological Survey, Menlo Park and ADGGS, Fairbanks. Residual gases, i.e., gases not absorbed in the sodium hydroxide solution (He, H_2, Ar, O_2, N_2, and CH_4) were analyzed on a dual-column gas-chromatograph with both argon and helium carrier gases. Moles of residual gas were calculated from measured gas pressure and head space volume. Carbon dioxide and hydrogen sulfide concentrations in the sodium hydroxide solutions were determined by titration and by ion chromatrography respectively, or by gravimetric methods using $SrCl_2$ and $BaCl_2$ to precipitate $SrCO_3$ and $BaSO_4$. The $SrCO_3$ precipitate was then reacted with phosphoric acid to determine CO_2 yield. The evolved gas was

saved and analyzed for $^{13}C/^{12}C$. Steam content of the gases was determined by weight difference before and after sampling. Ammonia was analyzed by specific ion electrode method.

Adjustments were made for head space gases dissolved in the solution using Henry's Law. Moles of each constituent collected were then determined and the mole percent of each constituent was calculated. A correction was then made for air contamination by using the ratio of oxygen in the sample to oxygen in air. The gas concentrations in mole percent were then recalculated on an air-free basis.

Helium isotope ratios ($^{3}He/^{4}He$) were determined at the Scripps Institute of Oceanography, La Jolla, California. Carbon isotope ratios in carbon dioxide ($^{13}C/^{12}C$) were analyzed at U.S. Geological Survey, Menlo Park, California.

The results of the analyses in mole percent are given in table 6-4. Sample AL-11 is from hot spring A3; sample AL-9 is from an acid-sulfate spring; and BN4, BN14, and RM3 are from fumaroles in the solfatara field. The much higher percentages of nitrogen and argon gases in hot spring A gases reflects a greater proportion of dissolved air in the thermal spring waters with oxygen being selectively removed through oxidation reactions. The fumarole samples are all relatively gas rich (Cf. Xg) and have similar proportions of major, minor, and trace gases. As is common for fumaroles associated with high temperature geothermal systems, these gases are rich in carbon dioxide and hydrogen sulfide. All the fumarole samples contain relatively large proportions of methane with very similar hydrogen-methane ratios. By comparison, the majority of fumaroles at the Makushin geothermal area have methane in only trace amounts and are very water rich with Xg's 1%.

Methane and hydrogen concentrations can be controlled by the reaction

$$CH_4 + 2H_2O \rightleftharpoons CO_2 + 4H_2$$

with higher temperatures favoring the right side of the equation (Giggenbach, 1980). Thus the high methane content and low H_2/CH_4 ratio could indicate a cooler geothermal system than at Makushin where reservoir temperature estimates range from 200 to 250°C. Alternatively, the higher methane content could reflect thermogenic breakdown of carbonaceous sediments. The carbon-13 compositions of the fumarolic carbon dioxide and methane are -11 and -35 per mil, respectively. Mantle-derived carbon dioxide is estimated to have carbon-13 compositions ranging from -4 to -9 per mil (Truesdell and Hulston, 1980) while mantle methane is estimated to range from -14 to -20 per mil (Welhan, 1981). Carbon dioxide derived from organic-sedimentary sources has carbon-13 compositions ranging from -12 to less than -20 per mil (Truesdell and Hulston, 1980); thermogenically derived methane has carbon-13 compositions ranging from -35 to -50 per mil (Scheoll, 1980). Thus the fumarolic methane may be primarily from thermogenic breakdown of organic sediments while the carbon dioxide is primarily mantle derived with a slight admixture of carbon dioxide from sedimentary sources.

At the elevation of the fumarole field the source of the organic material is unlikely to lie near the surface unless it is entrapped between layers of volcanic flows. A more likely source region would be deep-lying marine sandstones and shales which are thought to underlie the Aleutian Islands (Marlow and others, 1973). Circulation of thermal waters through such rocks could cause thermogenic reactions giving rise to the methane and the organic-sedimentary component of carbon dioxide found in the fumarole gases.

The contribution of gases from thermogenic breakdown of organic material must be greater at the hot springs to account for the larger proportion of

methane, and the lower carbon-13 compositions of the carbon dioxide (-18 per mil) and methane (-39 per mil) in the hot spring gases. The source region for the increased organic component could be the near-surface region beneath the valley floor where organic material may have become entrapped during infilling of the valley following deglaciation. Subsequent circulation of thermal waters through these recent valley sediments would have heated the organic material, causing the thermogenic breakdown.

The high helium isotope ratios ($^3He/^4He$ of 6.5-7.0) of both the springs and fumaroles do indicate a magmatic influence on the hydrothermal system. Procedures for determining helium isotope ratios and applying air corrections based on He/Ne ratios can be found in Poreda, 1983. Enrichments in ^3He with respect to atmospheric levels have been correlated with magmatic activity on a world-wide basis (Craig and Lupton, 1981). Values for the ratio of $^3He/^4He$ for Akutan fumarole and hot springs gases compared to atmospheric ratios (R/Ra) are typical of other island arc settings (Poreda, 1983). The excess $^3He/^4He$ ratio in gases from hydrothermal systems suggests a more direct connection to magmatic sources with little crustal contamination, although it may also result from leaching of young volcanic rock (Truesdell and Hulston, 1980). Lower values indicate a crustal influence of radiogenic ^4He.

D'Amore and Panichi (1980) have suggested a gas geothermometer for estimating reservoir temperatures based on the proportions of CO_2, H_2S, H_2, and CH_4. Application of this geothermometer to the 1983 gas analyses gives an estimated reservoir temperature of ~190°C which is consistent with both the geothermometry for the lower valley hot springs and the low H_2/CH_4 ratio in the fumarole gases. Although 190°C is considered relatively low, it nevertheless is sufficient for generation of electric power provided the reservoir has sufficient productivity.

The gases and steam emanating from the solfatara field probably originate from the boiling of a subsurface hot water reservoir similar to those supplying thermal waters to the lower valley springs. If the hot springs and fumaroles are all ultimately related to the same reservoir then the reservoir could cover a distance of over 4 km.

DISCUSSION

There is substantial evidence for the mixing of thermal waters with cold waters before the waters emerge as springs in the lower valley. Silica- and chloride enthalpy analyses and geologic considerations indicate the mixing occurs at depth with the mixing cooling the waters to temperatures ranging from 120° to 135°C. The waters then further cool by conduction upon lateral migration and ascent before emanating at the surface. A schematic cross-section of suggested hydrologic pathways is given in figure 6-6. The zone of mixing may be a seismically recognizable low-resistivity layer at a depth of 30 to 100 m discussed by Wescott and others, this report. Surface water on the valley floor cannot penetrate the relatively impermeable capping debris flow layer. Cold waters probably infiltrate along the valley sides and walls and migrate down-valley and laterally into the zone of mixing. There, they come into contact with thermal waters ascending from intermediate reservoirs.

Thermal waters and steam and gases emerging from the springs in the lower valley and from the fumarole field at the head of the valley appear to originate from different intermediate reservoirs having temperatures ranging from 170° to 190°C. The reservoir supplying waters to spring A has an estimated chloride concentration of ~600 ppm which is well below the chloride concentration of 3,000 ppm chloride found at the Makushin geothermal reservoir

on neighboring Unalaska Island (Motyka and others, 1985). Either a deeper, much more saline reservoir exists and supplies waters to the intermediate reservoirs of Akutan, or the Akutan hydrothermal system is considerably more dilute than the Makushin system.

Chloride-enthalpy analyses and Cl/B ratios suggest the existence of a deeper, hotter reservoir. However, the higher temperatures predicted by the chloride-enthalpy diagram are unsubstantiated by available geothermometry. If waters are ascending from a deep, master reservoir and mixing to form intermediate reservoirs, then the residence times in these intermediate reservoirs must be long enough to allow re-equilibration to geothermometer temperatures of 170° to 190°C. Carbon 13 data indicates that carbon dioxide emanating from the geothermal system is of a mixed origin: thermogenic breakdown of organic sediments plus outgassing from mantle material. Thermogenic breakdown may also be the source of the relatively high methane content of the gases. Helium isotope data confirm a magmatic influence on the Akutan geothermal system.

Heat discharge at the surface by spring flow from springs A through D referenced to 10°C is estimated at 4.4 to 7.4 MW. Substantially more thermal waters are probably discharging at the beach and directly into the sea beyond the end of the confining surface volcanic debris flow deposits. If the reservoirs supplying fluids to the fumaroles and hot springs are interconnected, the subsurface reservoir system may cover a distance of over 4 km. The estimated reservoir temperatures of 170-190°C are high enough for generation of electrical power provided the reservoir productivity is sufficiently high.

REFERENCES CITED

Arnorsson, Stefan, 1983, Chemical equilibria in Icelandic geothermal systems - implications for chemical geothermometry investigations: Geothermics, v. 12, no. 213, p. 119-128.

Arnorsson, Stefan, Gunnlaugsson, Finar, and Svavarsson, Hordur, 1983, The chemistry of geothermal waters in Iceland. III. Chemical geothermometry in geothermal investigations: Geochimica et Cosmochimica Acta, v. 47, no. 3, p. 567-578.

Baker, R.O., Lebida, R.C., Pyle, W.D., and Britch, R.P., 1977, An investigation of selected Alaska geothermal spring sources as possible salmon hatchery sites: National Technical Information Service IDO/1624-1, 173 p.

Byers, F.M., Jr., and Barth, T.F.W., 1953, Volcanic activity on Akun and Akutan Islands: Pacific Science Congress, 7th, New Zealand, 1949 Proceedings, v. 2, p. 382-397.

Craig, Harmon, 1961, Isotope variations in meteoric waters: Science, v. 133, p. 1702-1703.

Craig, H., and Lupton, J.E., 1981. Helium-3 and mantle volatiles in the ocean and the oceanic crust: The Oceanic Lithosphere: Vol. 7, The Sea, p. 391-428, New York, John Wiley & Sons.

D'Amore, F. and Panichi, C., 1980, Evaluation of deep temperatures of hydrothermal systems by a new gas geothermometer: Geochemica et Cosmochima Acta, v. 44, p. 549-556.

Fouillac, C., and Michard, G., 1981, Sodium/lithium ration in water applies to geothermometry of geothermal reservoirs: Geothermics, v. 10, no. 1, p. 55-70.

Fournier, R.O., and Truesdell, A.H., 1973, An empiracal Na-K-Ca geothermometer for natural waters: Geochimica et Cosmochimica Acta, v. 37, p. 1255-1275.

Fournier, R.O., and Potter, R.W., 1978, A magnesium correction for the Na-K-Ca chemical geothermometer: U.S. Geological Survey Open-file Report 78-468, 24 p.

Fournier, R.O., 1979, Geochemical and hydrologic considerations and the use of enthalpy-chloride diagrams in the prediction of underground conditions of hot-springs systems: Journal of Volcanology and Geothermal Research, v. 5, p. 1-16.

Fournier, R.O., 1981, Application of water chemistry to geothermal exploration and reservoir engineering, in Ryback, L., and Muffler, L.J.P., eds., Geothermal systems: Principles and case histories: New York, Wiley and Sons, p. 109-143.

Fournier, R.O., 1983, A method of calculating quartz solubilities in aqueous sodium chloride solutions: Geochemica et Cosmochimica Acta, v. 47, no. 3, p. 579-586.

Fritz, P., and Fontes, J.C., eds., 1980, Handbook of environmental isotope geochemistry; New York, Elsevier, p. 11-13.

Giggenbach, W.F., 1980, Geothermal gas equilibria: Geochemica et Cosmochimica Acta, v. 44, p. 2021-2130.

Marlow, M.S., Scholl, D.S., Buffington, D.S., and Alpha, T.R., 1973, Tectonic history of the central Aleutian arc: Geological Society of America Bulletin, v. 84, pp. 1555-1574.

McKenzie, W.F., and Truesdell, A.H., 1977, Geothermal reservoir temperatures estimated from the oxygen compositions of dissolved sulfate in water from hot springs and shallow drillholes: Geothermics, v. 5, p. 51-61.

Motyka, R.J., Moorman, M.A., and Liss, S.A., 1981, Assessment of thermal spring sites, Aleutian arc, Atka Island to Becharof Lake - preliminary results and evaluation: Alaska Division of Geological and Geophysical Surveys Open-file Report 144, 173 p.

Motyka, R.J., 1982, High temperature hydrothermal resources in the Aleutian arc: Alaska Geological Society Symposium on Western Alaska Geology and Resource Potential, Anchorage, Proceedings, p. 87-99.

Motyka, R.J., Queen, L.D., Nye, C.J., Janik, C.J., Sheppard, D.S., Poreda, R.J., Moorman, M.A., and Liss, S.A., 1985, 1983, and 1984 DGGS Geothermal fluids sampling and well-logging at the Makushin geothermal area: Alaska Division of Geological and Geophysical Surveys, Report of Investigations, submitted.

Panichi, C., and Gonfiantini, R., 1978, Environmental isotopes in geothermal studies: Geothermics, v. 6, p. 143-161.

Poreda, R.J., 1983, Helium, neon, water and carbon in volcanic rocks and gases: University of California, San Diego, Ph.D. thesis, 215 p.

Presser, T.S., and Barnes, Ivan, 1974, Special techniques for determining chemical properties of geothermal waters: U.S. Geological Survey Water Resources Investigations 22-74, 11 p.

Schoell, Martin, 1980, The hydrogen and carbon isotopic composition of methane from natural gases of various origins: Geochimica et Cosmochimica Acta, v. 44, pp. 649-661.

Truesdell, A.H., 1976, Geochemical techniques in exploration: United Nations Symposium on the Development and Use of Geothermal Resources, 2nd, San Francisco, 1975, Proceedings, v. 1, p. liii-lxxix.

Truesdell, A.H., and Hulston, J.R., 1980, Isotopic evidence on environments of geothermal systems, in Fritz, P., and Fontes, J.Ch., eds., Handbook of environmental isotope geochemistry, New York, Elsevier, p. 179-219.

Welhan, J.A., 1981, Carbon and Hydrogen Gases in Hydrothermal Systems: The Search for a Mantle Source: University of California, San Diego, Ph.D. thesis, 182 p.

Table 6-1. Chemical and stable isotope analyses of thermal waters from Hot Springs Valley, Akutan Island, Alaska.[a] (Values in mg/l unless otherwise specified).

Sample Code:	1. A3	2. A3	*. A3	3. B1	4. C4	5. D2	6. E	Fum acid spr
Cations								
Na	323.	328.	384.	172.	207.	128.	1660.	17.0
K	28.	26.	26.	16.	16.	9.3	74.	3.5
Ca	12.	12.	12.5	15.	18.	11.	130.	32.
Mg	0.9	1.0	.9	1.5	1.6	12.	320.	13.
Li	1.3	1.2	1.2	0.61	0.61	0.34	1.1	0.01
Sr	0.11	.12	nd	0.10	0.22	0.09	1.7	0.05
Anions								
HCO_3[b]	172.	nd	89.	116.	118.	128.	161.	nd
SO_4	43.	41.	54.	22.	43.	26.	495.	1300.
F	1.1	0.9	1.1	0.6	1.0	0.9	0.5	<0.1
Cl	420.	410.	424.	220.	280.	140.	3440.	5.2
Br	1.3	nd	nd	1.3	0.3	nd	17.	nd
I	0.4	nd	nd	0.1	0.6	nd	0.4	nd
SiO_2	145.	135.	140.	103.	133.	91.	121.	220.
H_2S[b]	0.50	nd	nd	nd	nd	nd	nd	nd
B	11.	12.	10.	5.9	7.0	3.4	4.5	<0.50
Fe	0.05	0.01	nd	0.57	<0.01	0.03	0.04	41.
TDS	1080.	nd	1100.	617.	762.	481.	6350.	1630.
pH[b]	7.0	nd	8.4	6.4	6.5	6.8	7.3	2.6
T(°C)	84.	84.	nd	47.4	73.4	58.8	67.	92.3

SC(μs/cm, at 25°C)[b]	,1775.	1500.	nd	1000.	1200.	700.	11000.	3500.
Date Sampled	8-07-80	7-10-81	8-31-83	7-09-81	7-09-81	8-08-80	7-12-81	7-09-81
$\delta 18_0$(SMOW)[c]	-9.2	(-10.5)[e]	nd	-10.8	-10.8	-9.2	-8.8	-1.4
δD(SMOW)[c]	nd	-70.35	nd	-71.5	-70.65	-68.67	-58.6	-38.7
^{3}H(T.U.)	20.3±0.6	nd	nd	nd	nd	nd	nd	nd
Cl/B	38	34	42	37	40	41	764	--

[a] Alaska Division of Geological and Geophysical Surveys, Fairbanks, Alaska, M.A. Moorman, analyst, except as noted.
[b] Determined in the field.
[c] R. Harmon and J. Borthwick, Southern Methodist University, Stable Isotope Laboratory, analyst, except as noted.
[d] N. Nehring, U.S. Geological Survey, Menlo Park, California, analyst.
[e] Suspect value.
[f] H. Gote Ostlund, U. of Miami, Miami, Florida, analyst.

nd = not determined
* = Analysis by D.S. Sheppaard, Dept. of Science and Industrial Research, New Zealand. pH and HCO_3 determined in the lab.

Table 6-2. Chemical and stable isotope analyses of surface streams in Hot Springs Bay, Akutan Island, Alaska.[a]
(Values in mg/l unless otherwise specified).

Sample Code:	7	8	9	10	11	12	13	14	15	16
Cations										
Na	6.7	4.0	4.1	8.6	9.4	7.3	9.1	9.9	37.	7.3
K	0.3	0.3	0.3	0.5	0.7	0.6	0.8	1.1	3.3	<0.1
Ca	11.	5.3	5.3	9.2	6.4	5.6	6.1	5.1	6.4	1.1
Mg	1.9	0.9	0.9	2.0	1.3	1.2	1.2	1.8	1.8	2.0
Li	<0.01	<0.01	<0.01	<0.01	0.01	0.01	0.01	0.02	0.11	nd
Sr	0.05	0.02	0.02	0.03	0.02	0.02	0.02	0.02	0.02	nd
Anions										
SO_4	4.	5.	6.	5.	6.	4.	6.	<1.	8.	2.
F	<0.01	<0.1	<0.1	<0.1	<0.1	<0.1	<0.1	<0.1	<0.1	0.1
Cl	6.9	7.1	3.2	9.6	10.	7.8	10.	11.	41.	10.
SiO_2	8.5	9.7	4.2	17.5	14.0	12.7	13.2	23.0	33.	19.4
B	0.50	0.50	0.50	0.50	0.50	0.50	0.50	0.50	1.7	nd
T(°C)[b]	9.	nd	nd	nd	nd	nd	8.	9.	16.	9.
SC(s/cm, at 25°C)[b]	100.	100.	100.	125.	100.	100.	nd	100.	250.	65.
Date Sampled	7-10-81	7-09-81	7-07-81	7-09-81	7-09-81	7-12-81	7-09-81	7-10-81	7-09-81	8-07-80
$\delta 18_O$(SMOW)[c]	nd	-11.6	-11.2 (-10.8)[d]	nd	nd	-10.3	nd	-10.9 (-10.8)[d]	(-9.2)[d]	(-9.3)[d]
δD(SMOW)[c]	nd	-75.	-73.	nd	nd	-72.	nd	-71. (-67.)[d]	(-68.)[d]	(-67.)[d]

Sample code:

7	Stream at head of main valley.
8	Upper west fork Hot Springs Creek.
9	Stream at head of tributary valley.
10	East fork, Hot Springs Creek above confluence.
11	Hot Springs Creek below confluence.
12	Hot Springs Creek at outlet.
13	West fork, Hot Springs Creek below springs D.
14	Tributary creek above springs A.
15	Tributary creek below springs A.
16	Cold spring near hot springs A.

[a] Alaska Division of Geological and Geophysical Surveys, Fairbanks, Alaska, M.A. Moorman, analyst.

[b] Determined in the field.

[c] R. Harmon and J. Borthwick, Southern Methodist University, Stable Isotope Laboratory, analyst, except as noted.

[d] 1980 value.

nd = not determined.

Table 6-3. Geothermometry of thermal waters of Hot Springs Bay, Akutan Island, Alaska. (Temperatures in °C).

Spring	Date	Qz. cond. (1)	Qz. adiab. (1)	Chal. cond.(1)	Na/K (2)	Na/K (3)	Na/K (4)	Na-K-Ca (5)	Mg. corr. Na-K-Ca (6)	Na/Li (7)	$\delta^{18}O$ H_2O-SO_4 (8)
A3	8-07-80	159	151	135	204	171	179	188	169	169	186[a]
A3	7-10-81	155	147	130	198	163	172	184	163	165	nd
A3	8-31-83	157	149	133	186	149	158	178	162	150	nd
B1	7-09-81	139	134	112	212	181	190	181	139	160	nd
C4	7-09-81	154	147	129	198	163	172	173	139	145	nd
D2	8-08-80	132	128	105	191	155	165	164	11	137	nd
E	7-12-81	148	142	123	156	114	124	161	2	56	nd

(1) Fournier, 1983, improved SiO_2.
(2) Fournier, 1981, Na/K.
(3) Truesdell, 1976, Na/K.
(4) Arnorsson, 1983, Na/K, Basalt.
(5) Fournier and Truesdell, 1973.
(6) Fournier and Potter, 1979.
(7) Fouillic and Michard, 1981.
(8) McKenzie and Truesdell, 1977.

[a] N. Nehring, U.S. Geological Survey, Menlo Park, California, analyst.
nd = not determined.

Table 6-4. Analysis of fumarolic and hot spring gases, Hot Springs Bay Valley, Akutan, Alaska.

Sample #	AL-11[a]	AL-9[a]	BN4[b]	BN14[b]	RM3[c]
Vent type[d]	AC-HS	AcS-HS	F	F	F
Date collected	7-09-81	7-07-81	8-31-83	8-31-83	8-31-83
T°C surface	84.5	86.6	98.5	98.5	98.5
RO_2[e]	0.000	0.000	0.000	0.002	0.001
Xg[f]	--	--	2.06	2.40	2.72
Air corrected analyses, mole %					
CO_2	10.27	92.53	95.47	94.35	95.03
H_2S	6.26	2.83	1.44	1.41	1.28
H_2	0.45	0.34	0.20	0.19	0.21
CH_4	4.58	1.32	0.92	0.91	1.05
NH_3	nd	nd	0.004	0.004	0.016
N_2	76.68	2.96	1.96	3.07	2.29
Ar	1.73	0.02	0.009	0.021	0.097
He	0.0012	0.0007	Tr	Tr	bd
Ratios					
N_2/Ar	44	148	215	154	23
C/S	2.4	33	67	68	75
H_2/CH_4	0.10	0.26	0.21	0.21	0.20
Gas Geothermometer[g]					
T°C	--	208	189	189	188
^{13}C composition and $^3He/^4He$ ratios					
$\delta^{13}C\text{-}CO_2$[h]	-18.1	-11.2	-10.9	-10.8	nd
$\delta^{13}C\text{-}CH_4$[h]	-39.2	-34.9	nd	nd	nd
Rc/Ra[i]	6.0-6.3	7.1	nd	nd	nd

[a] Collected by R. Poreda and R. Motyka. Analyzed by R. Poreda and J. Welhan, Scripps Institute of Oceanography, LaJolla, California, and R. Motyka, Alaska Division of Geological and Geophysical Surveys, Fairbanks, Alaska.

[b] Collected and analyzed by D. Sheppard, Department of Science and Industry Research, New Zealand.

c Collected by D. Sheppard; analyzed by R. Motyka.

d AC-HS = Alkali-chloride hot spring; AcS-HS = acidic-sulphate hot spring; F = fumarole.

e Ratio of mole % O_2 in sample to mole % O_2 in air.

f Gas-steam ratio, moles gas/moles steam, in percent.

g Gas geothermometer of D'Amore and Panichi (1980); PCO_2 assumed to be 1 bar.

h $\delta^{13}C$ in per mil referenced to "PDB" (Fritz and Fontes, 1980).

i Ratio of $^3He/^4He$ in sample (air corrected) to $^3He/^4He$ in atmosphere (Poreda, 1983).

FIGURE CAPTIONS

Figure 6-1: Thermal springs and stream water sampling locations in lower Akutan Srings Bay Valley.

Figure 6-2: Trilateral cation diagram for waters from Akutan Hot Springs Bay Valley.

Figure 6-3: Diagram of stable isotope composition of Akutan's waters. Values are relative to SMOW. Numbers are keyed to tables 1 and 2. Craig's (1961) meteoric water line and the Adak precipitiation line are included for comparison.

Figure 6-4: Silica - Enthalpy and mixing relationships for Akutan Hot Spring waters. Quartz soluability curve from Fournier (1983).

Figure 6-5: Chloride - Enthalpy relationships for Akutan Hot Springs.

Figure 6-6: Schematic cross-section of lower Hot Springs Bay Valley showing suggested hydrologic pathways for cold and hot waters. Meteoric waters percolate down along valley walls. The waters flow under capping volcanic debris flows and valley alluvium and infiltrate into a porous middle layer. Mixing with upwelling thermal water is thought to occur in a zone of low resistivity found to underlie the northwest corner of the valley. Subsurface boundaries are inferred from seismic and electrical resistivity surveys (Wescott and others, this report).

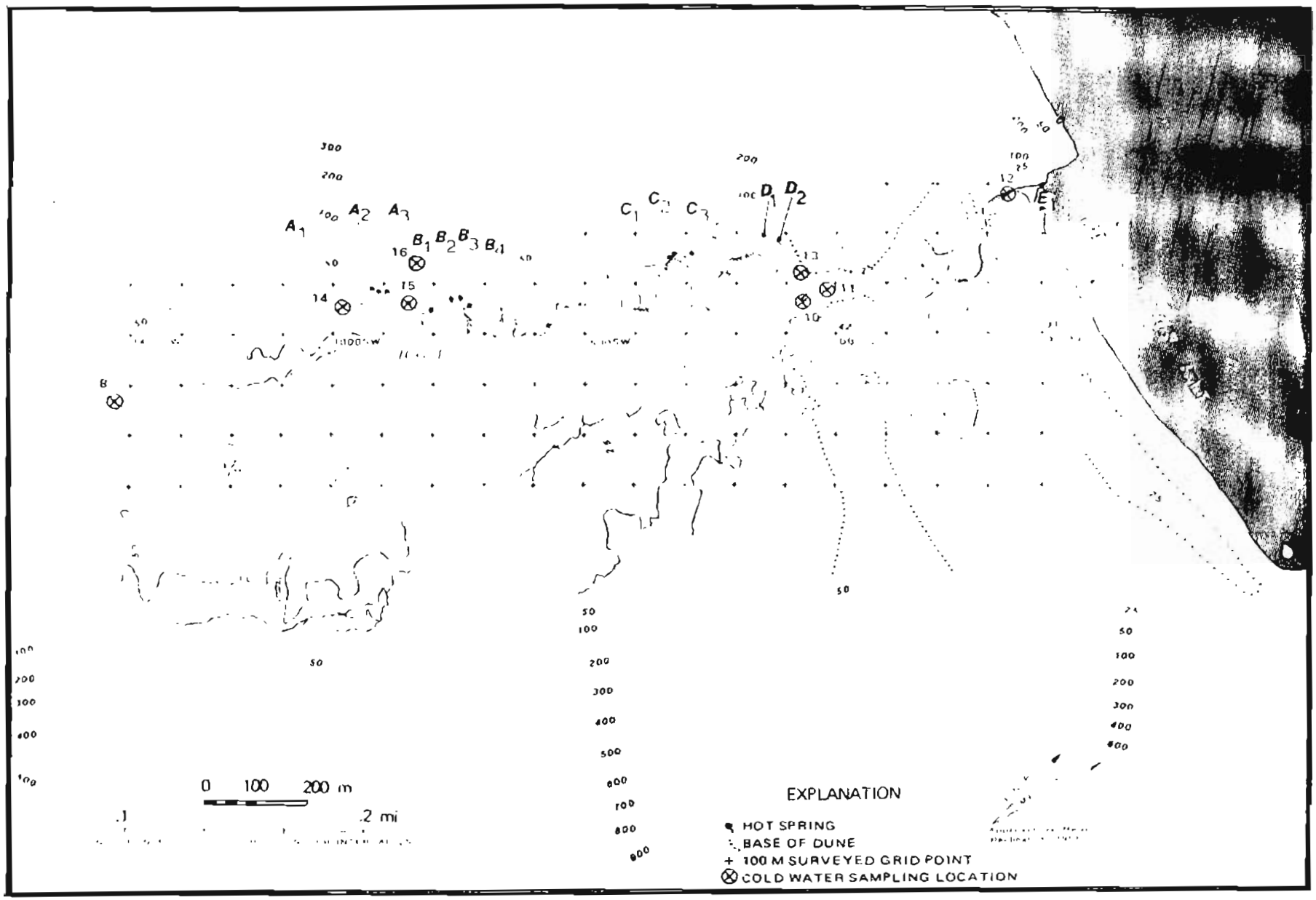
A1
A2
A3
B1
B2
B3
B4
C1
C2
C3
D1
D2
E1
B
10
11
12
13
14
15
16
0 100 200 m
.1 .2 mi
EXPLANATION
HOT SPRING
BASE OF DUNE
100 M SURVEYED GRID POINT
COLD WATER SAMPLING LOCATION

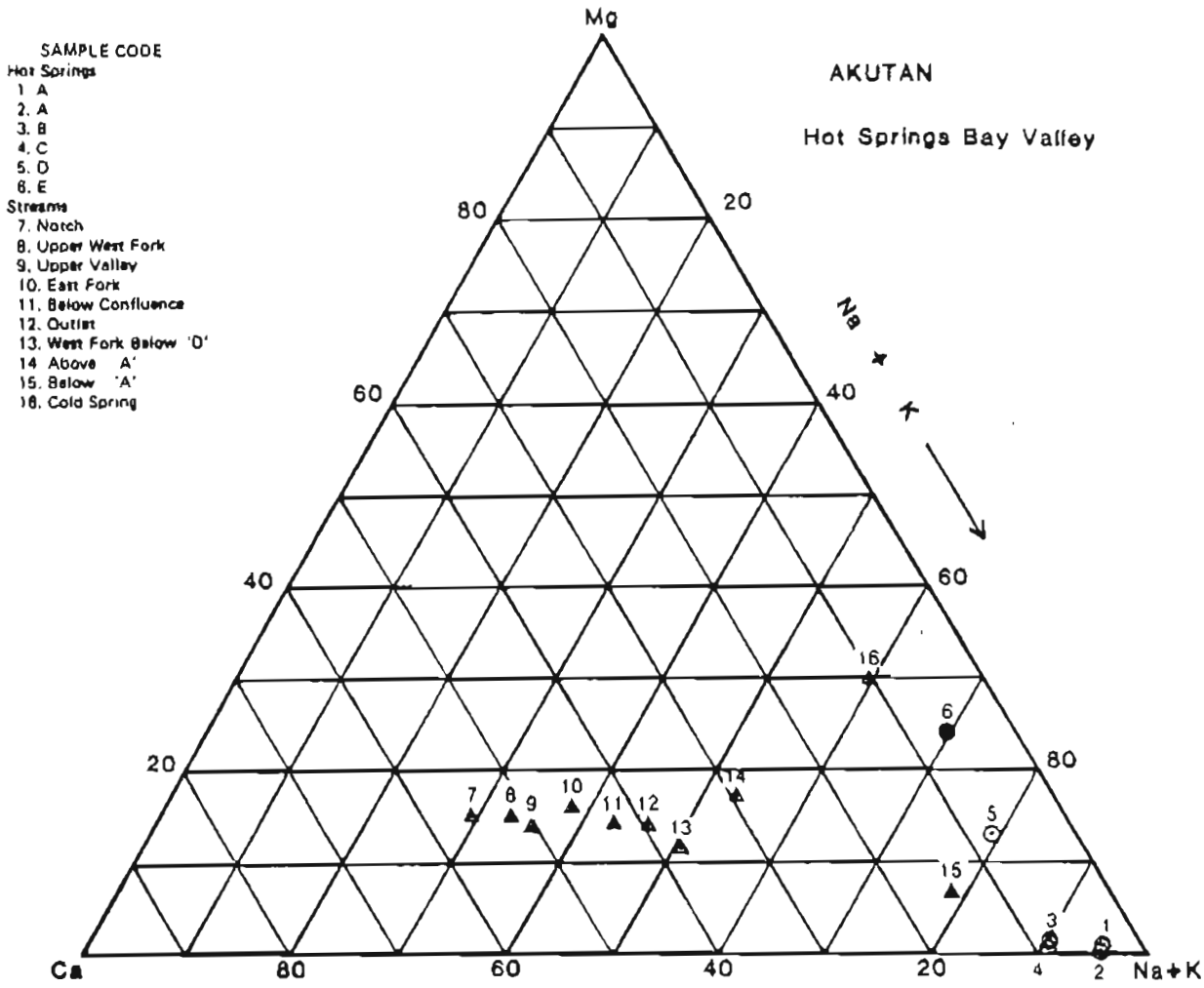
SAMPLE CODE
Hot Springs
1. A
2. A
3. B
4. C
5. D
6. E
Streams
7. Notch
8. Upper West Fork
9. Upper Valley
10. East Fork
11. Below Confluence
12. Outlet
13. West Fork Below 'D'
14. Above 'A'
15. Below 'A'
16. Cold Spring
AKUTAN
Hot Springs Bay Valley
Mg
Ca
Na+K
80
60
40
20
16
6
7
8
9
10
11
12
13
14
5
15
3
1
4
2

Hot Springs Bay, Akutan, Alaska

Stable Isotope Analyses

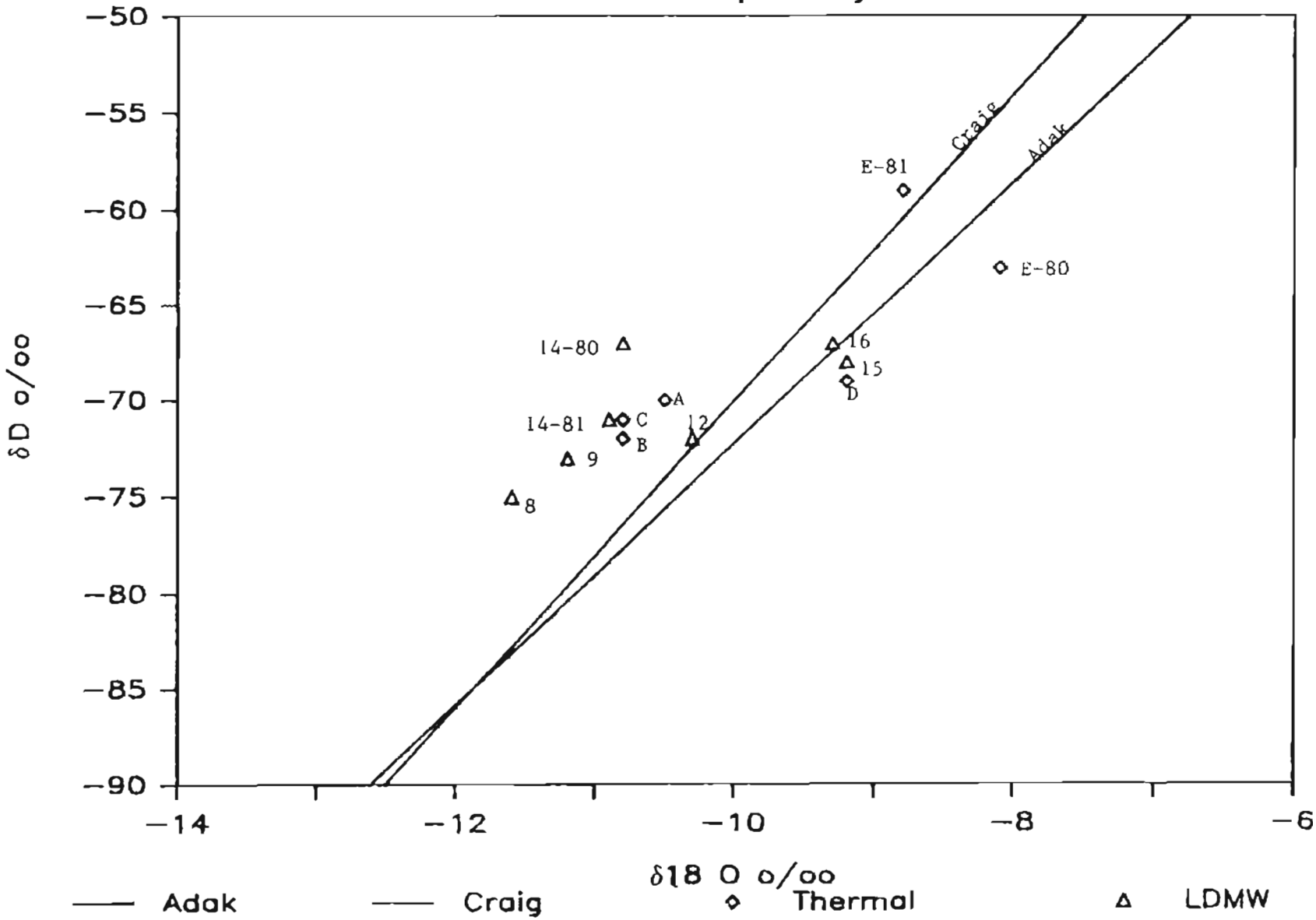

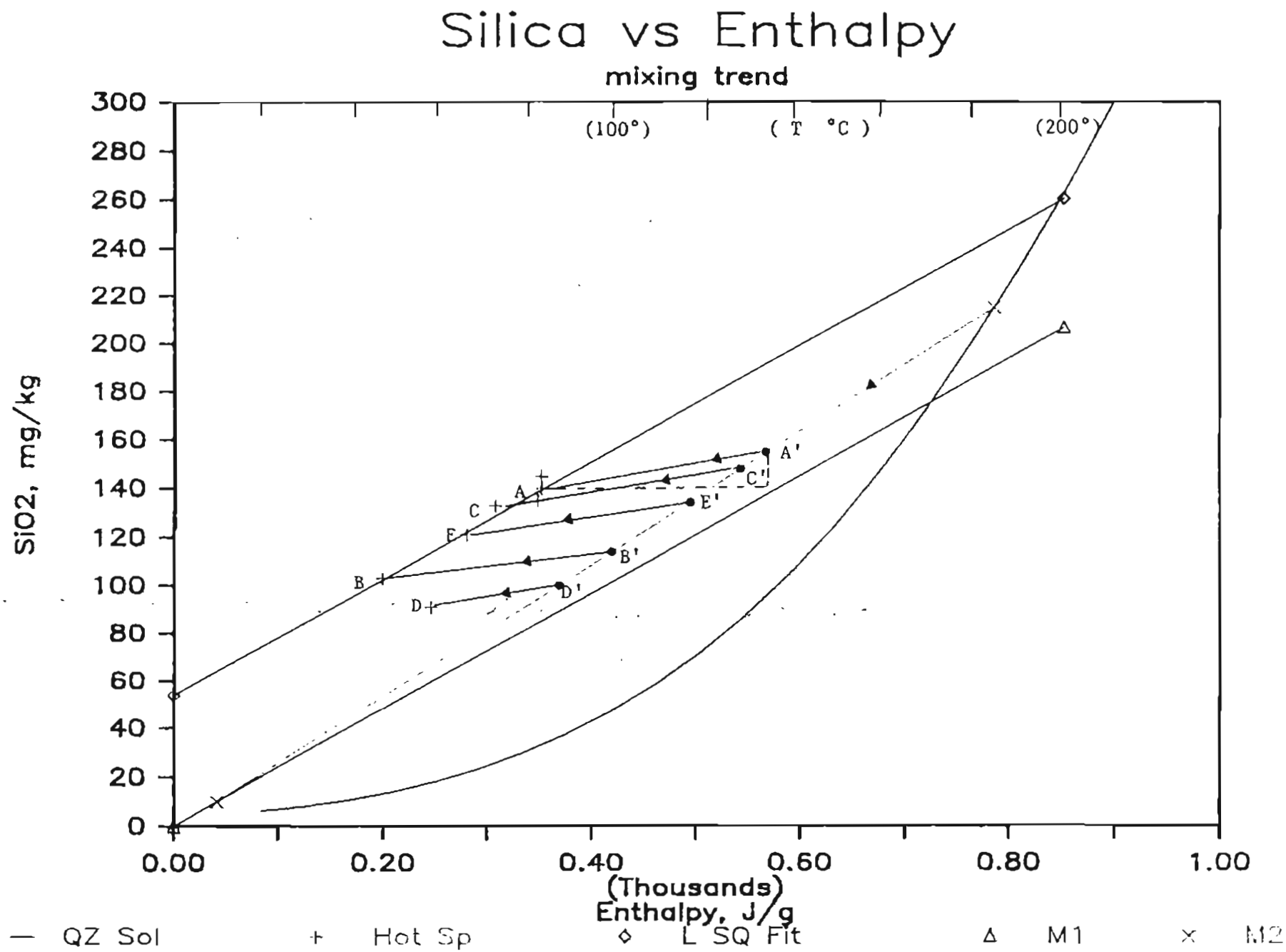
Silica vs Enthalpy
mixing trend
(100°)
(T °C)
(200°)
SiO2, mg/kg
300
280
260
240
220
200
180
160
140
120
100
80
60
40
20
0
0.00
0.20
0.40
0.60
0.80
1.00
(Thousands)
Enthalpy, J/g
A
A'
B
B'
C
C'
D
D'
E
E'
— QZ Sol
+ Hot Sp
◇ L SQ Fit
△ M1
× M2

Chloride — Enthalpy Analyses

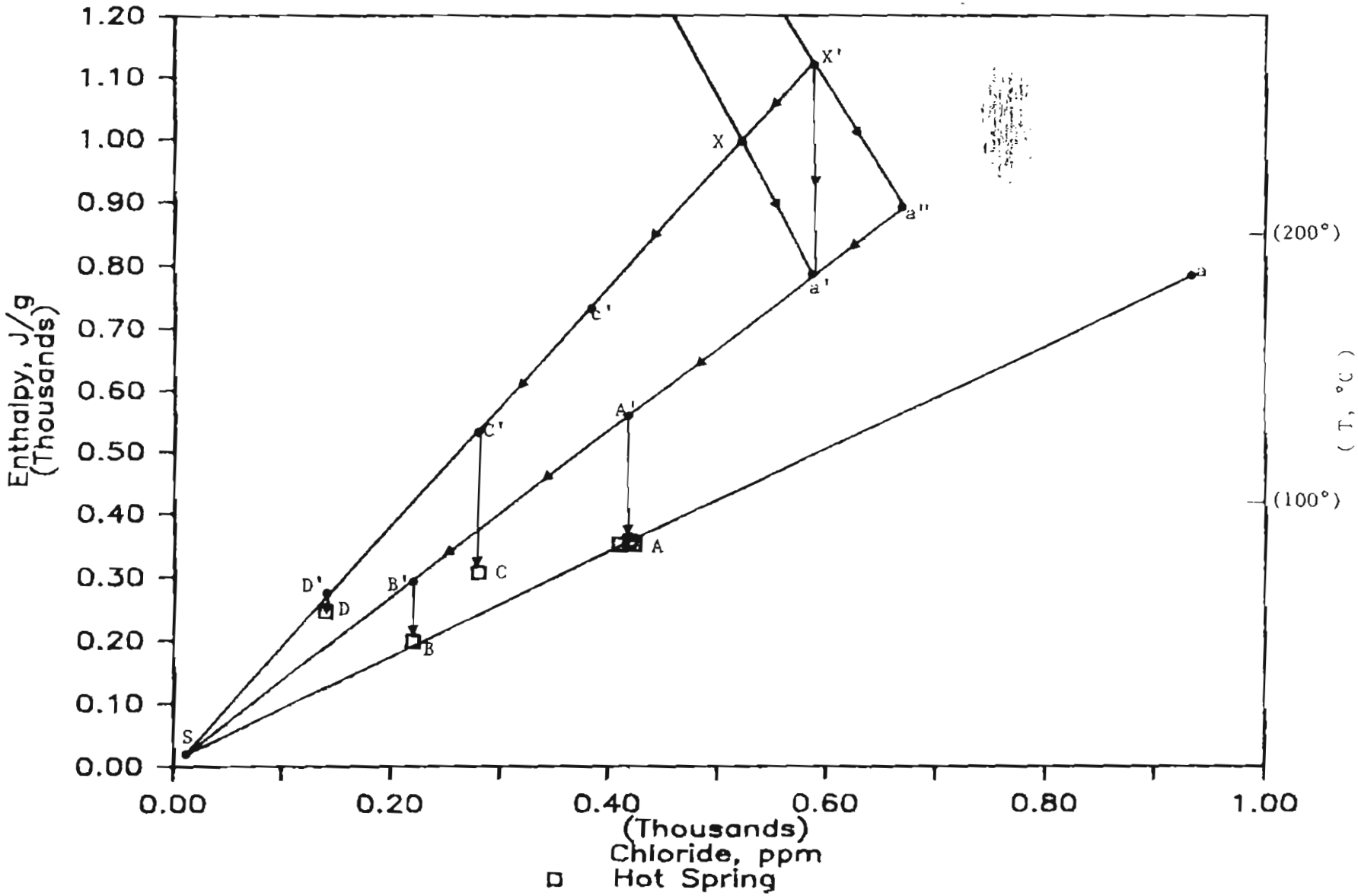

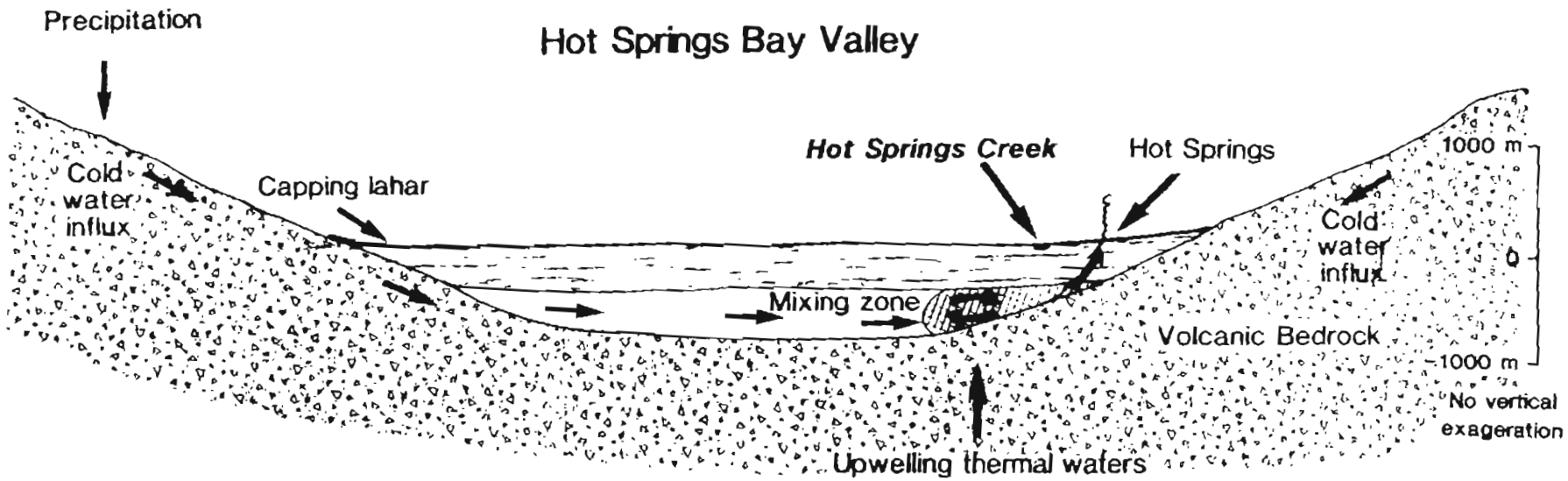
Precipitation
Hot Springs Bay Valley
Cold water influx
Capping lahar
Hot Springs Creek
Hot Springs
Cold water influx
1000 m
0
Mixing zone
Volcanic Bedrock
-1000 m
No vertical exageration
Upwelling thermal waters

CHAPTER 7

APPRAISAL OF GEOTHERMAL POTENTIAL

Roman J. Motyka,[1] Eugene M. Wescott,[2] Donald L. Turner,[2]
and Samuel E. Swanson[2]

[1]State of Alaska Division of Geological and Geophysical Surveys, Fairbanks, Alaska.
[2]Geophysical Institute, University of Alaska, Fairbanks.

MODEL

The results of our investigations allow development of a conceptual model of the geothermal regime at Hot Springs Bay Valley as depicted in figure 7-1. Seismic and resistivity surveys have delineated three fundamental layers in the valley: 1) an upper layer, 30-70 m thick with seismic velocity of 1630-1960 m/s, and resistivity of 100 ohm-m; 2) an intermediate-velocity layer of about 3240 m/s, 25 to 75 m thick which contains a region of low resistivity (3 ohm-m); 3) underlain by high-velocity (4900 m/s), high-resistivity (1500 ohm-m) volcanic bedrock presumed to be similar to the older volcanic breccias which form the steep valley walls. Detailed resistivity measurements suggest more complicated bedding structures within the three fundamental units.

Key features of the hydrothermal system include: 1) deep hydrothermal reservoirs at temperatures ranging from 170 to 190°C from which thermal waters with chloride concentrations of ~600 ppm, ascend to shallower levels; 2) a shallow mixing reservoir underlying the northwest corner of the valley and containing diluted waters with chloride concentrations of ~400 ppm and temperatures of 120 to 135°C; 3) a boiling hot-water reservoir feeding steam and gases into the fumarole field at the head of the valley; and 4) hot springs along the lower western margin of the valley.

The heat source driving the hydrothermal system is assumed to be a shallow-lying body of magma as suggested by petrologic and geochemical data and helium isotope ratios.

Upper layer - Hydrothermal Cap

The geophysical surveys have delineated an intermediate-resistivity, low-velocity upper layer in the valley that is 40 to 70 m thick near the valley center and which thins up-valley and towards the valley margins. The uppermost unit in this layer was found to be a volcanic debris flow of relatively recent age (<3000 ybp). By inference, the remainder of this layer is presumed to be composed of similar debris flows (such as are exposed in adjacent valleys), interbedded with valley alluvium. This layer appears to be acting as an impermeable cap on the shallow subsurface hydrothermal system except along the west side of the valley.

The thermal springs all occur along the lower west valley margin. Although searched for, no geologic or geophysical evidence could be found for fault control of the spring flow or fumarole emissions. The sinuous low-resistivity pattern of shallow ground EM-31 measurements suggests that the thermal spring waters are migrating along older stream channel gravels. The thermal springs presently occur on or very near stream banks and thermal waters are also discharging through stream-bed gravels directly into Hot Springs Creek. The creek has apparently cut through the uppermost volcanic debris flow layer which is probably thinnest along the valley margins. Interconnection with stream-cut channels embedded in the older debris flows would allow thermal waters under artesian pressure in the shallow mixing reservoir to migrate upward along the permeable gravels and emerge at the surface. The helium and mercury soil sample surveys (Wescott and others, this report) show anomalously high values away from the sinous pattern towards the center of the valley. This suggests the source of upwelling hot water to the mixing reservoir may be further out in the valley.

Intermediate Layer - Low Resistivity Zone of Mixing

The longitudinal seismic refraction survey BB' delineated a middle layer in the lower valley having a thickness of ~100 m near the ancient dune and thinning rapidly to less than 40 m, 500 m up-valley from the dune. The upper surface of this layer dips gently down-valley and lies at depths of 30 to 40 m. The interface of the layer with the underlying valley bedrock has a comparatively steeper slope with a depth to bedrock at the dune of 130 m vs. 75 m at 500 m up-valley.

This intermediate layer was not detected by the down-valley tranverse seismic survey AA' nor by the longitudinal survey CC' taken up-valley from BB'. However, Wescott and others have argued that a ghost layer up to 30 or 40 m could exist and go undetected by the seismic surveys. Furthermore the three layer model is in general agreement with the deep-sounding electrical resistivity surveys.

The composition of the intermediate layer is uncertain. The relatively high seismic velocity of this layer indicates a fairly rigid rock while electrical resistivity indicates a fairly porous or, alternatively, a clay-rich unit. Seismic profiles suggest that the lower valley bedrock was glacially carved. The intermediate layer could thus be composed of glacial till and glaciofluvial outwash deposited during the waning stages of the Wisconsinan Glaciation. The rigidity of the layer could arise from subsequent hydrothermal cementation. Alternately the layer could be composed of partially cemented ash flow tuffs which could account for both rigidity and porosity. In either case, the layer must also be relatively permeable to allow migration, mixing and upwelling of waters.

We next examine the possible causes of the low resistivity in the intermediate layer. The depth to bedrock near the ancient dune is 120 m below present mean sea level. Worldwide eustatic sea level depression during the Wisconsinan maximum is estimated to have been 75 to 100 m below the present mean sea level (Clark and Lingle, 1979). Relative sea levels and sea level changes during the late stages of the Wisconsinan Glaciation and during the Holocene in the Aleutians are not well-known because of the complications involved in unraveling isostatic, eustatic and tectonic processes (Black, 1982). However, it does appear possible that glaciofluvial sediments in lower Hot Springs Bay Valley were deposited in a marine environment during the waning stages of the Wisconsinan Glaciation. Thus the low resistivity could be due to the salinity of marine sediments. The low carbon-13 compositions of the carbon dioxide and methane and the large proportion of methane in hot springs gases does indicate a source of organic material exists in the near-surface region of the valley but we cannot distinguish whether this material is of marine or terrestial origin.

A second possibility is that coastal saltwater is currently infiltrating into the intermediate layer and is the cause of the low resistivity.

We reject both these possibilities and prefer to ascribe the low resistivity to the presence of thermal waters for the following reasons: 1) The hydraulic pressure head and the constant flow of meteoric water through the valley fill are probably sufficient to keep the valley flushed of salt water and cleansed of salts from any early Holocene marine sedimentation. 2) The region of low resistivity is confined to the west side of the valley and extends to within 30 m of the surface at 1 km from the present coast. If the low resistivity was due to marine sediments or salt water

intrusion, we would expect the low resistivity to extend across the entire width of the valley. It also seems improbable that salt water would penetrate as far inland as 1 km. 3) The most compelling reason for ascribing the low resistivity to thermal waters is the proximity of this zone to the location of hot springs.

Evidence from our fluid geochemistry indicates that the hot spring waters are a mixture of deeper thermal waters and shallow cold meteoric waters. We infer that the mixing occurs in the region of low resistivity within the intermediate layer. The ascending parent thermal waters ate estimated to be at temperatures of 170 to 190°C. These waters would normally begin boiling when they reached depths of 100 to 120 m but we believe meteoric waters infiltrating into the intermediate layer from the east side and from up-valley intercept the hot waters and either quench the boiling or prevent boiling from occurring at all. The mixed waters, initially at 120 to 135°C, are further cooled conductively as they migrate laterally towards the west and ascend under artesian pressure to the surface and emerge as hot springs.

Deep Reservoir

The high resistivity, high velocity bedrock underlying the valley is inferred to be a continuation of the Hot Springs Bay volcanics exposed in the valley walls. What underlies the volcanics is unknown. The depth of penetration of the geophysical surveys was insufficient to delineate conduits supplying geothermal fluids to the near surface and, although the existence of deeper reservoirs can be inferred from fluid geochemistry, the depths to

these reservoirs are unknown. At the Makushin geothermal area on neighboring Unalaska Island, an exploration well sited at 370 m (1200 ft) above sea level encountered a producing fracture in a hot-water system at a depth of 600 m (2000 ft), about 240 m below sea level. The water table of the Makushin hot-water system itself is estimated to be at about 120 m above sea level. Thus it seems reasonable to assume that the reservoirs at Akutan lie within 1 km of the surface and are perhaps as shallow as 300 m below the valley floor.

Although there are similarities in the compositions of the Akutan hot spring and fumarole gases and their $^{3}He/^{4}He$ ratios, the data are insufficient to unambiguously determine whether the thermal fluids supplying the two zones are derived from the same reservoir. However, gas geothermometry applied to the fumarole gas compositions gives results very similar to water geothermometry obtained for the hot springs.

The ultimate driving force for the geothermal system is presumed to be a shallow-lying body of magma. Akutan is a young, active volcano with a small recent collapse caldera, indicative of movement and storage of magma in the shallow crustal region of Akutan Island. Furthermore, geochemistry and petrology of volcanic rocks at Akutan Volcano are consistent with fractional crystallization of a single shallow magma system. Additionally, the helium isotope ratios and carbon-13 composition of the fumarole gases indicate a magmatic influence on the hydrothermal system.

GEOTHERMAL POTENTIAL

We attempt in this section to provide estimates of the energy potential of the geothermal resource base at Hot Springs Bay Valley. Our estimates are

necessarily preliminary because precise determination of parameters required for rigorous resource assessment, such as reservoir depth, volume, permeability, and temperature can only be obtained through an exploration drilling program. Our estimates are best for the near-surface region of lower Hot Springs Bay Valley where our investigations have concentrated. Estimates are more uncertain for the deeper reservoirs.

In making our estimates we have adopted the methodology developed by Brook and others (1979) for assessing geothermal systems that have not yet been drilled. The accessible geothermal resource base if a reservoir i.e., the total amount of thermal energy available in the reservoir, is given by:

$$Qr = \rho c \, V \, (T - Tref) \qquad (7\text{-}1)$$

where,

Qr = accessible reservoir thermal energy in joules

ρc = volumetric specific heat of rock plus water

V = reservoir volume

T = reservoir temperature

Tref = reference temperature.

The reference temperature, Tref, is the mean annual surface temperature which for Akutan is approximately 10°C.

The recoverable geothermal energy, i.e., the amount of heat that can actually be extracted at the wellhead, Qwh, is estimated by Natheson and Muffler (1975) to be approximately 25 percent of the stored energy. In making the latter estimate Natheson and Muffler assume that thermal energy in the reservoir can be additionally extracted by a sweep process involving

injection of cold water into the reservoir to replace the original hot water withdrawn during production. If cold-water reinjunction is not done, the recoverable energy would be somewhat less, although colder groundwaters would still be expected to replace some of the extracted thermal water.

Electricity is produced from geothermal resources by converting part of the thermal energy into mechanical energy (work) and then using this work to generate electrical energy. The change in fluid enthalpy minus the waste heat involved in the process is the work that is available, Ea.

The ratio of work to the accessible energy base, Qr/Ea, has been calculated by Brook and others (1979) for hot-water systems for a broad range of temperatures and for reservoir depths of 1 and 3 km using a number of simplifying assumptions. The reader is referred to Brook and others (1979) for details on the calculations and assumptions made. For a reservoir depth of 1 km and temperature of 180°C, conditions we might expect for the deeper reservoirs at Akutan, the ration Qr/Ea is 0.0525.

Shallow Reservoir

Stored Energy

The volume of the shallow reservoir residing in the intermediate layer was estimated by assuming the reservoir occupies only the western half of the lower valley, that it has a valley-center thickness of 100 m at the coast, and that the reservoir layer gradually thins to 0 m, 1.5 km up-valley. The reservoir layer is also assumed to gradually thin to 0 m at the western valley margin to give the reservoir width of 0.25 km. The resulting volume is $\sim 9.4 \times 10^6$ m^3.

Wescott and others (this report) estimate the reservoir porosity at 33 to 47 percent. For this analysis we use the more conservative porosity estimate to allow for the possible presence of clays, which would shift calculated porosity toward the higher end of the estimated range. The volumetric specific heat of rock, $(\rho c)r$, is 2.5 $J/cm^3/°C$, and that of water, $(\rho c)w$, is 4.1 $J/cm^3/°C$ giving an overall average specific heat for the reservoir of 3.0 $J/cm^3/°C$. Fluid geochemistry and mixing relationships suggest reservoir temperatures are 120 to 135°C and a mean value of 127°C is used in this analysis. The resulting estimates of stored heat energy obtained by applying equation 7-1 is given in table 7-1.

Because the shallow reservoir is relatively small, the amount of energy stored would be depleted in relatively short time. However this does not take into account the fact that the reservoir would be constantly replenished by natural flow-through discharge of the system. In fact, as will be shown, this natural heat discharge itself appears to be more than sufficient to meet the present needs of the Akutan community.

Flow-Through Heat Discharge

The rate at which heat is being discharged from the geothermal system by natural fluid flow in the lower valley was estimated at 5 to 10 MW. This power represents the rate at which heat could potentially be extracted from the system indefinitely without significant drawdown or depletion of shallow reservoir energy. The estimate of natural heat discharge is based on thermal spring flow measurements, estimates of thermal water discharge directly into Hot Springs Creek, and the discharge of thermal waters at and beyond the Hot

Springs Bay beach. If these thermal waters, which are presumably under artesian pressure in the shallow reservoir, could be tapped and diverted by drilling, the heat energy could be used for direct heat applications. Since the thermal spring waters appear to have cooled by conduction during their ascent from the reservoir, the available heating power could be higher than the 5 to 10 MW estimate.

We now attempt to estimate the number of dwellings that could be potentially heated by this natural flow-through discharge. Using available data on the efficiency of conversion of wellhead heat energy to direct-heat use, Sorey and others (1983) derived an empiracal relationship between the usable temperature drop, ΔT, that occurs as energy is extracted in some process, such as district heating, and the reservoir temperature, T:

$$\Delta T = 0.6\ (T - 20°C)\ . \qquad (7\text{-}2)$$

Thus if waters are extracted from the wellhead at a temperature of 127°C at approximately the rate of natural discharge. then approximately one-half of 5 to 10 MW or 2.5 to 5 MW would potentially be available for heating purposes.

Based on data obtained for the Western United States, the maximum heat loss of normal-size residential buildings was found to vary between 47 to 189 W/m^2 of floor area, depending upon insulation and inside-outside temperature difference (Anderson and Lund, eds., 1979). For Akutan we assume that the average house is $100m^2$ ($1000\ ft^2$) and is moderately insulated. For outside temperatures of -25°C (-14°F) (the probable coldest winter temperatures at Akutan), the maximum heat loss is 100 W/m^2 or 10,000 W per household.

Assuming a 20 percent heat loss in the pipeline and distribution network, 2.5 to 5 MW of heat energy would be capable of heating 200 to 400 homes during the coldest periods at Akutan.

The wellhead thermal-water flow, in liters per second, required to supply this heat is given by

$$W(l/s) = HL/(4.22\ \Delta T) = 9.2 \text{ to } 18.4\ l/s \qquad (7\text{-}3)$$

where HL is the heating load in KW and ΔT is in °C. Such flow-rates could be provided by one or two shallow wells if the reservoir pressure is sufficiently high.

In addition to district heating, the geothermal heat energy could be used for a variety of industrial and agricultural applications. For an informative discussion of these potential applications the reader is referred to 'Direct Utilization of Geothermal Energy: A Technical Handbook,' Anderson and Lund, eds., 1979.

Deep Reservoir

Thermal fluid geothermometry indicates the existence of deeper hydrothermal reservoirs ranging in temperature from 170 to 190°C. Geochemistry and mixing models indicate the reservoir waters are relatively dilute with chloride concentrations of ~600 ppm. Although the depth and volume of these reservoirs are unknown, we can still attempt an appraisal of their geothermal potential by making reasonable estimates of these parameters. As discussed previously, geothermal drilling at neighboring Unalaska Island intersected a producing hot-water fracture zone at a depth of

approximately 600 m below the point of drilling. It thus seems reasonable to assume that reservoirs at Akutan lie within 1 km of the surface and are perhaps shallower.

Brook and others (1979) estimate that the minimum volume of a hot-water reservoir is 1 km^3. Using the mean temperature of our geothermometry, 180°C, and the preceeding parameters in equation 7-1, and using a Qr/Ea ratio of 0.0525 gives the results in table 7-1. Thus a single reservoir at 180°C, 1 km depth, and 1 km^3 in volume could provide 9.2 MW of electrical power for a period of 30 years. Higher temperatures and larger or multiple reservoirs, as suggested by the presence of the fumarole field, would significantly increase the estimated electric power potential at Akutan. However, even our minimum estimate of the electric power potential at Akutan would be more than sufficient to meet the energy needs of the Akutan community for he forseeable future.

RECOMMENDATIONS

The proximity of the Hot Springs Bay Valley geothermal resource area to Akutan village and harbor make this resource a particularly attractive one for continued exploration and development. The resource area lies near the coast and is accessible by sea. Exploration and drilling equipment can be brought to the site by barge and tractor, and would not require much, if any, helicopter support. Development of the resource could be tailored to the needs of the Akutan community. If district heating of the village and industrial direct heat applications are the goals of then we recommend shallow drilling (100 to 150 m) into the reservoir suspected to underlie the lower northwest corner of Hot Springs Bay Valley. Sampling and analysis of

fluids produced from the well would be required to determine whether there are any potential environmental problems. The analyses would also be used to refine mixing models and provide better estimates of deep reservoir temperatures.

If higher temperature resources capable of producing electrical power is the desired target then we recommend the following exploration program:

Phase 1

1) Electrical resistivity survey of the entire valley and extending over areas over the pass to Akutan harbor with depths of penetration of over 1 km. A 2 km transmitting dipole for controlled source audio magnetotelluric surveying could be installed in Broad Bight valley on the south side of the island for these measurements.
2) A detailed helium and mercury soil-survey of the valley.
3) Self-potential survey of the valley.
4) Continued monitoring of thermal springs and fumaroles.

Phase 2

1) Siting of exploratory test well based on results of phase 1.
2) Drilling of well to appropriate depth.
3) Sampling and analyses of well thermal fluids.
4) Well test and reservoir engineering analysis.

The goal of the first phase is to refine estimates of reservoir size and temperature and to determine the locations of potential reservoirs and conduit systems in order to help guide the siting of exploration and

production wells. If the results of phase 1 are promising then drilling of an exploratory well should proceed. If the results of the phase 1 exploration are particularly encouraging then the exploration well could be designed to become a production well after completion of the well tests.

REFERENCES CITED

Anderson, D.A., Lund, J.W., eds., 1979, Direct Utilization of Geothermal Energy: A Technical Handbook: Geothermal Resources Council Special Report No. 7.

Black, R.F., 1980, Isostatic, tectonic, and eustatic movements of sea level in the Aleutian Islands, Alaska, in Earth Rheology, Isostasy and Eustasy, Nils Axel Morner, ed., J. Wiley and Sons, p. 231-248.

Brook, C.A., Mariner, R.H., Mabey, D.R., Swanson, J.R., Guffacti, Marianne, and Muffler, L.J.P., 1979, Hydrothermal convection systems with reservoir temperatures >90°C, in Muffler, L.J.P., ed., Assessment of geothermal resources of the United States - 1978: U.S. Geological Survey Circular 790, p. 18-85.

Clark, J.A., and Lingle, C.S., 1979, Predicted relative sea-level changes (18,000 years B.P. to present) caused by late-glacial retreat of the Antarctic ice sheet: Quaternary Research, v. 11, p. 279-298.

Natheson, Manuel, and Muffler, L.J.P., 1975, Geothermal resources in hydrothermal convection systems and conduction-dominated areas, in White, D.E., and Williams, D.L., eds., Assessment of geothermal resources of the United States - 1975: U.S. Geological Survey Circular 726, p. 104-121.

Sorey, M.L., Natheson, Manuel, and Smith, Christian, 1983, Methods for assessing low-temperature geothermal resources, in Reed, M.J., ed., Assessment of low-temperature geothermal resources of the United States - 1982: U.S. Geological Survey Circular 892, p. 17-30.

Table 7-1. Estimates of energy potential of Hot Springs Bay Valley, Akutan Island, Alaska.

Shallow Reservoir

Temperature	127°C
Volume	9.4×10^6 m^3
Stored energy, Qr	3.3×10^{15} J
Flow-through heat discharge	5 to 10 MW
Heat discharge potentially available at wellheads	5 to 10 MW
Estimated utilization factor	0.5
Heat discharge potentially available for district heating and industrial purposes	2.5 to 5 MW

Deep Reservoir

Temperature	180°C
Assumed volume	1 km^3
Stored energy, Qr	4.1×10^{17} J
Wellhead energy, Qwh	1.0×10^{17} J
Work available, Wa	0.22×10^{17} J
Electrical energy, E	0.087×10^{17} J
Electrical power production (30 yr)	9.2 MW

FIGURE CAPTION

Figure 7-1. Model of geothermal system at Hot Springs Bay Valley, Akutan Island, Alaska. Thermal waters from deep reservoirs ascend into a porous layer underlying the lower valley. The thermal waters are diluted with infiltrating cold meteoric waters in a zone of mixing then ascend and emanate as hot springs. Steam and gases evolving from either the same reservoirs or different reservoirs feed fumaroles at the head of the valley. The underlying driving force is assumed to be a shallow-lying body of magma associated with active Akutan Volcano.

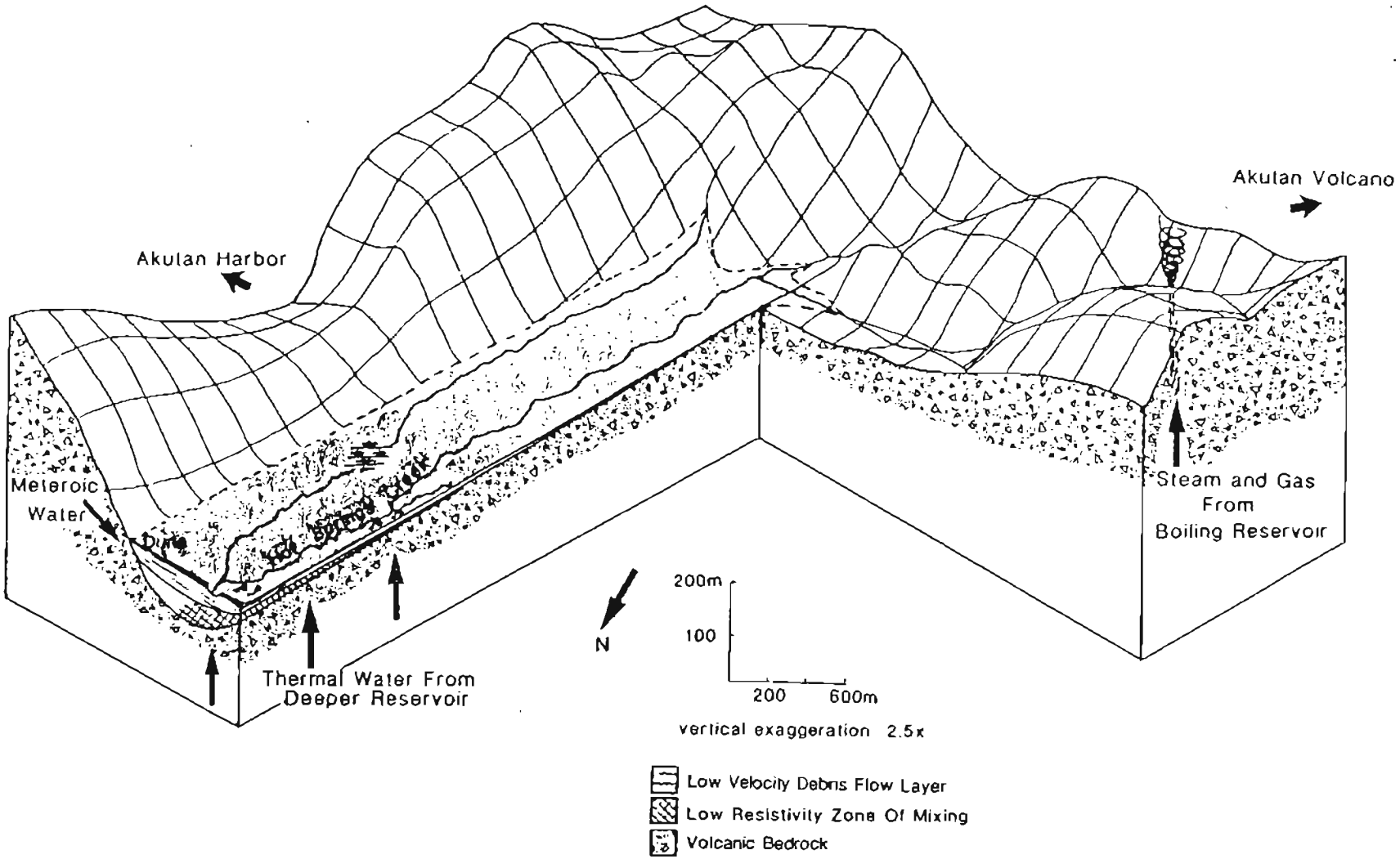
Akulan Harbor
Akulan Volcano
Meteroic
Water
Steam and Gas
From
Boiling Reservoir
Thermal Water From
Deeper Reservoir
N
200m
100
200
600m
vertical exaggeration 2.5x
Low Velocity Debris Flow Layer
Low Resistivity Zone Of Mixing
Volcanic Bedrock